

Needles in a Haystack: Identification and Characterization of Inhibitors of Lassa Virus RNA-
Dependent RNA Polymerase

by

Gabrielle Gate

A thesis submitted in partial fulfillment of the requirements for the degree of

Master of Science

in

Virology

Department of Medical Microbiology and Immunology
University of Alberta

Abstract

The all-too-recent coronavirus disease 2019 (COVID-19) pandemic is a case study in what happens when suitable antiviral measures are not in place prior to an outbreak. Severe acute respiratory syndrome virus 2 (SARS-CoV-2) was the causative agent of the COVID-19 pandemic, and has claimed more than 6.5 million lives since its discovery in 2019¹. During the scramble to find effective treatments for COVID-19, our lab demonstrated the potency of the nucleotide analogue remdesivir as an inhibitor of the SARS-CoV-2 RNA-dependent RNA polymerase (RdRp)². To date, remdesivir remains one of only a handful of approved treatments for COVID-19³. Unfortunately, it has also been shown that mutations in the RdRp can confer resistance to remdesivir⁴. As such, it is crucial to continue to expand the arsenal of antiviral agents available, not only for SARS-CoV-2, but for other viruses with high epidemic potential.

The viral RdRp replicates the viral genome, and is essential for the viral life cycle of most RNA viruses, making it a logical target for drug development^{5,6}. While nucleotide analogues like remdesivir have been successfully used to target RdRps in the past, allosteric inhibitors may also be used. Allosteric inhibitors are especially attractive in that they are less likely to be toxic *in vivo* than their substrate analogue counterparts⁷. Allosteric inhibitors can also be used in conjunction with nucleotide analogues, which can increase the efficacy of treatment and reduce the potential for resistance⁷. The goal of this project was to screen for novel allosteric compounds that inhibit the RdRp, or L-protein, of Lassa fever virus (LASV). This virus, like SARS-CoV-2, was identified by the

World Health Organization as a priority pathogen back in 2017, noted for its pandemic potential⁸. Unlike SARS-CoV-2, there is currently no approved vaccine for LASV, although a vaccine is currently in clinical trials⁹. In addition, data supporting the antiviral drug ribavirin as an effective treatment for LASV is limited¹⁰.

In the interest of pandemic preparedness, the goals of this project were to: 1) identify small molecule inhibitors of LASV RdRp, and 2) assess various properties of those inhibitors to identify which compounds warrant further investigation as candidates for drug development into new antiviral drugs to treat LASV and related viruses. Beginning with a library of 100,000 compounds, we used an *in vitro* polymerase activity assay to systematically narrow a pool of candidate compounds based on their potency (ie. half-maximal inhibitory concentration, IC₅₀), selectivity, chemical stability, and mechanism of action. Ultimately, we identified five chemically stable compounds with high potency and appropriate selectivity. Of these, three compound appeared to be competitive, while the other two appeared to be allosteric inhibitors, although the possibility of covalent inhibition couldn't be ruled out in this study. As such, while further investigation is still required, these five candidates provide a solid foundation for future LASV drug development efforts.

Preface

Construct design and expression of the various polymerases used in this project were established by Dr. Egor Tchesnokov in the Götte lab. Purification of human mitochondrial polymerase was performed by Dr. Dana Kocincova and Emma Woolner in the Götte lab. Dr. Egor Tchesnokov and Dr. Dana Kocincova also provided LASV, CCHFV, and SARS-CoV-2 polymerases for the first six months of the project. For the remainder of the project, LASV, CCHFV, and SARS-CoV-2 polymerases were purified by myself.

One human polymerase IC_{50} replicate and one SARS-CoV-2 IC_{50} replicate for compound BTB-11392 (Fig. 4.1.3), as well as one SARS-CoV-2 IC_{50} replicate for compound LS-6 (Fig. 4.1.2) were performed by Dr. Egor Tchesnokov, although these gels are not shown. The gels shown were my own experimental work.

Dr. Tracey Campbell at McMaster University performed the initial fluorescence-based screening of 100,000 compounds in section 3.1. Dr. Dana Kocincova and Emma Woolner purified the recombinant SARS-CoV-2 and LASV polymerases for this.

Dedication

To a silly little horse and a big silly dog.

Acknowledgements

There are so many people who have played a part in the journey that led me to where I am today. Most of them have made the journey better, a few have made the journey much worse. I am grateful for both; I pray that God blesses them equally and abundantly. That being said, there are a few people that I would specifically like to thank:

My parents, who created the happy accident you see before you today. Thanks especially to my mom, who willingly housed a parasite in her body for nine months and in her house for the last 26 years. And to my dad, for teaching me how to fix pretty much anything, and the best grilled cheese for the last 26 years. Thank you both for everything.

My sister, who for some reason still seems to think I'm something special when she's been a supernova since the day she was born. I'm so crazy proud of you, kid. I love you.

My best friend Emily, who despite having known me through ALL of my awkward phases doesn't pretend not to know me in public. You are the strongest, bravest, most fiercely loyal person I know, and I am the luckiest person in the world to be able to call you my best friend. I'm so glad you haven't gotten sick of me yet, and I will happily continue to eat all the tomatoes you pick out of your food until the day I die.

To my dauntless editors, Grace and Emily, who not only agreed to proofread this thesis, but actually volunteered to do so, completely unprompted. Not only were you willing to pour your blood, sweat, and tears into this, but you treated it as an honour, not a burden. Your generosity overwhelms my heart to the point that a little bit of gratitude spills out of my eyes, even as I write this. How blessed I am to have friends like you.

To my three favourite science teachers: Mr. Morgan Reed, Ms. Leslie Heinsen, and Dr. Jonathan Parrish. I'm not sure if what you've unleashed on the world is good or bad, but I am especially fond of you regardless.

To Dr. Matthias Götte, for the opportunity to work in his lab. I learned so many things, most of which I did not expect, but was pleasantly surprised to discover.

To my “lab dad”, Dr. Egor Tchesnokov, for answering all of my dumb questions, yet never making me feel dumb for asking them. You’ve been a joy to work with and I will miss you dearly.

To Emma and Dana for their unwavering encouragement and support. Yes, your efforts made this work possible, but more than that, you make the world a far more pleasant place to live and work.

To Tabitha, whose tireless miracle-working is probably second only to Jesus himself.

To my good cop and bad cop, Dr. David Marchant and Dr. Amit Bhavsar. I’m still not sure which one of you is supposed to be bad cop, and to be honest, I don’t think you know either. The two of you make marshmallows look foul-tempered.

To Dr. Lorne Tyrrell, who always seemed to magically appear whenever I most needed a word of encouragement. If fairy godfathers are a thing, you must be mine.

To Bradley Dubrule, for saving what remained of my sanity by helping me format the page numbers in my thesis.

And finally, to my fellow trainees, who restore a great deal of my faith in humanity. I think the future is in good hands. You are bright, you are hardworking, but most importantly, you are kind. Good trees produce good fruit. I believe you are good trees.

Table of Contents

1	Introduction	1
1.1	Introduction to LASV	1
1.1.1	History	1
1.1.2	Classification and genome organization	2
1.1.3	Epidemiology and climate change	3
1.2	Current antiviral strategies to treat LASV	5
1.2.1	Vaccines	5
1.2.2	Antiviral drugs	6
1.2.3	Other strategies	7
1.3	Viral polymerases as therapeutic targets	8
1.3.1	LASV viral life cycle.....	8
1.3.2	Evolutionary conservation	11
1.3.3	Allosteric inhibitors versus substrate analogues	13
1.4	Objectives.....	18
2	Methods.....	19
2.1	Polymerase expression and purification	19
2.2	High-throughput screening assay	19
2.3	Chemical Preparation.....	20
2.4	Chemical stability assay.....	20
2.5	Gel-based assay.....	21
2.6	Data analysis.....	21
3	Identification of small molecule inhibitors of LASV polymerase	23
3.1	Initial Screening	23
3.2	Reproducibility and hit confirmation	25
3.3	Exploration of chemical classes.....	27
3.4	Selection of compounds for further characterization	32
4	Characterization of small molecule inhibitors of LASV polymerase	34
4.1	Selectivity	34
4.1.1	Human mitochondrial polymerase	34
4.1.2	Crimean-Congo hemorrhagic fever virus.....	35

4.1.3	Severe acute respiratory syndrome virus 2	35
4.2	Chemical stability	36
4.3	Mechanism of Action	38
4.4	Compounds for future investigation	42
5	Discussion and Future Directions	43
	References.....	48
	Appendix.....	55

List of Tables

(All tables are located in the appendix, beginning on pg. 55)

Table 2.1 Polymerase purification buffers.....	85
Table 2.2 <i>in vitro</i> polymerase activity assay conditions.....	86
Table 3.1 Compounds with $\geq 80\%$ inhibition of LASV polymerase at 100 μM	87-90
Table 3.2 Representative compounds from 16 distinct structural groups.....	91-93
Table 3.3 Summary of derivatives tested for each parent compound.....	94
Table 3.4 Derivatives with $\geq 80\%$ inhibition of LASV polymerase at 100 μM	95-98
Table 4.1 IC_{50} determination of select compounds against LASV and other polymerases.....	99-100
Table 4.2 IC_{50} of select compounds against LASV under different reaction conditions.....	101-102

List of Figures

(Figures found on page 55 or subsequent are located in the appendix)

Figure 1.1 Genome organization of LASV.....	3
Figure 1.2 LASV outbreak distribution map.....	5
Figure 1.3 LASV viral life cycle.....	10
Figure 1.4 LASV polymerase structure.....	13
Figure 1.5 Types of inhibitors.....	16
Figure 1.6 HIV reverse transcriptase inhibitors.....	17
Figure 2.1 <i>in vitro</i> polymerase activity assays.....	55
Figure 3.1 Compound selection process schematic.....	24
Figure 3.2 Compound screening with the gel-based assay.....	26
Figure 3.3 Structural comparison of xanthine and caffeine against parent compound ENM-29.....	29
Figure 3.4 Structural comparison of active vs inactive derivatives of parent compound BTB-11392.....	30
Figure 3.5 Screening of additional derivatives.....	31
Figure 4.1 IC ₅₀ of select compounds against LASV and other polymerases.....	56-63
4.1.1 ENM-29.....	56
4.1.2 LS-6.....	57
4.1.3 BTB-11392.....	58
4.1.4 1073.....	59
4.1.5 CBM-11.....	60

4.1.6 6336.....	61
4.1.7 5912.....	62
4.1.8 5588.....	63
Figure 4.2 Chemical stability of select compounds in DMSO and reaction buffer.....	64-76
4.2.1 DMSO.....	64
4.2.2 L-SAR-4.....	65
4.2.3 ENM-29.....	66
4.2.4 L-SAR-5.....	67
4.2.5 LS-4.....	68
4.2.6 LS-5.....	69
4.2.7 LS-6.....	70
4.2.8 BTB-11392.....	71
4.2.9 1073.....	72
4.2.10 CBM-11.....	73
4.2.11 6336.....	74
4.2.12 5912.....	75
4.2.13 5588.....	76
Figure 4.3 Mechanism of action reaction set-up.....	40
Figure 4.4 IC ₅₀ of select compounds against LASV under different reaction conditions.....	77-84
4.4.1 ENM-29.....	77
4.4.2 LS-6.....	78
4.4.3 BTB-11392.....	79

4.4.4 1073.....	80
4.4.5 CBM-11.....	81
4.4.6 6336.....	82
4.4.7 5912.....	83
4.4.8 5588.....	84

List of Abbreviations

CCHFV: Crimean-Congo hemorrhagic fever virus

CDC: Centers for Disease Control and Prevention

COVID-19: coronavirus disease 2019

°C: degrees Celsius

dsDNA: double-stranded DNA

ELISA: enzyme-linked immunosorbent assay

GPC: glycoprotein precursor, glycoprotein complex

HIV: Human immunodeficiency virus

hmtRNAP: human mitochondrial polymerase

IC₅₀: half-maximal inhibitory concentration

LASV: Lassa fever virus

μM: micromolar

mM: millimolar

MOPV: Mopeia virus

nm: nanometers

NP: nucleoprotein

NTPs: nucleotides

RdRp: RNA-dependent RNA polymerase

RME: receptor-mediated endocytosis

RT: reverse transcriptase

RT-PCR: reverse transcriptase polymerase chain reaction

SAR: structure-activity relationship

SARS-CoV-2, SARS-2: severe acute respiratory syndrome virus 2

VSV: vesicular stomatitis virus

WHO: World Health Organization

1 Introduction

1.1 Introduction to LASV

1.1.1 History

Lassa fever virus (LASV) was first identified in 1969 in Ms. Laura Wine, a mission hospital nurse in the rural town of Lassa, Nigeria¹¹⁻¹³. Ms. Wine died from infection within 6 days of symptom onset¹¹. Ms. Lily “Penny” Pinneo, one of two nurses that tended to Ms. Wine, also became infected, and was the first identified survivor of LASV^{11,12}. The other nurse, Ms. Charlotte Shaw, died 11 days after symptom onset¹¹. LASV was first isolated by Dr. Jordi Casals-Ariet at Yale University in 1969 from the sera of Ms. Wine, Ms. Shaw, Ms. Pinneo, and himself, as he became infected during the course of investigation¹¹. Fortunately, he recovered after treatment with convalescent plasma from Ms. Pinneo^{11,12}. The virus isolated from Ms. Pinneo’s sample became the prototype strain^{11,12}. Notably, a small 2013 study of IgG antibodies against LASV in previously infected individuals, including Ms. Pinneo herself, suggested that the first case of LASV may have actually been in 1952, 17 years before the first reported case^{11,14}.

Between 1970-1976, several small LASV outbreaks occurred in Nigeria and Sierra Leone¹¹. Some were nosocomial outbreaks due to improper equipment sterilization and insufficient safety measures, while others were acquired from the surrounding community¹¹. The 1972 outbreak led to the identification of the rodent reservoir^{11,12}. In 1976, the Centers for Disease Control and Prevention (CDC) set up a long-term research project in Kenema, Sierra Leone, which enabled characterization of the virus¹¹. While this was certainly a step in the right direction, the Blood Diamond conflict caused research to grind to a halt from 1991 to 2002^{11,12}. The Ebola virus outbreak of 2013-2016 was also detrimental to LASV research efforts, as resources were diverted¹². A number of different groups have since renewed investigation and surveillance efforts in West Africa, including the Institute of Lassa Fever Research and Control, Kenema Government Hospital (KGH), the National Public Health Institute of Liberia (NPHIL), the Irrua Specialist Teaching Hospital (ISTH), and the African Center of Excellence for the Genetics of

Infectious Diseases (ACEGID)^{11,12}. In 2017, the World Health Organization (WHO) identified LASV as a priority pathogen, noted for its pandemic potential⁸. Shortly thereafter, a LASV outbreak in 2018 reported 1,893 cases^{15,16}. Of the 423 laboratory-confirmed cases, 106 deaths were reported, for a case-fatality rate of 25%¹⁶. 2023 saw the largest LASV outbreak to date, with 4702 suspected cases in just 15 weeks^{15,17}. Among the 877 confirmed cases, 152 deaths were reported, for a case-fatality rate of 17%¹⁷. Trends in the last few decades suggest that LASV outbreaks are not only becoming larger, but also more frequent, highlighting the need for development of therapeutics to treat LASV^{12,13,15}.

1.1.2 Classification and genome organization

LASV is a segmented, single-stranded RNA virus belonging to the *Arenaviridae* family (see [Fig. 1.1](#), taken from [18])^{12,19,20}. Its genome is ambisense, meaning that it encodes proteins in both the positive and negative direction^{12,19,20}. The relative simplicity of the LASV genome reduces the number of possible therapeutic targets available. Its two gene segments encode four proteins: the large 7.3 kb segment (L) encodes the RNA-dependent RNA polymerase (RdRp), or L protein, as well as the matrix, or zinc-binding protein (Z)^{12,19,20}. The polymerase is required for transcription and genome replication, while the zinc-binding protein plays a role in virion assembly¹². The small 3.4 kb segment (S) encodes the nucleoprotein (NP), and the glycoprotein precursor (GPC), which is post-translationally cleaved into glycoprotein 1 (GPC1) and glycoprotein 2 (GPC2)^{12,19,20}. Nucleoproteins are required for genome management: regulation of transcription vs. replication, as well as packaging once it's time for virion assembly^{12,21}. Glycoproteins 1 and 2 are involved in viral attachment and entry into the host cell¹². LASV virions are pleomorphic, enveloped, and range in size from 50-300 nm in diameter^{19,21}. Virions contain host ribosomes, which resemble grains of sand, hence the name *Arenaviridae* from the Latin "arenos", meaning "sandy"¹². LASV is an Old-World arenavirus²¹.

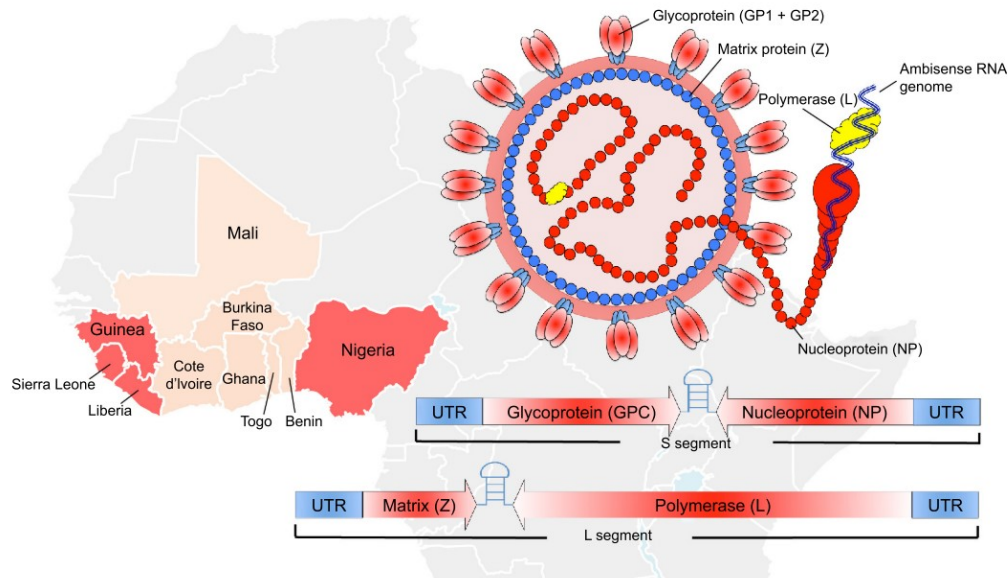


Figure 1.1 Genome organization of LASV. Taken from [18]. LASV contains two gene segments encoding four proteins: the polymerase (L protein), the matrix (Z) protein, the nucleoprotein (NP), and the glycoprotein precursor (GPC). The two segments are ambisense, meaning they are read in both directions. The orientation of these segments is depicted above. A schematic of the virion is also shown. UTR: untranslated region

1.1.3 Epidemiology and climate change

LASV is a hemorrhagic fever virus that displays a wide spectrum of symptoms. 80% of cases are asymptomatic, while the remaining 20% are severe cases that can lead to multi-organ failure and death²¹⁻²⁴. Mild symptoms include fever, headache, muscle aches and pains, and fatigue²¹⁻²⁴. As the infection progresses, symptoms may include sore throat, chest pain, abdominal pain, nausea, vomiting, diarrhea, and cough²¹⁻²⁴. In severe cases, symptoms can include swelling, fluid accumulation in the lungs, bleeding from various orifices or the gastrointestinal tract, seizures, shock, and neurological effects²¹⁻²⁴. 25% of cases also result in deafness, which may be permanent or temporary²¹⁻²⁴. Symptoms appear within 1-3 weeks post-infection, and infection persists for 1-4 weeks²¹⁻²⁴. Typically, severe cases will result in death within 14 days²¹⁻²⁴. Pregnant women are the most at risk, with 80% of women experiencing spontaneous abortion upon LASV infection, particularly in the third trimester²¹⁻²⁴.

Diagnosis of LASV is difficult, as it resembles several other fever viruses in its symptomology²²⁻²⁴. Diagnosis is further complicated by a lack of resources and appropriate biosafety level 4 facilities in affected areas¹⁹. While the gold standard for diagnosis is virus isolation by cell culture, LASV is more commonly diagnosed using enzyme-linked immunosorbent assay (ELISA) to detect anti-LASV IgM or IgG antibodies or LASV antigens, or to use reverse transcriptase polymerase chain reaction (RT-PCR) to detect viral RNA^{21,23}. Recently, progress has been made towards a field-ready rapid test kit²⁵, but surveillance efforts remain a top priority. Early detection is critical in both treatment of LASV, as well as limiting its spread in the event of an outbreak.

LASV is a zoonotic virus endemic in Nigeria, Sierra Leone, Liberia, Guinea, Ghana, Mali, and Senegal (see [Fig. 1.2](#), taken from [22])²¹. Phylogenetic analysis suggests that LASV originated in Nigeria over a thousand years ago, and only migrated into neighbouring West African countries in the last few hundred years²⁰. The reservoir for LASV is the multimammate rat, *Mastomys natalensis*, which is found throughout West Africa²¹⁻²⁴. LASV has also been detected in other rodent species, including *Hylomyscus pamfi* and *Mastomys erythroleucus*²¹. This, coupled with climate change, is serious cause for concern, as the LASV endemic area continues to expand^{13,20}. Reports of imported cases of LASV in North America, Europe, and Asia are few, but globalization can rapidly facilitate the spread of a virus, as seen with the COVID-19 pandemic^{10,12,21}. Transmission is more commonly reservoir to human than human to human, although human to human transmission is common in a nosocomial context^{20,21}. Humans can acquire LASV from rats via direct contact with infected rodents or bodily fluids, inhalation of excrement/urine, indirect contact via contaminated surfaces or food, and consumption of infected rodents^{21,23,24}. Human to human transmission requires direct contact with bodily fluids from an infected individual, including blood, saliva, excrement/urine, and semen^{21,23,24}. LASV is estimated to infect 300,000 to 500,000 people per year, and cause 5,000 to 10,000 deaths²¹⁻²⁴. These figures are likely an underrepresentation, as LASV is

frequently underreported due to lack of diagnosis and lack of resources in rural areas where LASV is most prevalent. The official case-fatality rate is only 1-2%, but climbs to 15% in hospital outbreaks^{21,22}.

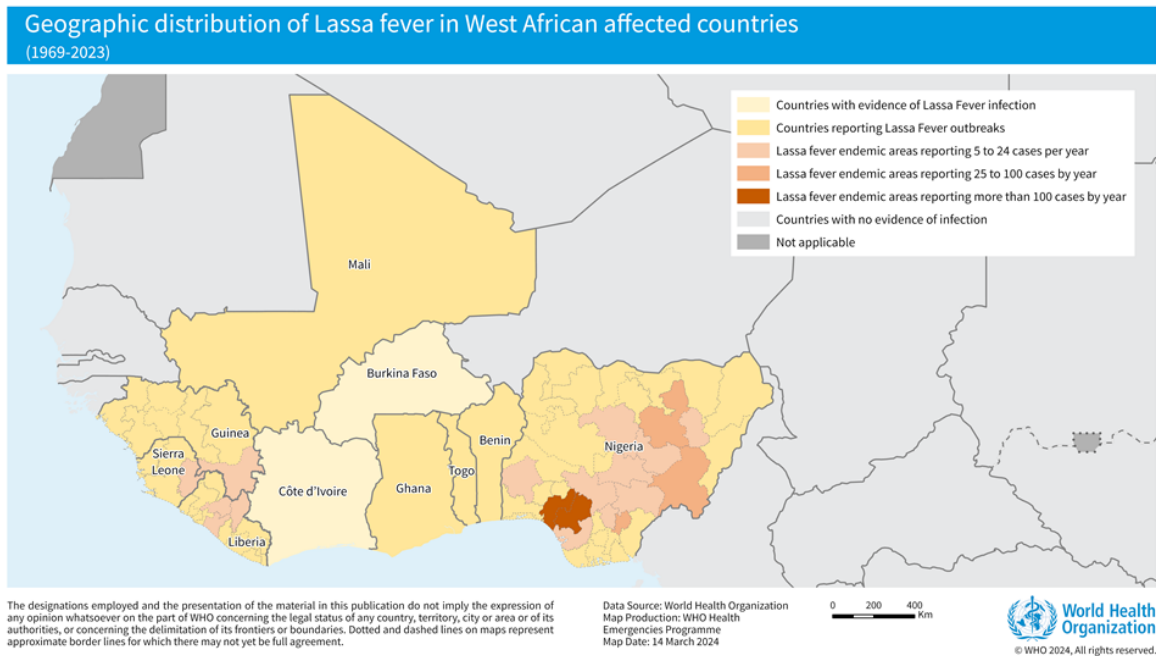


Figure 1.2 LASV outbreak distribution map. Taken from [22]. While LASV is believed to have originated in Nigeria over 1,000 years ago, it is now prevalent in a number of West African countries. There are seven different strains, or clades of LASV: clades I-III and VI are found in Nigeria, clade IV is found in Sierra Leone, Guinea, and Liberia, clade V is found in Mali and Côte d'Ivoire, and lineage VII is found in Benin, Ghana, and Togo. The genetic diversity of LASV, as well as the effects of climate change on the rodent reservoir are both causes for concern.

1.2 Current antiviral strategies to treat LASV

1.2.1 Vaccines

There are currently no approved vaccines for LASV, although several candidates are in clinical trials^{9,19,26}. Three of these candidates rely on recombinant viruses: the first, a live-attenuated measles virus, has been engineered to express either LASV glycoprotein precursor (GPC) and nucleoprotein (NP) or glycoprotein precursor (GPC) and Z protein^{9,26}. Another, a recombinant vesicular stomatitis virus (VSV), has been engineered

to express LASV glycoprotein precursor (GPC), rather than its own glycoprotein^{9,26}. Notably, this VSV vector strategy was used to create the Ebola Zaire vaccine, ERVEBO^{®9}. The third, a reassortment clone dubbed ML29, was generated by substituting the LASV L gene into another *Arenavirus*, the non-pathogenic Mopeia virus (MOPV)²⁶. A DNA vaccine strategy is also underway. IN-4500 is a DNA vaccine that encodes the LASV glycoprotein precursor (GPC)^{9,26}. Other vaccine candidates are also in development, but are still restricted to testing in murine models^{21,26}.

A major challenge with vaccine development is that LASV is highly genetically diverse, with seven distinct lineages, or clades, which are distributed geographically.²¹ Lineages I–III are found in Nigeria, as well as lineage VI; lineage IV is found in Sierra Leone, Guinea, and Liberia^{12,21}. Lineage V is present in both Mali and Côte d'Ivoire, and lineage VII is present in Benin, Ghana, and Togo^{12,21}. Each of these lineages has a number of distinct strains, with up to 32% nucleotide variation in the L segment alone²⁰. Most vaccine development has been done with the Josiah strain from Sierra Leone, which raises concerns about the likelihood of creating a universal LASV vaccine²⁶.

1.2.2 Antiviral drugs

There are currently no approved antiviral drugs to treat LASV^{21-23,26}. Historically, the nucleoside analogue ribavirin has been used, but data regarding its safety and efficacy is limited^{10,21,24,27}. Ribavirin is also known to have serious side-effects, including hemolytic anemia and teratogenic effects in animal models¹⁹. Furthermore, ribavirin only seems to be effective if administered within 6 days post-infection^{10,21,27}. Favipiravir, a nucleotide analogue, has shown promising results in guinea pigs and non-human primates, with up to 100% survival even when treatment is delayed until 7 days post-infection^{10,27}. In all comparative animal trials, favipiravir treatment has shown greater benefit than ribavirin treatment^{10,27}. Favipiravir was successfully used to treat two cases of LASV in humans, although no clinical trials have been done to date¹⁰. Favipiravir is currently licensed for use in Japan to treat influenza^{10,27}.

A derivative of the reverse transcriptase inhibitor d4T has also been evaluated for efficacy in treating LASV. This nucleoside analogue, stampidine, increased survival rates from 28% to 75% in infected mice, but has yet to be tested in any other models¹⁰. A viral entry inhibitor, ST-193, and its derivative LHF-535 both improved survival rates and showed IC₅₀ values in the nanomolar range when tested against LASV, but have only been tested in guinea pigs^{10,27}. As such, there is a critical need for investigation into drugs to treat LASV.

1.2.3 Other strategies

Most treatment of LASV consists of either supportive care or rodent control strategies^{10,21-24}. Support care includes bedrest, fluids, electrolytes, oxygen supplementation, and dialysis as needed to treat symptoms^{21,24}. To date, the most effective weapon against LASV infection is education²¹⁻²⁴. Equipment sterilization and proper use of protective equipment by healthcare workers can limit spread in a nosocomial setting²¹⁻²⁴. Good “community hygiene” practices, including adequate sanitation and garbage disposal, placing rodent traps and/or keeping cats, and storage of food and grain in rodent-proof containers all help to reduce human contact with the reservoir²²⁻²⁴. As multimammate rats are endemic, they cannot be completely eliminated. Thus, most strategies targeting LASV are preventative, rather than therapeutic.

Convalescent plasma from Ms. Pinneo was successfully used to treat Dr. Jordi Casals-Ariet when he acquired a laboratory infection of LASV^{11,12}. Unfortunately, animal studies have shown that this strategy is only effective if: 1) treatment begins within 6 days post-infection, 2) LASV-specific antibody concentration is high enough, and 3) the donor and recipient have been infected with the same or a very similar strain of LASV^{10,27}. A single follow-up study in humans revealed no benefit, although convalescent plasma continues to be used in a patient setting^{10,27}. In a similar vein, monoclonal antibody cocktails are currently being investigated for treatment of LASV. Of 113 LASV-specific antibodies

identified in survivors of LASV, 16 showed potent inhibition of LASV *in vitro*¹⁰. Three were active against multiple clades¹⁰. When tested in guinea pigs and non-human primates, these antibodies showed variable protection against LASV, anywhere from 20-100%^{10,27}. While no human trials have been conducted, monoclonal antibody treatment offers a safer and more practical option than convalescent plasma, although production cost is still a significant barrier to low-income areas where LASV is prevalent¹⁰. Due to the nature of the political and economic circumstances in areas where LASV is endemic, any therapeutics must be inexpensive and easy to produce to ensure accessibility for the vulnerable populations that need it most.

1.3 Viral polymerases as therapeutic targets

1.3.1 LASV viral life cycle

While not truly living organisms, viruses do still have a pseudo “life cycle”, which may be exploited for therapeutic purposes. [Figure 1.3](#), taken from [12], shows a schematic representation of the LASV viral life cycle, which can be broken down into the following steps:

1) Virion binding to host cell receptor: Like other Old-World *Arenaviruses*, LASV relies on receptor-mediated endocytosis (RME) to enter host cells^{21,28}. The main receptor for LASV entry is α -dystroglycan (α -DG), although a few other receptors have been implicated as well^{12,21,28}. α -dystroglycan is a transmembrane protein that binds extracellular matrix proteins^{21,28}. Importantly, α -dystroglycan requires a special *O*-mannosylation for both biological function and LASV binding²⁸.

2) Virion entry into host cell via endocytosis: The LASV glycoprotein complex (GPC) binds to the matriglycan on α -dystroglycan (α -DG), stimulating cellular uptake²⁸. Acidification of the endosome causes a conformational change in the glycoprotein complex (GPC), resulting in a loss of affinity for α -dystroglycan (α -DG) and an increase in affinity for an endosomal membrane receptor called lysosome-associated membrane protein 1 (LAMP1)²⁸. This is known as the “receptor switch”^{12,28}. Binding of LASV glycoprotein

complex (GPC) to LAMP-1 facilitates viral egress from the endosome, or “uncoating”^{12,28}.

3) Genome replication and template synthesis by the viral polymerase: Transcription occurs in the cytoplasm, and requires the virally-encoded polymerase (L protein), as well as several host factors, including DEAD-Box RNA Helicase 3 (DDX3)^{12,21,28}. As LASV is ambisense, it must synthesize complementary/anti-genomic RNA in order to then replicate the viral genome and produce all four encoded proteins.

4) Translation and protein synthesis: Translation also occurs in the cytoplasm. Viral polymerase (L protein) and nucleoprotein (NP) are synthesized during early transcription; matrix (Z) protein and glycoprotein precursor (GPC) are synthesized during late transcription¹². Translation and processing of glycoprotein precursor (GPC) occurs in the Golgi apparatus¹².

5) Virion assembly at the cell membrane: Nucleoprotein (NP) binds to both viral RNA and matrix (Z) protein²⁹. As intracellular levels of matrix (Z) protein increase, both nucleoprotein (NP) and the viral genome are recruited to the cellular membrane²⁹. Z protein can also bind to the viral polymerase (L protein), ensuring proper packaging of all viral components into the virion²⁸. At this point, processed glycoprotein 1 (GPC1) and glycoprotein 2 (GPC2) arrive at the cellular membrane as well, en route from the Golgi apparatus¹².

6) Virion budding and release: Association of all viral components at the cellular membrane facilitates virion budding from the host cell^{12,28,29}.

Any one of these steps could be targeted therapeutically, and have been exploited for other viruses in the past. However, this project focuses on the viral RdRp, as it is absolutely essential for the viral life cycle of most RNA viruses, and therefore a logical target for drug design^{5,6}.

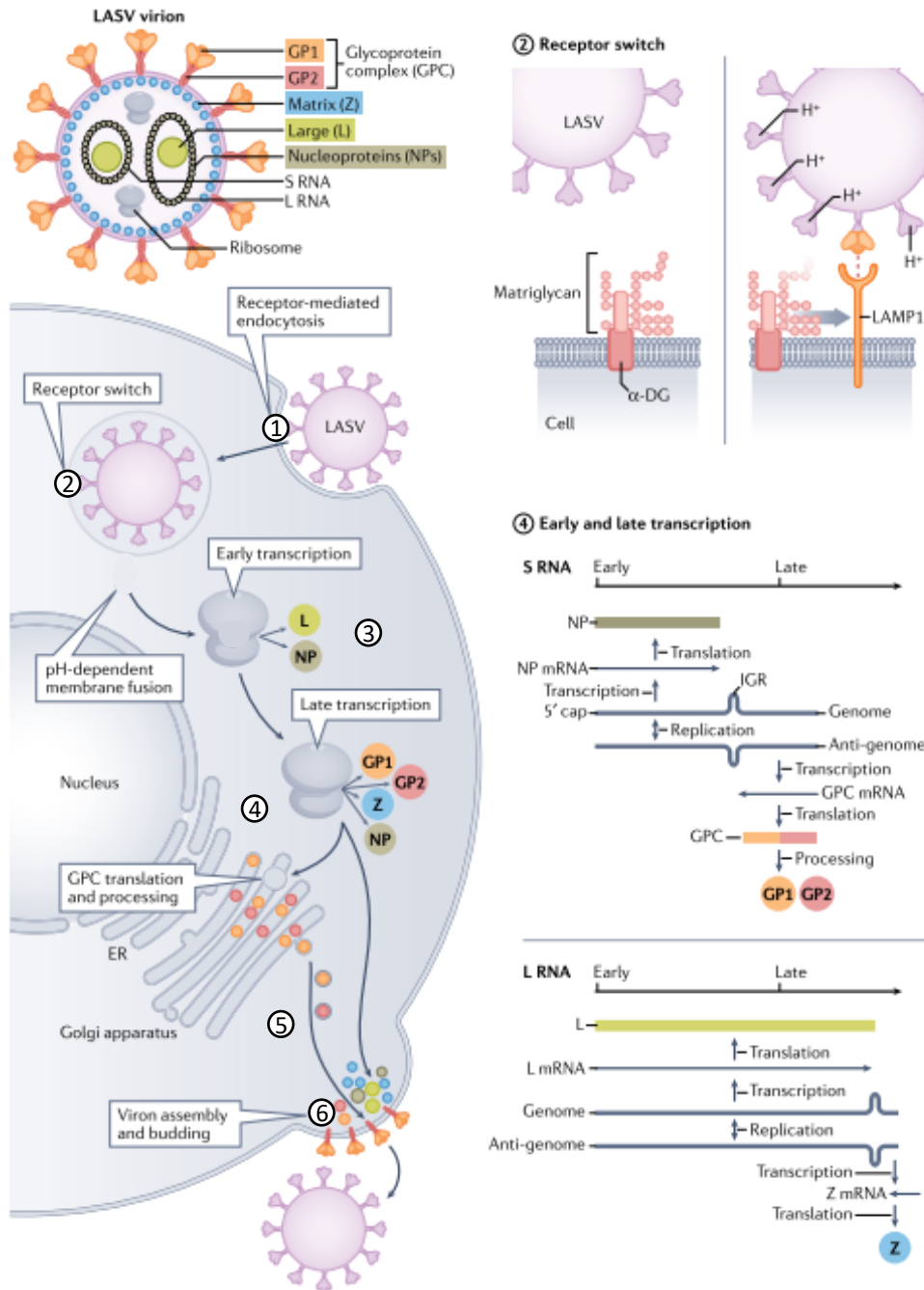


Figure 1.3 LASV viral life cycle. Taken from [12]; please note numbering scheme has been changed to reflect steps outlined in introduction. Briefly: 1) Virion binding to host cell receptor, 2) Virion entry into host cell via endocytosis, 3) Genome replication and template synthesis by the viral polymerase, 4) Translation and protein synthesis, 5) Virion assembly at the cell membrane, and 6) Virion budding and release.

1.3.2 Evolutionary conservation

Viral polymerases are also an excellent therapeutic target because they're highly evolutionarily conserved^{6,31-33}. Viral evolutionary analysis relies on broadly conserved genes, referred to as "viral hallmark genes"³¹. RdRps are one of only six viral hallmark genes³¹. They also contain an RNA recognition motif (RRM) which is found in all viral polymerases³¹. RdRps are also the only gene that is universally conserved among all RNA viruses (with the exception of reverse-transcribing RNA viruses, which utilize reverse transcriptase instead)^{31,33}. By contrast, double stranded DNA (dsDNA) viruses do not have any universally conserved genes³¹. This high level of conservation reflects the evolutionary constraints on genes that are critical for viral replication³¹. While polymerases *can* mutate, there is a limit to how far polymerases can mutate before they lose functionality. While drug-resistance mutations are not uncommon, these mutations often result in decreased viral fitness^{4,34}.

Structurally, all polymerases share an overall architecture analogous to a human right hand: the core catalytic domain is located in the palm, the fingers position the template and incoming NTPs, and the thumb interacts with the product nucleic acid^{6,32,33}. Evolutionarily, the palm domain is the oldest, and contains two invariant aspartate residues that coordinate the metal cofactors required for catalysis^{6,32}. As every good biochemist knows, structure equals function, so while there can be considerable variation in the sequence of different polymerases, the overall structure remains consistent^{6,32}. RdRps contain seven highly conserved structural motifs, A through G^{6,32,33}. Motifs A through E are located in the palm domain, G and F are in the fingers, and some viruses have an additional motif H in the thumb^{6,32,33}. Motifs A and C are the most conserved, as they contain the invariant aspartate residues^{32,33}. LASV polymerase has three distinct domains: the RdRp, a cap-binding domain, and a nuclease domain^{30,61}. The RdRp forms the core of the polymerase, and is required for RNA synthesis³⁰. The cap-binding domain and the endonuclease domain work in conjunction to 'steal' the 5' cap of host mRNAs, which are then used as primers for transcription³⁰. The cap-binding

domain, located in the C-terminal domain, binds host 5' mRNA caps^{30,61}. The endonuclease domain, located at the N-terminus, then cleaves the bound host mRNA, releasing the 5' cap^{30,61}. Influenza polymerase contains the same three domains, but influenza polymerase is a heterotrimeric complex, while LASV polymerase is a single chain^{30,61}. [Figure 1.4](#) (taken from [61]) shows the overall architecture of LASV polymerase. As the structure of LASV polymerase has not yet been fully elucidated, homology modelling is often based on other polymerases from more well-characterized viruses, like influenza, or on genetically similar viral polymerases, like Machupo (MACV) virus⁶¹. A comprehensive model of LASV polymerase is absolutely critical for drug design, not only for screening purposes, but for mechanistic studies as well, so this remains an important area for investigation.

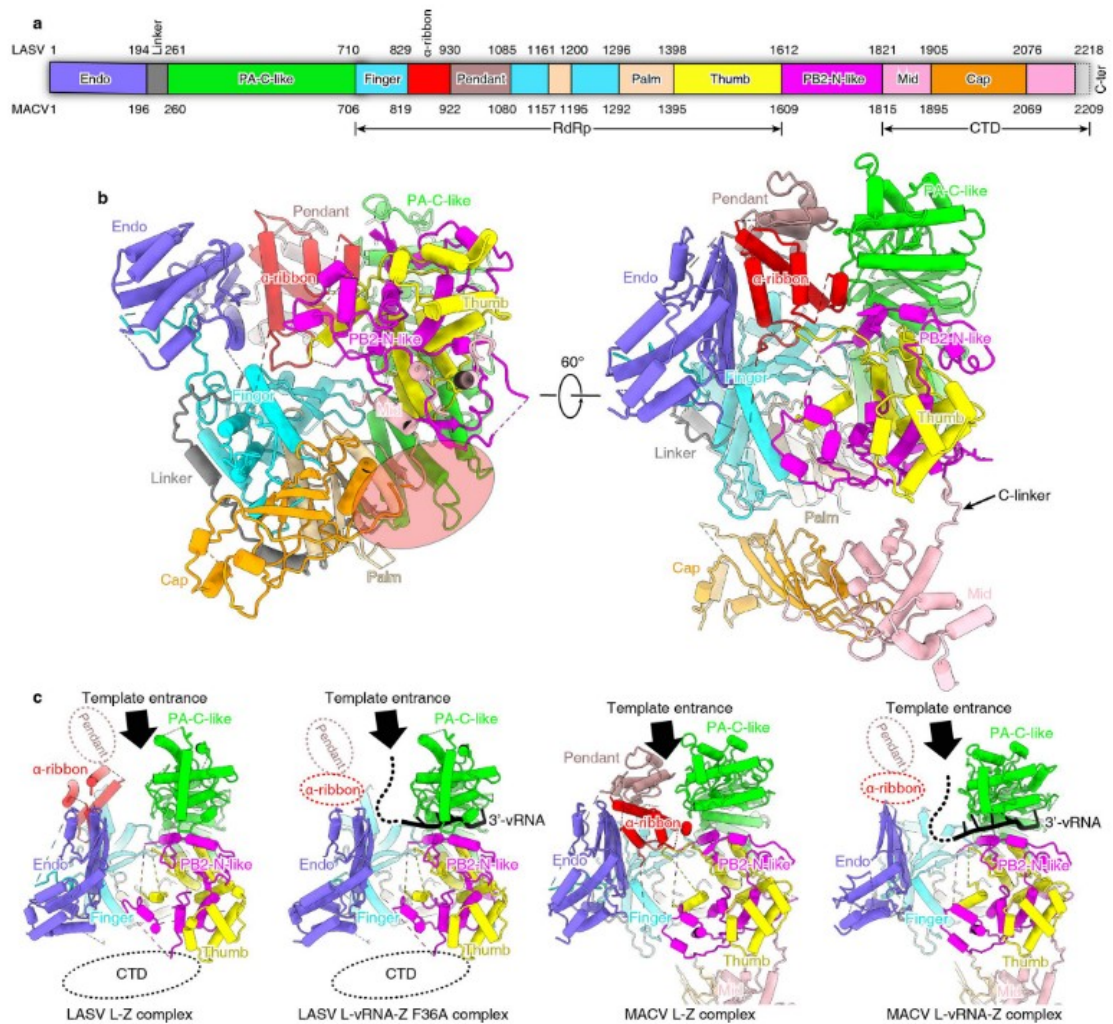


Figure 1.4 LASV polymerase structure. Taken from [61]. LASV polymerase structure is contrasted with a related virus, Machupo (MACV), polymerase. a) Schematic representation of the overall architecture of LASV and Machupo (MACV) polymerases, with amino acid residues denoted. b) Ribbon diagram of Machupo (MACV) polymerase. Note that ribbon diagram is colour-coded to match a). c) Comparison of LASV and Machupo (MACV) polymerases with or without RNA. Unresolved domains are indicated by dashed ovals.

1.3.3 Allosteric inhibitors versus substrate analogues

There are two main types of enzyme inhibitors: allosteric inhibitors and competitive inhibitors³⁵. [Figure 1.5](#) shows the mechanism of action of these two types of inhibitors. Covalent inhibitors are an additional type, but will not be discussed further here, as they

are not the focus of this project. Competitive inhibitors are so named because they compete with the enzyme's natural substrate(s)³⁵. In the context of polymerases, these would be nucleoside/nucleotide analogues, which tend to be broad-spectrum inhibitors. They mimic the natural substrate, binding in the same active site as the natural counterpart³⁵. For this reason, they are also called substrate analogues³⁵. Competitive inhibitors may or may not undergo catalysis³⁵. In contrast, allosteric inhibitors bind in a site other than the active site and do not compete with the natural substrate(s)³⁵. Allosteric inhibitors may bind to just the enzyme-substrate complex (uncompetitive inhibition), or to either the enzyme or enzyme-substrate complex (non-competitive inhibition)³⁵. Allosteric inhibitors most often inactivate enzymes by causing a conformational change which either prevents substrate binding, or "locking" the enzyme in one position so catalysis cannot occur³⁵. As non- nucleoside/nucleotide inhibitors are usually allosteric, they are typically specific to a subset of viruses, and are not generally broad-spectrum. However, in some cases, non-nucleoside/nucleotide inhibitors may be competitive.

For polymerases, both allosteric and competitive inhibitors are effective strategies, although a combinatorial approach is usually best^{7,35,36}. Human immunodeficiency virus (HIV) reverse transcriptase (RT) is an example of a viral polymerase that has been successfully targeted with this combination approach^{7,35,36}. Nucleoside/nucleotide analogues used to treat HIV reverse transcriptase (RT) include: azidothymidine (AZT, deoxythymidine analogue), stavudine (d4T, deoxythymidine analogue), lamivudine (3TC, deoxycytidine analogue), abacavir (ABC, deoxyguanosine analogue), and tenofovir (TFV, deoxyadenosine analogue), among others^{7,36-38}. The structures of some of these inhibitors, as well as the natural counterparts, are shown in [Figure 1.6](#). All of these analogues lack the 3' hydroxyl group required for elongation of the primer strand, and therefore act as immediate chain terminators³⁶. Allosteric inhibitors for HIV reverse transcriptase (RT) include: nevirapine, doravirine, and efavirenz, among others^{7,37-39}. Despite very different structures, all three of these compounds bind in the same

allosteric pocket located 10 Å from the reverse transcriptase (RT) active site^{7,39}. The structures of these compounds are also shown in [Figure 1.6](#).

There are a few problems with nucleoside analogues, however. First, they must be triphosphorylated by host machinery before they can be used^{7,36}. This is a very slow and rate-limiting step³⁶. Second, because they resemble natural nucleotides, which are also the natural substrate of host polymerases, there is always the risk of cross-reactivity and off-target effects^{7,35,36}. Third, resistance mutations are common^{35,36}. In contrast, allosteric inhibitors generally do not require modification by the host cell, and are usually quite selective, as they target a unique pocket other than the active site⁷. This also reduces the likelihood of cytotoxic effects⁷. While resistance mutations can still arise against allosteric inhibitors, using a combination of allosteric and competitive inhibitors can help reduce the incidence of resistance^{7,35,36}. For this reason, it is absolutely crucial to continue exploration into various types of inhibitors for polymerases of concern.

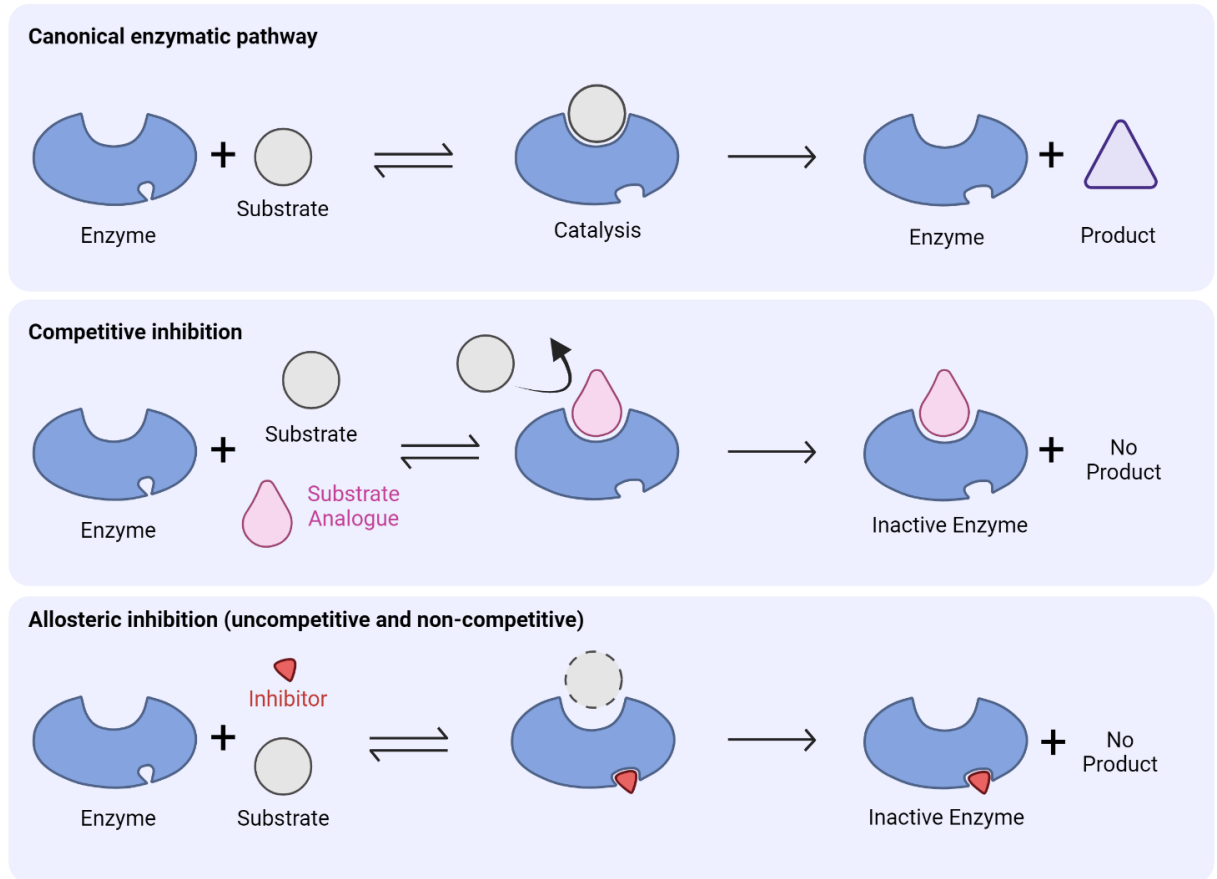


Figure 1.5 Types of inhibitors. Top panel shows enzyme in absence of inhibitor. Middle panel shows competitive inhibition, where the natural substrate and a substrate analogue compete for binding to the active site. Bottom panel shows allosteric inhibition, where inhibitor inactivates enzyme by binding in a site other than the active site. Substrate may or may not be bound when allosteric inhibitor binds, depending on type of allosteric inhibition. Created with BioRender.

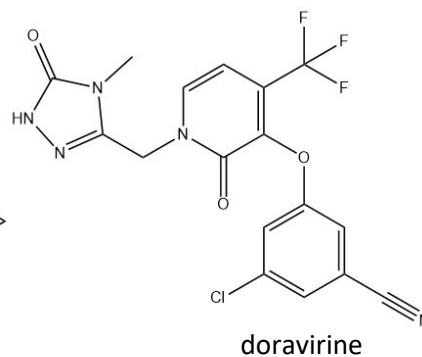
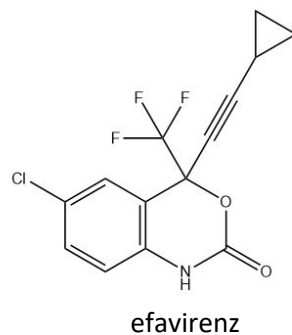
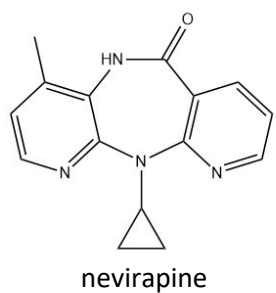
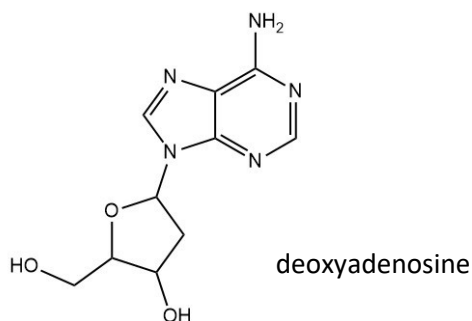
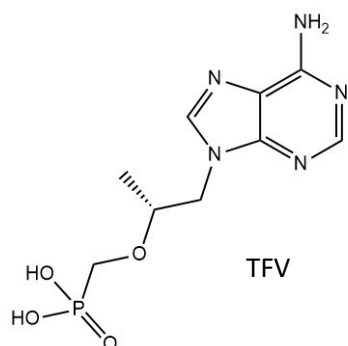
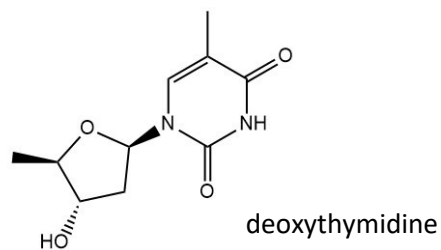
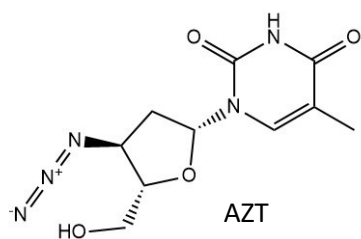


Figure 1.6 HIV reverse transcriptase (RT) inhibitors. Above dashed line: substrate analogues and their natural counterparts. Both zidovudine (AZT) and tenofovir (TFV) lack the 3' hydroxyl on the sugar moiety, and therefore act as immediate chain terminators. Below dashed line: allosteric inhibitors. Despite vastly different structures, all three of these inhibitors bind in the same allosteric pocket 10 Å from the active site.

1.4 Objectives

In the interest of pandemic preparedness, the goals of this project are to: 1) identify small molecule inhibitors of LASV polymerase, and 2) assess various properties of those inhibitors to identify which compounds warrant further investigation as potential candidates for drug development into new antiviral drugs to treat LASV and related viruses. To accomplish this, we used a systematic approach to narrow down our pool of candidate compounds: First, we generated and purified recombinant His-tagged LASV polymerase using a baculovirus expression system and nickel affinity chromatography. We then used that purified recombinant LASV polymerase in a high-throughput polymerase activity assay to rapidly assess 100,000 compounds for inhibition of LASV polymerase. Compounds with inhibition below a certain threshold were eliminated. Next, we used an orthogonal polymerase activity assay to confirm the inhibitory effect of the compounds we identified in the high-throughput assay. Again, compounds with inhibition below a certain threshold were eliminated. From there, we used the same orthogonal activity assay to assess the potency and selectivity of compounds of interest. We also determined their chemical stability. Compounds with the greatest potency, selectivity, and stability were selected for structure-activity relationship (SAR) analyses. Derivatives were assessed in the same fashion as the parent compounds. Preliminary investigation into the mechanism of action was only conducted for compounds with sufficient potency, selectivity, and stability. This approach ensured that we focused our efforts on only the most promising candidates for future antiviral drug development.

2 Methods

2.1 Polymerase expression and purification

Both viral and human polymerases were generated and purified as described previously⁴⁰⁻⁴⁴. Briefly, recombinant polyhistidine-tagged polymerases were generated using the pFastBac-1 (Invitrogen) system to express various replication complexes in insect cells (Sf9, Invitrogen). Please note that different buffer conditions were used for SARS-2, while the same conditions were used for LASV, CCHFV, and hmtRNAP, as listed in [Table 2.1](#). SARS-2 is purified from the cytosolic fraction, while the other three enzymes are purified from whole cell lysates. All lysis buffers contained one Roche Ultra Complete EDTA Free Protease Inhibitor tablet. Pellets were resuspended in lysis buffer and lysed with a Dounce homogenizer. For SARS-2 only, the lysed solution was spun at 1,000 x g for 25 minutes at 4°C to pellet nuclei, then the supernatant was transferred to a new tube and solid NaCl was added to a final concentration of 1M. At this point, the purification schemes for all four polymerases are the same. Lysed solutions were centrifuged at 30,000 x g for 30 minutes. Supernatant was incubated with 500 µL (1 column volume) of Thermofisher His-Pur™ NiNTA resin for one hour at 4°C. Non-specific proteins were removed with 10 column volumes of wash buffer, then 6 column volumes of 50 mM imidazole elution buffer to improve stringency. His-tagged constructs were eluted off Ni-NTA columns with 5 column volumes of elution buffer with either 100 or 200 mM imidazole. Eluted fractions were concentrated by centrifugation at 4,000 x g as needed at 4°C, and either flash-frozen and stored at -80°C until use, or glycerol was added to a final concentration of 40% and purified enzyme was stored at -20°C. Purity and activity of elution fractions were assessed using SDS-PAGE and the gel-based assay, respectively.

2.2 High-throughput screening assay

Initial screening was performed by Dr. Tracey Campbell at McMaster using the method previously described⁴⁵. A schematic is shown in [Fig. 2.1](#). Briefly, compounds of interest were pipetted into 384-well black flat bottom plates at a final concentration of 100 µM. A reaction mixture containing ~0.1-0.2 µM polymerase, 25 mM Tris-HCl (pH 8), 100x diluted PicoGreen

(Invitrogen, P7581), 10 μ M NTPs (ATP, GTP, CTP equimolar), 0.3 μ M RNA template (3'-UGCGCUUGUU(13xU)-5'), and 10 μ M RNA primer (5'-pACGC-3') was added to each well. The reaction was started with 5 mM MgCl₂ and PicoGreen fluorescence was measured in 30-60 second intervals over a period of 45 minutes, or until plateau was reached. Plate was read with an excitation wavelength of 480 nm and an emission wavelength of 530 nm. Screening assays were performed in duplicate or triplicate. Fluorescence was plotted as a function of time, and the resulting slopes were normalized to treatment with vehicle only (10% DMSO).

2.3 Chemical Preparation

Compounds of interest were purchased from a number of companies, including Enamine, Chembridge, Maybridge, Akos, Sigma-Aldrich, and MolPort. A number of compounds were also provided by collaborators at the University of California, San Francisco. Compounds were dissolved in 100% DMSO to a final concentration of 10 mM. Resuspended compounds were then centrifuged at 13,000 x g for 5 minutes to remove any insoluble particulates, and the top fraction was used to generate 1 mM stocks of each chemical. Compounds with poor solubility (ie. visible particulates) were noted.

2.4 Chemical stability assay

10 mM stocks of compounds (100% DMSO) were diluted to 1 mM with either reaction buffer (25 mM Tris HCl, 5 mM MgCl₂, 50 mM EDTA; 10% DMSO final concentration) or 100% DMSO (100% DMSO final concentration). Diluted compounds were then centrifuged at 13,000 x g for 5 minutes to pellet any insoluble particulates prior to measuring absorbance with a NanoDrop. UV-Vis spectra were collected at time = 0, 0.5, 1, 2, and 18 hours, and the spectra were plotted using Prism. % degradation over time was calculated by determining absorbance at a particular time as a fraction of absorbance at time = 0. For ease of measurement, the wavelength at the highest point of the largest/most distinct peak was used for calculating % degradation.

2.5 Gel-based assay

Polymerase activity and products were monitored using the previously described radiolabelled gel-based assay^{40,42-44}. A schematic is shown in [Fig. 2.1](#). Briefly, final reaction mixtures contain compound of interest (0-100 μM), polymerase (~ 0.1 μM , up to 0.2 μM), 25 mM Tris HCl (pH 8), 50 mM EDTA, RNA template (2 μM), RNA primer (200 μM), and [α -³²P]GTP (0.1 μM). NTPs (ACU) and MgCl_2 concentration varies depending on enzyme, as indicated in [Table 2.2](#). The order of addition of these components varies, as indicated. Some polymerases tolerate the inclusion of detergent (TritonX-100) and/or NaCl in the reaction mixture as well, also indicated in [Table 2.2](#). Pre-incubation was carried out at room temperature for 10 minutes, then reaction tubes were transferred to 30°C (except hmtRNAP, which is optimized at room temperature) and incubated an additional 10 minutes. Reactions were started with the addition of substrates or co-factor as indicated, and reactions were allowed to proceed for 30-45 minutes at 30°C (or room temperature for hmtRNAP). Reactions were stopped with a mixture of formamide and EDTA (50 mM), then incubated at 95°C for 7 minutes. RNA products were visualized by electrophoresis on denaturing urea-PAGE (20% acrylamide) and phosphor imaging with Typhoon TRIP, variable mode imager (GE Healthcare Bio-Science, Uppsala, Sweden). Quantification was performed with ImageQuant software (GE Healthcare Bio-Science, Uppsala, Sweden) and QuantityOne software (Biorad). Data analysis was performed with GraphPad Prism (Graphpad, San Diego, California). Templates and primers were 5'-phosphorylated and purchased from Dharmacon (Lafayette, CO). NTPs were purchased from GE Healthcare; [α -³²P]GTP was purchased from PerkinElmer Life Sciences.

2.6 Data analysis

Quantification was performed with ImageQuant software (GE Healthcare Bio-Science, Uppsala, Sweden) and QuantityOne software (Biorad). Data analysis was performed with GraphPad Prism (Graphpad, San Diego, California) as previously described^{43,44,46}. Briefly, full-template length product signal is normalized to the signal of vehicle control. This helps to account for the considerable variation in radioactive signal. Normalized signals are plotted as

a percentage (ie. of the vehicle control, with control = 100%). For IC_{50} determination, these normalized percentages are plotted against chemical concentration, and Prism software fits a non-linear regression with a variable slope.

3 Identification of small molecule inhibitors of LASV polymerase

3.1 Initial Screening

A library of 100,000 compounds was screened against purified recombinant SARS-CoV-2 polymerase and LASV polymerase using the fluorescent plate reader assay described (see methods section 2.2). Dr. Dana Kocincova and Emma Woolner provided the purified recombinant polymerases for this. Candidates that showed at least a 40% reduction in slope (ie. 40% inhibition compared to vehicle) were classified as 'initial hits'. 377 compounds were identified for SARS-CoV-2; 695 were identified for LASV (see [Fig. 3.1](#) for a schematic representation). Compounds that showed consistent inhibition across multiple (n=2 or 3) replicates were classified as 'reconfirmed hits'. Of 377 initial hits, only 130 were reconfirmed for SARS-CoV-2. Of 695 initial hits, 349 were reconfirmed for LASV. Overlapping compounds that showed inhibition of both polymerases were excluded, as these were predicted to have poor selectivity. Based on this, only 64 of the 130 reconfirmed SARS-CoV-2 compounds were predicted to be selective for SARS-CoV-2. These compounds were investigated by Dr. Egor Tchesnokov in the Götte lab. Of the 349 reconfirmed LASV compounds, 240 were predicted to be selective for LASV. These 240 LASV-specific compounds became the focus of the remainder of this project.

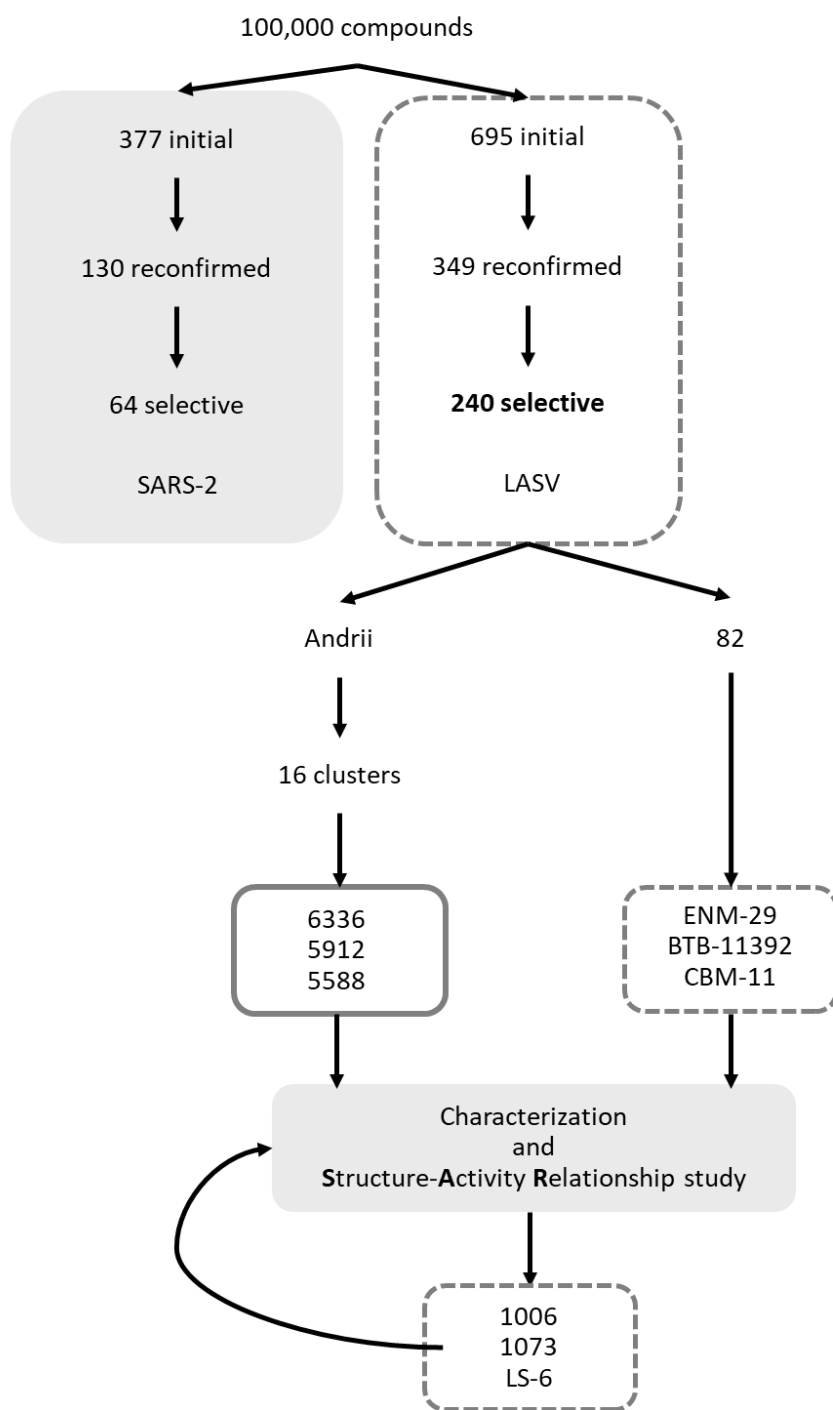


Figure 3.1 Compound selection process schematic. Derivatives that were identified in the structure-activity relationship study were subject to the same criteria and characterization process as their parent compounds.

3.2 Reproducibility and hit confirmation

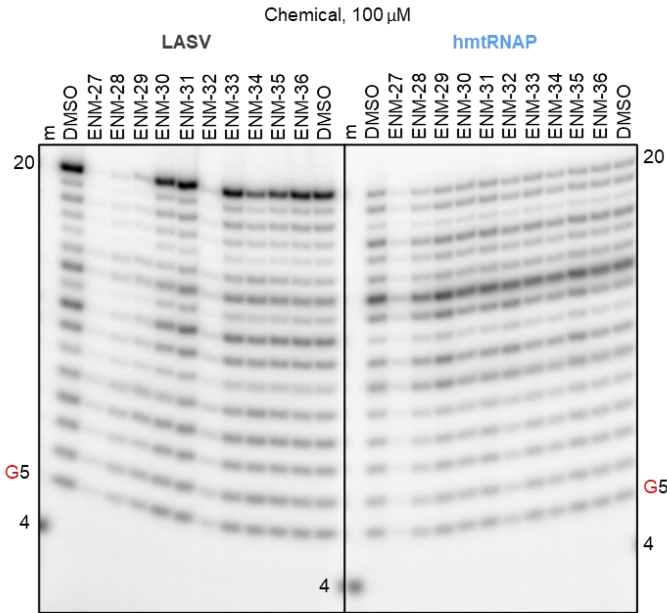
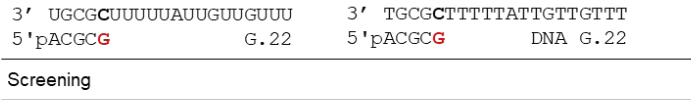
Given the somewhat poor reconfirmation rate obtained with the fluorescence-based assay (130 out of 377 for SARS-CoV-2 equates to a 34% reconfirmation rate; 349 out of 695 for LASV equates to a 50% reconfirmation rate), we first wanted to verify that these reconfirmed compounds did in fact inhibit LASV polymerase using an orthogonal assay. Here, we opted to use the gel-based assay described in methods section 2.5. However, as radiolabelled nucleotides are quite expensive, we wanted to further limit the number of compounds we would be testing. Therefore, the 240 aforementioned LASV-specific compounds were analyzed with two different, but parallel methods as follows:

The first method was undertaken in the Götte lab. First, compounds containing heavy metals were excluded, as these are likely to be toxic³⁵. Second, only compounds showing a slope of 0.34 RFU/second or less in the plate reader assay were considered for further investigation. A slope of 0.34 RFU/second or less would correspond to approximately 60% inhibition or greater as compared to a normalized slope of 1.0 RFU/second for vehicle. Theoretically, this should capture all compounds with a half-maximal inhibitory concentration (IC_{50}) of 100 μ M or less. Finally, a number of compounds were excluded for practical considerations, including cost, shipping, etc. This yielded 82 candidate compounds which were screened against LASV polymerase at 100 μ M using the radiolabelled gel-based assay. [Figure 3.2](#) shows an example screening gel. Of the 82 compounds tested, only 24 showed 80% or greater inhibition of LASV polymerase in the gel-based assay. These 24 compounds are shown in [Table 3.1](#).

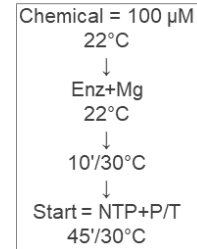
The second method was primarily computational, and was undertaken by a collaborator, Dr. Andrii Kyrylchuk, at the University of California, San Francisco. His analysis sorted all 240 compounds into 16 distinct structural groups. One compound from each of those 16 groups was chosen at random as a representative of that chemical group. Of note, this analysis was based exclusively on the structures of the compounds, as no data from the initial screening in section 3.1 was included. These compounds were screened in the

same manner as above. [Table 3.2](#) shows the % inhibition of these compounds against LASV. Of the 16 compounds, only three showed 80% or greater inhibition of LASV polymerase in the gel-based assay.

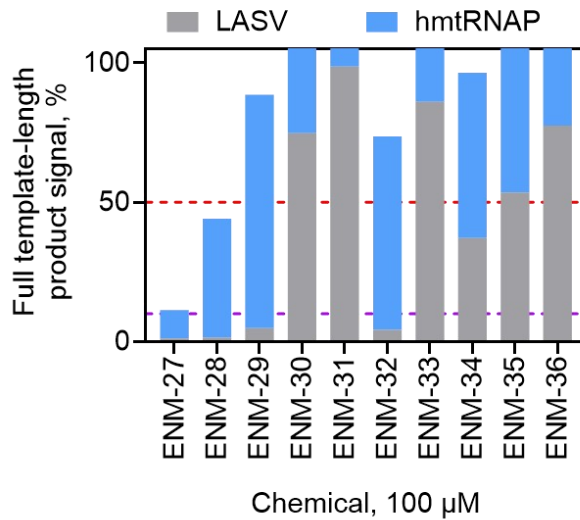
A



B



C



D

Chemical	% inhibition	
	LASV	hmtRNAP
ENM-27	99	90
ENM-28	99	57
ENM-29	95	16
ENM-30	25	12
ENM-31	1	0
ENM-32	96	31
ENM-33	14	14
ENM-34	63	41
ENM-35	47	18
ENM-36	23	15

Figure 3.2 Compound screening with the gel-based assay. Compounds were initially screened at 100 μM against LASV and hmtRNAP polymerases. A) Synthesis of full-template length product.

5'-phosphorylated templates and primers used are shown. A radiolabelled 4 nt RNA serves as a marker. A representative gel is shown for a selection of compounds. B) Reaction set-up. C) Quantification of full-template length signal in A). % signal is normalized to DMSO control. Note A) and C) are colour-coordinated. D) % inhibition of compounds against LASV and hmtRNAP. % inhibition is calculated as 100% - % signal.

3.3 Exploration of chemical classes

Structure-activity relationship (SAR) analyses are often used to identify any critical functional groups involved in potency, selectivity, stability, and solubility of a particular compound, with the goal of optimizing those characteristics³⁵. For five of the six compounds identified in section 3.2, we conducted a limited SAR analysis by catalogue in order to identify key chemical motifs. We anticipated that small modifications of the parent scaffold may improve the potency and/or selectivity of the compounds. As is often the case in science, we met with mixed results. The majority of the derivatives tested showed little to no inhibition of LASV. Of those that were active, most were on par with their parent, not improved. While the size of this SAR study limited our ability to draw definitive conclusions, we did note a few key findings, detailed below. [Table 3.3](#) summarizes the number of derivatives tested for each parent compound. In total, 124 derivatives were screened against LASV at 100 μ M. Of these, 19 compounds showed 80% or greater inhibition of LASV polymerase in the gel-based assay. [Table 3.4](#) shows the % inhibition of these compounds against LASV.

ENM-29 was the first compound we identified, so we had the opportunity to test a large number of derivatives of this compound. The O-NH-O motif of ENM-29 appeared to be important for inhibition of LASV, as this motif consistently showed up in active compounds. Selectivity and stability of these compounds seemed to be affected by another part of the molecule, however, although we were unable to determine which part exactly. For example, compound L-SAR-2 and L-SAR-5 differed greatly in selectivity against hmtRNAP, despite their remarkable structural similarity. Compounds LS-4, LS-5, and LS-6 showed similar potency despite more substantial differences in structure

between them, suggesting some tolerance for modification in the vicinity of the O-NH-O motif region. While none of the derivatives tested showed improved potency or selectivity compared to the parent (discussed further in section 3.4 and section 4.1, respectively), compound LS-6 showed improved chemical stability (see section 4.2), a factor we hadn't previously considered up until this point in the project. This was an unexpected benefit of our SAR efforts, and highlights the importance of SAR studies.

During investigation, it was noted that ENM-29 has a very similar structure to both xanthine and caffeine (see [Fig. 3.3](#)), both of which are stimulants. Xanthine derivatives are often used as bronchodilators⁴⁷, which are useful in mitigating some symptoms of respiratory viruses. Both xanthine and caffeine, as well as 33 derivatives of these compounds, were screened against LASV at 100 μ M as above. None of these compounds showed any inhibition of LASV polymerase.

Twelve derivatives of BTB-11392 were tested. Interestingly, the only compound that showed inhibition of LASV polymerase (1073) contained the same conjugated system as the parent compound (see [Fig. 3.4](#)), suggesting this feature may be important in the mechanism of action of this compound, although this is discussed further in section 4.3.

Additional derivatives were ordered recently for compounds 6336, 5912, and 5588, as these three compounds identified by our collaborator Dr. Kyrilchuk all showed promising results. Unfortunately, only about half of these compounds had arrived by April 2024, so analysis of these compounds was limited by time constraints. The compounds that did arrive were screened against LASV at 100 μ M in the gel-based assay as before (see [Fig. 3.5](#)). Nine out of the 22 compounds showed 80% or greater inhibition of LASV polymerase, all nine of which are derivatives of compound 5588, suggesting that this may be an important chemotype for future investigation.

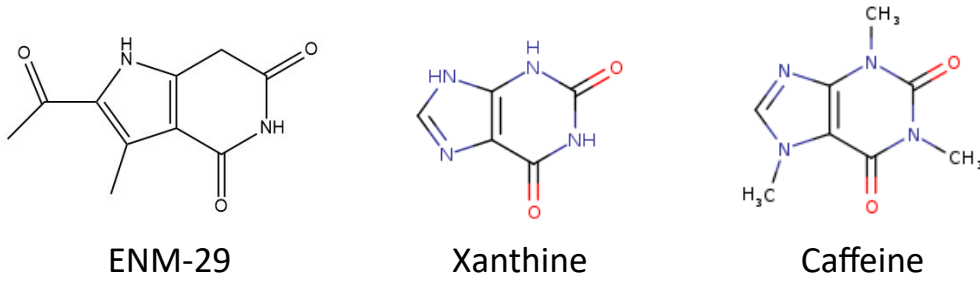


Figure 3.3 Structural comparison of xanthine and caffeine against parent compound ENM-29.

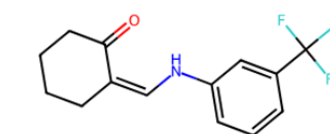
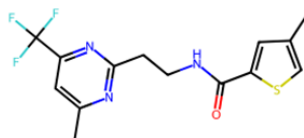
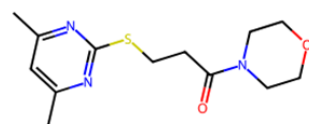
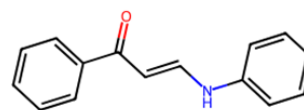
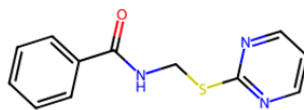
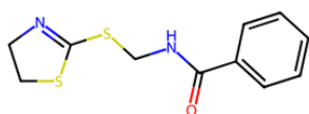
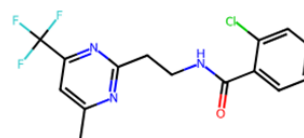
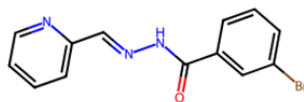
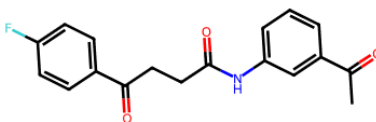
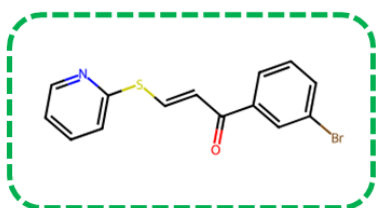
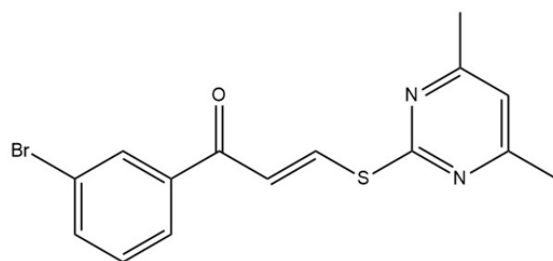


Figure 3.4 Structural comparison of active vs inactive derivatives of parent compound BTB-11392. Parent is shown above solid line; derivatives are shown below. Dashed green rectangle indicates active derivative.

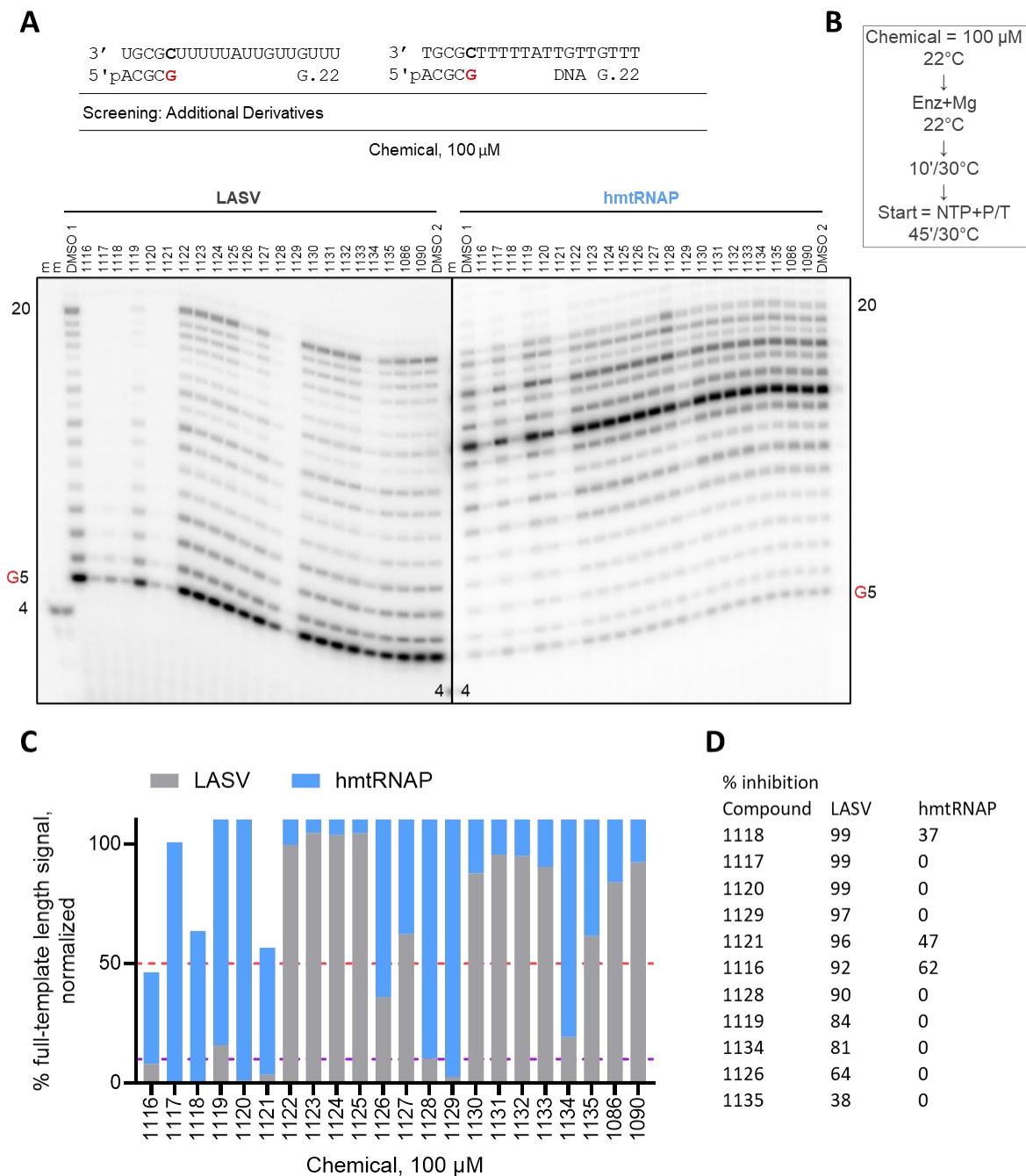


Figure 3.5 Screening of additional derivatives. Compounds were initially screened at 100 μ M against LASV and hmtRNAP polymerases. A) Synthesis of full-template length product. 5'-phosphorylated templates and primers used are shown. A radiolabelled 4 nt RNA serves as a marker. Due to time constraints, these compounds were not further characterized. B) Reaction set-up. C) Quantification of full-template length signal in A). % signal is normalized to DMSO control. Note A) and C) are colour-coordinated. D) % inhibition of compounds against LASV and hmtRNAP. % inhibition is calculated as 100% - % signal.

3.4 Selection of compounds for further characterization

In order to limit our study to only the most promising candidates, we further restricted our search based on two additional criteria: 1) high potency against LASV, and 2) little to no inhibition of human mitochondrial polymerase (hmtRNAP). Potency was assessed by determining the IC₅₀ against LASV using the gel-based assay (methods section 2.5). Ideally, the IC₅₀ against the target polymerase should be as low as possible, while host polymerases should be unaffected. Representative gels are shown in [Figure 4.1](#); IC₅₀ values are listed in tables [3.1](#), [3.2](#), and [3.4](#). An example is shown below; all chemicals are shown in the appendix. hmtRNAP is a good rule of thumb for cytotoxicity^{48,49}, although as this study was conducted *in vitro*, technically this would be a measure of selectivity, not cytotoxicity. hmtRNAP is discussed in more detail in section 4.1.1. At this stage, candidate compounds were screened against hmtRNAP at 100 μM in the same fashion as LASV in section 3.2. Tables [3.1](#), [3.2](#), and [3.4](#) list the % inhibition values for hmtRNAP. An example screening gel is shown in [Figure 3.2](#). Only compounds with an IC₅₀ less than or equal to 10 μM against LASV *and* little to no inhibition of hmtRNAP were considered for further evaluation. Based on this criteria, six compounds from our screening in section 3.2, and two derivatives from section 3.3 were selected for further characterization.

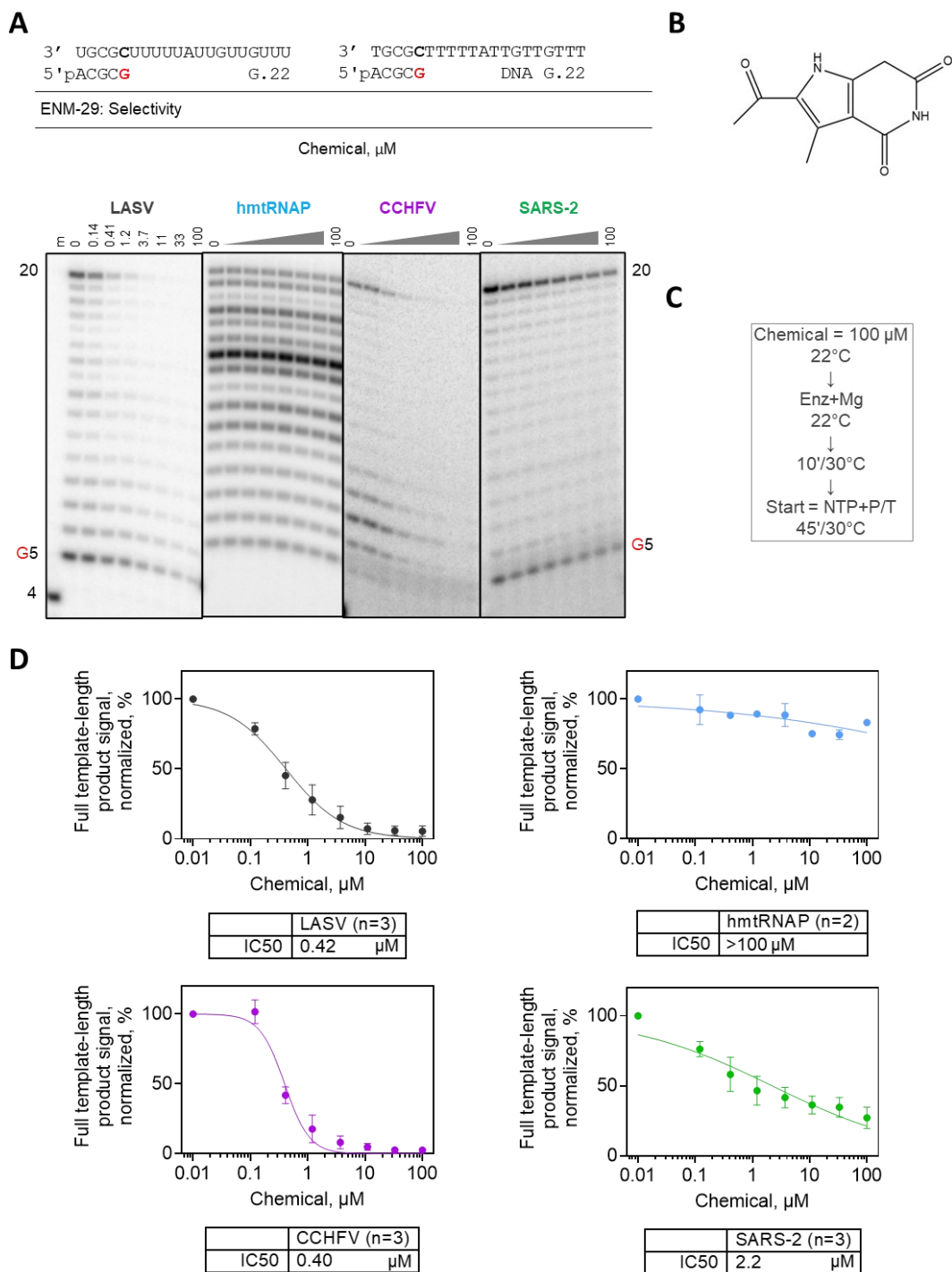


Figure 4.1.1 IC₅₀ of compound ENM-29 against LASV and other polymerases. A) Synthesis of full-template length product by various polymerases at increasing concentrations of chemical. 5'-phosphorylated templates and primers used are shown. A radiolabelled 4 nt RNA serves as a marker. Representative gels are shown for each polymerase. B) Chemical structure. C) Reaction set-up. D) Quantification of full-template length signal in A). IC₅₀ curves and values calculated with Prism software. Note A) and D) are colour-coordinated.

4 Characterization of small molecule inhibitors of LASV polymerase

4.1 Selectivity

We wanted to limit our study to compounds that selectively inhibit a subset of viral polymerases, but do not inhibit human polymerases. Analogous to antibiotics and bacteria, different types of antiviral drugs are more or less effective against different types of viruses. We would expect to identify inhibitors that are effective against related viruses, but may be less effective against more distantly related viruses. While inhibitors of human polymerases may be useful as chemotherapeutic drugs, that is not the focus of this project, and in this case is likely to be detrimental to the host. Therefore, in order to identify compounds that selectively inhibit a subset of viral polymerases, but do not inhibit human polymerases, we determined IC₅₀ values for our top compounds against three additional polymerases: Crimean-Congo Hemorrhagic Fever virus (CCHFV), SARS-CoV-2, and human mitochondrial polymerase (hmtRNAP). [Table 4.1](#) summarizes the IC₅₀ values obtained for these three polymerases, as well as LASV, while the corresponding gels and graphs are shown in [Figure 4.1](#). An example is shown above; all chemicals are shown in the appendix. Overall, our top compounds showed little to no inhibition of hmtRNAP, and variable inhibition of CCHFV and SARS-CoV-2, with most compounds showing similar potency against CCHFV as compared to LASV, and slightly reduced potency against SARS-CoV-2.

4.1.1 Human mitochondrial polymerase

Human mitochondrial polymerase (hmtRNAP) is a convenient tool for drug screening, as inhibition of hmtRNAP directly correlates with cytotoxicity in cell culture and off-target effects in clinical trials^{48,49}. Related to bacteriophage T7 polymerase, hmtRNAP is also a relatively small (~134 kDa), single-subunit polymerase, enabling easier purification of recombinant enzyme⁴⁹. As a follow-up to the screening conducted in section 3.4, we also determined IC₅₀ values for our top compounds against hmtRNAP in the same manner as LASV, as shown in [Fig. 4.1](#). As expected, none of the compounds showed inhibition of hmtRNAP, with the exception of compound 1073, which showed 38% inhibition at 100 μM. For most of the other compounds, graphical analysis predicted very high IC₅₀ values;

this is a computational artefact of the software, and it would be more accurate to say that the IC_{50} is simply greater than 100 μM . Of note, compound 6336 shows the inverse of what we expect, with increased signal at higher concentrations of chemical (see [Fig 4.1.6](#)). While this is unusual, it still indicates that this compound does not inhibit hmtRNAP. A similar, but less pronounced effect is also seen with compound 5912 (see [Fig 4.1.7](#)).

4.1.2 Crimean-Congo hemorrhagic fever virus

Crimean-Congo Hemorrhagic Fever virus (CCHFV) is a member of the same order as LASV (*Bunyavirales*), but a different family (*Nairoviridae* as opposed to *Arenaviridae*)¹¹. CCHFV was also identified by the World Health Organization as a priority pathogen back in 2017, along with LASV⁸. Similar to LASV, there is currently no approved vaccine for CCHFV, but a vaccine is in clinical trials¹⁰. Ribavirin has been used to treat CCHFV, but data supporting its effectiveness is limited. Therefore, CCHFV was chosen as a representative virus that is similar to LASV. With the exception of compound ENM-29, all compounds showed similar but slightly higher IC_{50} values against CCHFV compared to LASV. Compound ENM-29 was actually slightly more effective against CCHFV than LASV, with an IC_{50} of 0.40 μM , as opposed to 0.42 μM . All compounds showed an IC_{50} of less than 10 μM against CCHFV, with the exception of compound 6336, with an IC_{50} of 11 μM .

4.1.3 Severe acute respiratory syndrome virus 2

Severe acute respiratory syndrome virus 2 (SARS-CoV-2, or SARS-2) is a member of the *Coronaviridae* family, putting it into a different phylum than LASV and CCHFV¹¹. SARS-CoV-2 was also identified by the World Health Organization as a priority pathogen back in 2017, along with LASV⁸. SARS-CoV-2 was the causative agent of the COVID-19 pandemic, and has claimed more than 6.5 million lives since its discovery in 2019¹, although there are now several vaccines and treatments available for SARS-CoV-2³. Given its taxonomy and its global significance, SARS-CoV-2 was chosen as a representative virus that is evolutionarily distinct from LASV. With the exception of compounds 6336 and LS-6, all compounds showed higher IC_{50} values against SARS-CoV-2

than LASV, but still showed IC₅₀ values less than 10 μM against SARS-CoV-2. Compounds 6336 and LS-6 showed IC₅₀ values of 21 μM and 45 μM, respectively, suggesting that these two compounds are much more selective towards LASV than SARS-CoV-2 (see [Fig 4.1.6](#) and [Fig 4.1.2](#), respectively). Of note, LS-6 appears to have increased selectivity compared to its parent compound, ENM-29, although it shows reduced potency.

4.2 Chemical stability

We wanted to assess the chemical stability of our top compounds in order to remove confounding variables that could affect the interpretation of future cell culture and/or pharmacokinetic studies. Degradation, poor solubility, poor absorption into the cell, and rapid efflux out of the cell can all cause a drug to appear less effective than it actually is. [Figure 4.2](#) shows the UV-Vis spectra of our top candidates in both DMSO and in reaction buffer over time. An example is shown below; all chemicals are shown in the appendix. % degradation over time was calculated by determining absorbance at a particular time as a fraction of absorbance at time = 0. For ease of measurement, the wavelength at the highest point of the largest/most distinct peak was used for calculating % degradation. Where applicable, the wavelength used to calculate % degradation is indicated by a vertical red line on the spectrum. L-SAR-4 was chosen as a negative control, as it shows no inhibition of LASV polymerase in the gel-based assay. Presence of additional spectral peaks in reaction buffer, but not DMSO is not unusual. No apparent decrease in absorbance over time in either sample suggests that the compound is stable in both DMSO and reaction buffer over time (see [Fig 4.2.2](#)).

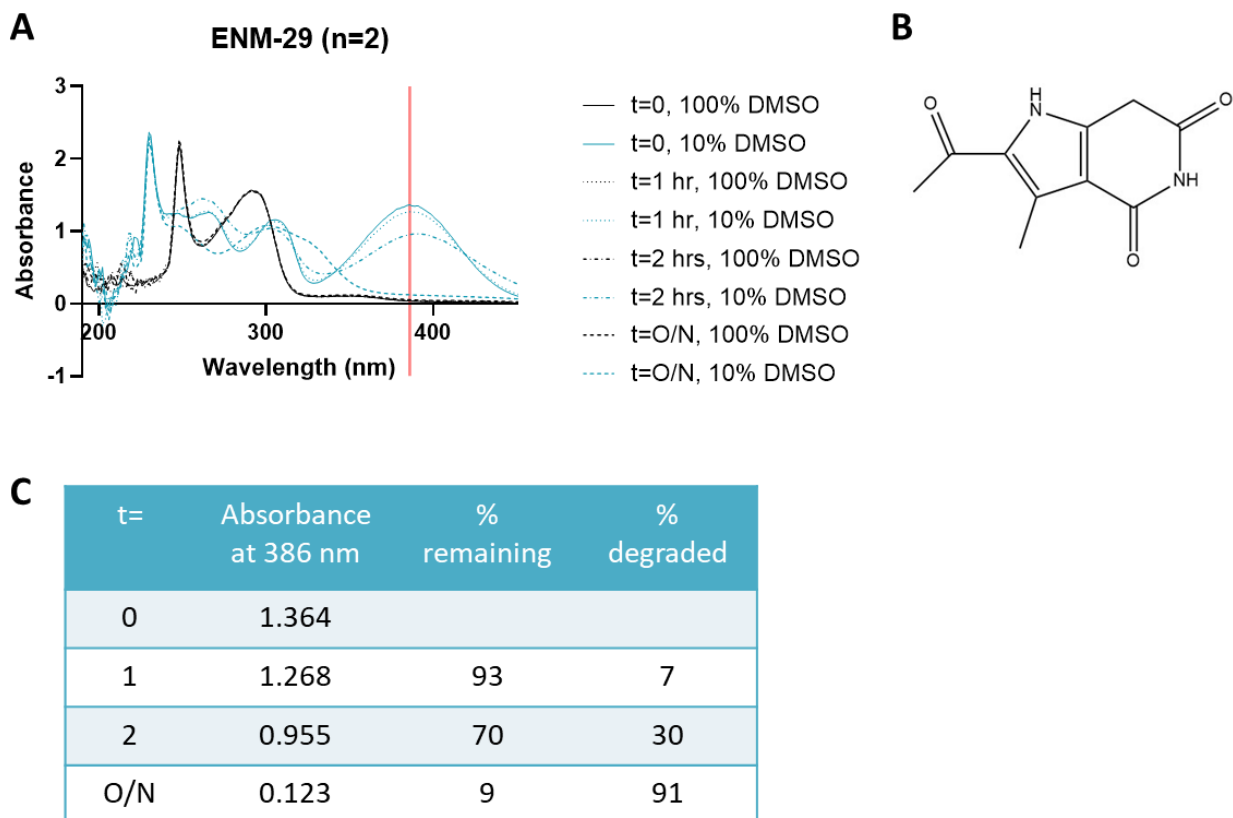


Figure 4.2.3 Chemical stability of ENM-29 in DMSO and reaction buffer (10% DMSO) overnight. A) Absorbance spectrum of compound in DMSO (black) or reaction buffer (teal). Replicate spectra are plotted on the same graph. B) Chemical structure. C) Degradation of compound over time, as calculated by disappearance of spectral peak indicated by red line in A). Please note this is an example, and spectra for all other chemicals are shown in the appendix.

All compounds appeared stable in DMSO, with the exception of compounds LS-4 and LS-5 (see [Fig 4.2.5](#) and [Fig 4.2.6](#), respectively). Replicate spectra for LS-4 did not show consistent features, suggesting that while this compound is stable over time in either DMSO or reaction buffer, it's likely unstable over multiple freeze-thaw cycles, although no precipitate was observed. Replicate spectra for LS-5 show similar spectral features, but at reduced magnitude in the second replicate, suggesting that this compound is unstable over multiple freeze-thaw cycles. Immediate precipitation was observed upon resuspension in reaction buffer, therefore the signal remaining in the aqueous samples (teal) likely represents the soluble fraction of the organic samples (black).

Compounds ENM-29 ([Fig 4.2.3](#)), L-SAR-5 ([Fig 4.2.4](#)), CBM-11 ([Fig 4.2.10](#)), and 6336 ([Fig 4.2.11](#)) all showed substantial degradation over time in reaction buffer, as evidenced by disappearance of spectral features over time. LS-6 also showed some degradation over time, but very minimal degradation, as only 11% degradation occurred overnight (see [Fig 4.2.7](#)).

Compounds BTB-11392 and 5912 had poor solubility upon initial resuspension in 100% DMSO, and showed immediate precipitation upon resuspension in reaction buffer. This seems incongruous with the relatively low IC₅₀ values obtained with these compounds, but the concentration of chemical used in the stability assay is ten times that of the gel-based assay (1 mM vs 100 μM, respectively), which could at least partially explain this phenomenon. The lack of signal in the aqueous samples (teal) is likely due to precipitation as well.

Compound 5588 not only shows very similar spectra for both aqueous and organic samples, but shows no apparent precipitation or change in spectral features over time, suggesting that this compound is stable in both DMSO and reaction buffer over extended periods of time, as well as over multiple freeze-thaw cycles.

4.3 Mechanism of Action

In the interest of determining a cursory mechanism of action for our top eight candidates, we set up a series of experiments in which we altered the order of addition of substrates and co-factor (see [Fig 4.3](#) for a schematic representation). In one condition, the compound is allowed to access the polymerase *before* any of the substrates, then the reaction is started by the addition of the substrates (ie. RNA primer, RNA template, and NTPs), hence this is referred to as an 'RNA start'. In the other condition, the compound accesses the polymerase *at the same time* as the substrates, and the reaction is started by the addition of Mg²⁺ co-factor, hence this is referred to as a 'Mg start'. By comparing the IC₅₀ under these two different conditions, we were able to determine whether these compounds were behaving as competitive or allosteric inhibitors. We would expect a competitive inhibitor to be much more effective, or have a lower IC₅₀,

when the substrates are absent, as in the RNA start condition. In the Mg start condition, we would expect a much higher IC_{50} for a competitive inhibitor, as now the inhibitor will be competing with one or more substrates. By contrast, we would expect an allosteric inhibitor to show virtually identical IC_{50} values in either condition, as the presence or absence of substrates is irrelevant (unless we were trying to distinguish between uncompetitive and non-competitive inhibition, but that is outside the scope of this project). [Figure 4.4](#) shows the IC_{50} determination for each of the top eight compounds under different reaction conditions. The extra sum of squares F-test was used to determine whether the IC_{50} values for the two conditions were significantly different from each other or not. An F-test compares the fit of one curve for all data sets against the fit of individual curves for each data set. The smaller the p value, the more likely that the two data sets are best described by two different curves. In this case, the smaller the p value, the more likely that the compound is competitive. These values are summarized in [Table 4.2](#). An example is shown below; all chemicals are shown in the appendix. Compounds 6336 ([Fig 4.4.6](#)), 5912 ([Fig 4.4.7](#)), and 5588 ([Fig 4.4.8](#)) all show nearly identical IC_{50} curves under both conditions, and their IC_{50} values differ by less than one order of magnitude, suggesting that these compounds are likely allosteric. However, the results of the F-test suggest that only compound 5912 is actually allosteric. Compound BTB-11392 and its derivative 1073 both show nearly identical curves, but their IC_{50} values differ by an order of magnitude, although they only roughly double (see [Fig 4.4.3](#) and [Fig 4.4.4](#), respectively). We would expect a similar mechanism of action for a parent and derivative, but based on the F-test, compound BTB-11392 is more likely to be an allosteric inhibitor, while its derivative 1073 is more likely to be competitive. Of note, compounds 5912, BTB-11392, and 1073 all contain conjugated systems, and therefore may be covalent inhibitors. Compound ENM-29 shows vastly different curves and IC_{50} values under different conditions, by two orders of magnitude (see [Fig 4.4.1](#)). Its derivative, LS-6, shows a similar pattern, albeit to a lesser degree (see [Fig. 4.4.2](#)). This could potentially be due to differences in affinity, given the slightly higher baseline IC_{50} of LS-6 compared to ENM-29 (3.6 μ M vs 0.42 μ M). LS-6 also has a side chain off the

nitrogen atom, so perhaps there are steric clashes with binding site residues that do not affect binding of the smaller ENM-29. However, both of these compounds appear to be competitive based on the F-test. Compound CBM-11 appears to be competitive based on the results of the F-test. While the IC_{50} curves are noticeably different, the IC_{50} values are not, and only roughly double (see [Fig 4.4.5](#)). CBM-11 does bear some structural similarity to ENM-29 and LS-6, but compared to the other compounds, so there may be similarities in the mechanism of action as well.

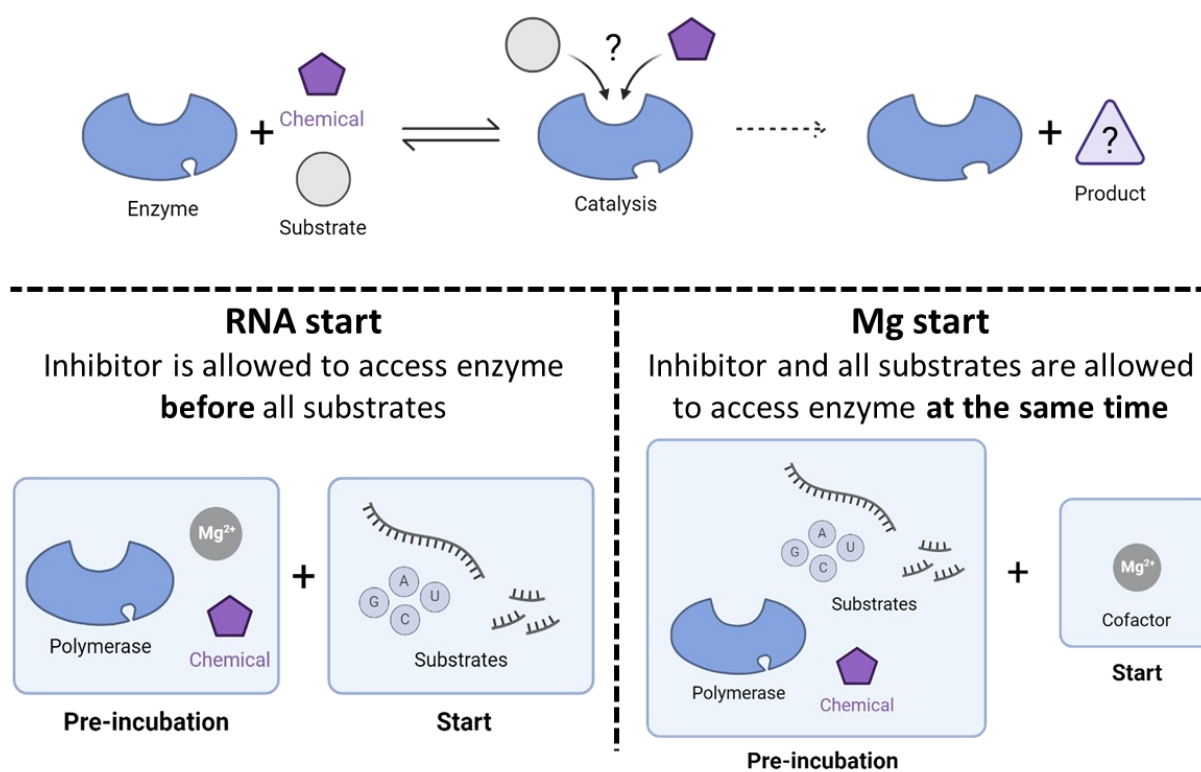


Figure 4.3 Mechanism of action reaction set-up. Substrates and inhibitor are incubated with polymerase at different times. Comparing the IC_{50} under these two different conditions allows identification of competitive or allosteric inhibitors. Allosteric inhibitors should have virtually identical IC_{50} values in either condition, as they do not compete with substrate(s). Competitive inhibitors are more effective, or have a lower IC_{50} , when the substrates are absent, as in the RNA start condition.

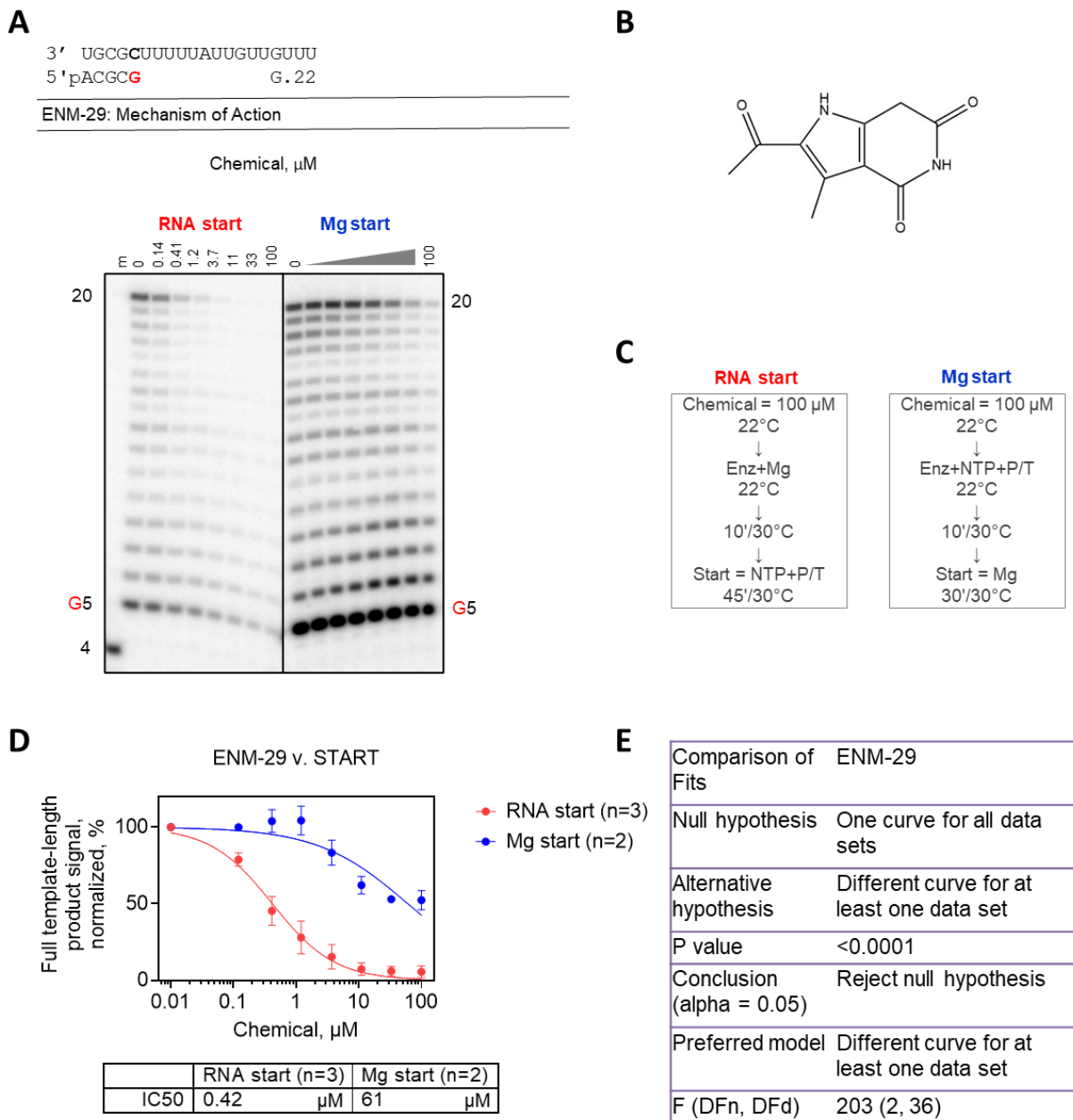


Figure 4.4.1 IC₅₀ of compound ENM-29 against LASV under different reaction conditions. A) Synthesis of full-template length product at increasing concentrations of chemical. 5'-phosphorylated templates and primers used are shown. A radiolabelled 4 nt RNA serves as a marker. Representative gels are shown for both conditions. B) Chemical structure. C) Reaction schemes. D) Quantification of full-template length signal in A). IC₅₀ curves and values calculated with Prism software. E) Extra sum of squares F-test. Note A) and D) are colour-coordinated.

4.4 Compounds for future investigation

Beginning with a library of 100,000 compounds, we systematically narrowed a pool of candidate compounds based on their potency, selectivity, chemical stability, and mechanism of action. Ultimately, only five compounds showed acceptable potency, selectivity, and chemical stability based on our criteria: LS-6, BTB-11392, 1073, 5912, and 5588. Compounds LS-6, 1073, and 5588 appeared to be competitive, while compounds BTB-11392 and 5912 appeared to be allosteric inhibitors. Of note, compounds 5912, BTB-11392, and 1073 all contain conjugated systems, and therefore may be covalent inhibitors. Additional SAR analyses should be conducted for each of these compounds, and further investigation into their mechanisms of action is required. However, these five compounds lay a solid foundation for future LASV drug development efforts.

5 Discussion and Future Directions

In 2017, the World Health Organization identified a number of viruses, including LASV, as priority pathogens, given their pandemic potential⁸. LASV remains a virus of concern, as there is currently no approved vaccine for LASV, nor conclusive data to suggest that the antiviral drug ribavirin is effective at treating LASV^{9,10}. LASV is an RNA virus, and is therefore dependent on its own encoded polymerase^{12,28}. The viral polymerase is an essential component of the viral life cycle of most RNA viruses, and therefore a logical target for drug design^{5,6}. This strategy has been used successfully in the past^{7,35,36}. Allosteric inhibitors are particularly desirable, as they are less prone to cytotoxicity issues than their substrate analogue counterparts, and they can be used in conjunction with nucleotide analogues, which can increase the efficacy of treatment⁷. The goal of this project was to identify compounds that inhibit LASV polymerase, and then characterize those compounds to determine which, if any, warrant further investigation as candidates for drug development into new antivirals to treat LASV.

Beginning with 100,000 compounds, this project systematically narrowed a pool of candidates based on their potency, selectivity, and chemical stability. Preliminary investigation into the mechanism of action was also conducted for the most promising candidates. Ultimately, we identified five promising compounds. All five compounds have an IC₅₀ against LASV of 10 μM or less, indicating that they are potent inhibitors of the target. All five compounds appear to be somewhat selective, as they inhibit LASV and the related CCHFV to a similar extent, but they are less effective against the unrelated SARS-2, and they do not inhibit hmtRNAP. All five compounds appear to be relatively chemically stable, as they show little to no decrease in absorbance over time, as measured by UV-Vis. Three compounds appear to be competitive inhibitors, while the other two appear to be allosteric inhibitors, although the possibility of covalent inhibition cannot be ruled out at this stage. Of note, this study identified compounds that represent promising chemical *classes* for future investigation. Further work is

required to fully elucidate their mechanisms of action and to optimize their characteristics.

Prior to this study, a high-throughput fluorescence-based screening campaign of 100,000 compounds revealed 349 compounds that showed consistent inhibition of LASV polymerase *in vitro*. There are a number of benefits with this approach, the main one being that high-throughput assays are very fast. Thousands of compounds can be screened in a short period of time, which streamlines drug development considerably. In addition, *in vitro* approaches like this one are also much safer, as they circumvent the need for biosafety level 4 labs required for many viruses. However, the reproducibility of fluorescence-based assays leaves something to be desired, as seen with the poor reconfirmation rate in section 3.1. This necessitated the use of an orthogonal assay, in this case our gel-based assay, to confirm the inhibitory activity of compounds identified in the initial screen. A low discovery rate is not unusual, much like trying to find a needle in a haystack. High-throughput methods, while less consistent, rapidly narrow down the candidate pool, while slower, more precise assays can be used to both verify results and further characterize compounds of interest. More recently, *in silico* screening has grown in popularity, and has been successfully used to identify drugs to treat hypertension, flu, and HIV, among others⁵⁰. This approach may be useful, but still requires a second method to verify its results. When narrowing down our candidate pool, we opted to use two parallel methods of analysis, as described in section 3.2. Our analysis yielded 82 candidates, while our collaborator Dr. Kyrilchuk's method yielded 16 for the same 240 compound pool. Three of these compounds overlapped, although compound ENM-80 was never tested as it was never received. In total, 95 compounds were tested against LASV polymerase. Of these, only six went on to be fully characterized. Three of these were identified in our analysis, while the other three were identified by Dr. Kyrilchuk. This suggests that while either approach is a valid strategy, a combinatorial approach is likely best in order to avoid missing any useful compounds. Of note, one of our top

candidates, compound CBM-11, was also identified in a poliovirus RNA polymerase screen with an IC_{50} of $82 \mu M$ ⁵¹.

The effectiveness of a particular drug is determined by a number of factors, including its size, composition, solubility, and chemical stability^{35,52}. Structure-activity relationship (SAR) studies are often used to identify key functional groups that affect these characteristics, in order to optimize a drug's properties^{35,53-55}. In this study, limited SAR studies were conducted for the most promising candidates. Of the 140 derivatives tested, only two showed promising results. This could be due, at least in part, to the limitations of this particular component of the project. Namely, we were restricted to compounds readily available for purchase. In an ideal world, we would be able to partner with an organic chemistry group that could synthesize custom compounds, enabling us to test specific, individual modifications of compounds. Being limited to a catalogue causes too many gaps in available structures, which makes interpretation difficult. That being said, our SAR study did have two unexpected benefits: first, we identified compound LS-6 as a more stable derivative of ENM-29, albeit with reduced potency. Second, 9 out of 12 derivatives of compound 5588 showed at least 80% inhibition of LASV polymerase when screened at $100 \mu M$, suggesting that this is an important chemical class for future investigation. Indoles may also be a chemical class for further investigation. Compound ENM-29 is an indole, and indoles are a common therapeutic scaffold⁵⁶. ENM-29 also bears some similarity to the 2-pyridone scaffold. A number of naturally occurring 2-pyridone-containing compounds have been identified as inhibitors of the SARS-CoV-2 protease⁵⁷. It would be interesting to see if any of the compounds identified in our study show activity against other viral targets as well.

While broad-spectrum antivirals are certainly useful, extensive use of broad-spectrum drugs raises concerns with the development of resistance^{4,7,34}. As such, selectivity is an important parameter to consider in antiviral development. In this study, assessment of selectivity was determined based on four polymerases: LASV (target), hmtRNAP (ballpark of cytotoxicity), CCHFV (related virus), and SARS-CoV-2 (unrelated virus).

Fortunately, our top compounds showed little to no inhibition of hmtRNAP, with most compounds showing similar potency against CCHFV as compared to LASV, and slightly reduced potency against SARS-CoV-2, as expected. This section of the project could have been expanded to include other viral polymerases, and in the future it may be useful to test additional related and unrelated viruses to determine the exact niche of the top candidates. Although this may depend on the particular mechanism of action of these compounds as well. In this study, hmtRNAP was used as a rule of thumb for potential toxicity, as the simplicity of hmtRNAP makes it a practical option. While other human polymerases could have been used, at this point it would be more efficient to begin cell culture work, especially since viral infection is studied in the context of host cells. Chemical stability is an important consideration when moving into cell culture work and pharmacokinetic studies. In this study, we used a common method, UV-Vis spectroscopy, to monitor chemical stability over time, as it's both fast and inexpensive. This method is not a foolproof way to assess stability however, as some compounds lack distinct spectral features. In addition, disappearance of peaks may be due to factors other than degradation, like precipitation or change in protonation state. Liquid chromatography and mass spectrometry can be used to monitor degradation with high precision, but this is a far more time consuming and expensive technique⁵⁸.

Historically, combination antiviral treatments have been more effective than single-drug regimens^{7,36}. For this reason, understanding the mechanism of action of a particular drug is essential when designing a treatment plan. Investigation into the mechanism of action of the compounds identified in this study was only preliminary. However, results suggest at least two different mechanisms of action, with three compounds appearing to be competitive, and two appearing to be allosteric, although at this stage the possibility of covalent inhibition cannot be ruled out. As such, there is considerable follow-up investigation to be done in this area. At the time of writing, exploration into the mechanism of action using mass spectrometry is currently being done in collaboration with Dr. John Klassen's lab here at the University of Alberta⁵⁹. Microscale thermophoresis is a relatively new technique that enables determination of binding

affinities of small molecules, so this technique may prove useful in the future as well⁶⁰. In 2021, two new crystal structures were published for LASV polymerase, so perhaps computational approaches like 3D-modelling could be used^{61,62}. The fluorescence-based plate reader assay described in section 2.2 could potentially be adapted to study enzyme kinetics. There are well-established parameters for this, *a la* Michaelis-Menten and Lineweaver-Burk³⁵.

Overall, this study demonstrates a streamlined method for drug discovery. Using a systematic approach, we narrowed a pool of 100,000 compounds down to five candidates for future investigation based on their potency, selectivity, chemical stability, and mechanism of action. These compounds were: LS-6, BTB-11392, 1073, 5912, and 5588. Additional SAR analyses should be conducted for each of these compounds, and further investigation into their mechanisms of action is required. However, these five compounds lay a solid foundation for future LASV drug development efforts, and demonstrate the validity of our approach. This method can be applied to any viral polymerase, facilitating antiviral development for not just LASV, but a number of viruses with pandemic potential. While this study is only the first leg of the drug development relay race, identification of several promising candidates puts us one step closer to an effective treatment for LASV.

References

1. Lu, R., Zhao, X., Li, J., Niu, P., Yang, B., Wu, H., Wang, W., Song, H., Huang, B., Zhu, N., Bi, Y., Ma, X., Zhan, F., Wang, L., Hu, T., Zhou, H., Hu, Z., Zhou, W., Zhao, L., Chen, J., Meng, Y., Wang, J., Lin, Y., Yuan, J., Xie, Z., Ma, J., Liu, W. J., Wang, D., Xu, W., Holmes, E. C., Gao, G. F., Wu, G., Chen, W., Shi, W., and Tan, W. (2020) Genomic characterisation and epidemiology of 2019 novel coronavirus: implications for virus origins and receptor binding. *Lancet* **395**, 565-574
2. Gordon, C. J., Lee, H. W., Tchesnokov, E. P., Perry, J. K., Feng, J. Y., Bilello, J. P., Porter, D. P., and Gotte, M. (2022) Efficient incorporation and template-dependent polymerase inhibition are major determinants for the broad-spectrum antiviral activity of remdesivir. *J Biol Chem* **298**, 101529
3. Centers for Disease Control and Prevention. (Last reviewed March 15, 2023) CDC Museum COVID-19 Timeline. [online] <https://www.cdc.gov/museum/timeline/covid19.html#print> (Accessed May 17, 2024).
4. Stevens, L. J., Pruijssers, A. J., Lee, H. W., Gordon, C. J., Tchesnokov, E. P., Gribble, J., George, A. S., Hughes, T. M., Lu, X., Li, J., Perry, J. K., Porter, D. P., Cihlar, T., Sheahan, T. P., Baric, R. S., Gotte, M., and Denison, M. R. (2022) Mutations in the SARS-CoV-2 RNA-dependent RNA polymerase confer resistance to remdesivir by distinct mechanisms. *Sci Transl Med* **14**, eabo0718
5. Maheden, K., Todd, B., Gordon, C. J., Tchesnokov, E. P., and Gotte, M. (2021) Inhibition of viral RNA-dependent RNA polymerases with clinically relevant nucleotide analogs. *Enzymes* **49**, 315-354
6. de Farias, S. T., Dos Santos Junior, A. P., Rego, T. G., and Jose, M. V. (2017) Origin and Evolution of RNA-Dependent RNA Polymerase. *Front Genet* **8**, 125
7. Sluis-Cremer, N., and Tachedjian, G. (2008) Mechanisms of inhibition of HIV replication by non-nucleoside reverse transcriptase inhibitors. *Virus Res* **134**, 147-156
8. World Health Organization. (2023) Prioritizing diseases for research and development in emergency contexts. [online] <https://www.who.int/activities/prioritizing-diseases-for-research-and-development-in-emergency-contexts> (Accessed May 17, 2024).

9. Sulis, G., Peebles, A., and Basta, N. E. (2023) Lassa fever vaccine candidates: A scoping review of vaccine clinical trials *Tropical Medicine & International Health* **28**, 420-431 <https://doi.org/10.1111/tmi.13876>
10. Hansen, F., Jarvis, M. A., Feldmann, H., and Rosenke, K. (2021) Lassa Virus Treatment Options. *Microorganisms* **9**
11. Monath, T. P. (2019) A short history of Lassa fever: the first 10-15 years after discovery *Curr Opin Virol* **37**, 77-83 [10.1016/j.coviro.2019.06.005](https://doi.org/10.1016/j.coviro.2019.06.005)
12. Garry, R. F. (2023) Lassa fever — the road ahead *Nature Reviews Microbiology* **21**, 87-96 [10.1038/s41579-022-00789-8](https://doi.org/10.1038/s41579-022-00789-8)
13. Tewogbola P, Aung N (2020) Lassa fever: History, causes, effects, and reduction strategies, *Int. J. One Health*, 6(2): 95-98. doi: [www.doi.org/10.14202/IJOH.2020.95-98](https://doi.org/10.14202/IJOH.2020.95-98)
14. Bond, N., Schieffelin, J. S., Moses, L. M., Bennett, A. J., and Bausch, D. G. (2013) A historical look at the first reported cases of Lassa fever: IgG antibodies 40 years after acute infection *Am J Trop Med Hyg* **88**, 241-244 [10.4269/ajtmh.2012.12-0466](https://doi.org/10.4269/ajtmh.2012.12-0466)
15. Naeem, A., Zahid, S., Hafeez, M. H., Bibi, A., Tabassum, S., and Akilimali, A. (2023) Re-emergence of Lassa fever in Nigeria: A new challenge for public health authorities *Health Sci Rep* **6**, e1628 [10.1002/hsr2.1628](https://doi.org/10.1002/hsr2.1628)
16. Ilori, E. A., Furuse, Y., Ipadeola, O. B., Dan-Nwafor, C. C., Abubakar, A., Womi-Eteng, O. E. *et al.* (2019) Epidemiologic and Clinical Features of Lassa Fever Outbreak in Nigeria, January 1-May 6, 2018 *Emerg Infect Dis* **25**, 1066-1074 [10.3201/eid2506.181035](https://doi.org/10.3201/eid2506.181035)
17. World Health Organization (2023) Disease Outbreak News; Lassa Fever – Nigeria. [online] <https://www.who.int/emergencies/disease-outbreak-news/item/2023-DON463> (Accessed May 20, 2024).
18. Warner, B. M., Safronetz, D., and Stein, D. R. (2018) Current research for a vaccine against Lassa hemorrhagic fever virus *Drug Des Devel Ther* **12**, 2519-2527 [10.2147/DDDT.S147276](https://doi.org/10.2147/DDDT.S147276)
19. Garnett, L. E., and Strong, J. E. (2019) Lassa fever: With 50 years of study, hundreds of thousands of patients and an extremely high disease burden, what have we learned? *Current Opinion in Virology* **37**, 123-131 <https://doi.org/10.1016/j.coviro.2019.07.009>

20. Andersen, K. G., Shapiro, B. J., Matranga, C. B., Sealfon, R., Lin, A. E., Moses, L. M. *et al.* (2015) Clinical Sequencing Uncovers Origins and Evolution of Lassa Virus Cell **162**, 738-750 10.1016/j.cell.2015.07.020
21. Government of Canada. (Last date modified: 2024-02-12) Lassa virus: Infectious substances pathogen safety data sheet. [online] <https://www.canada.ca/en/public-health/services/laboratory-biosafety-biosecurity/pathogen-safety-data-sheets-risk-assessment/lassa-virus.html> (Accessed May 22, 2024).
22. World Health Organization. (2024) Lassa Fever. [online] https://www.who.int/health-topics/lassa-fever#tab=tab_1 (Accessed May 22, 2024).
23. World Health Organization. (2017) Lassa Fever Fact Sheet. [online] <https://www.who.int/news-room/fact-sheets/detail/lassa-fever> (Accessed May 22, 2024).
24. Centers for Disease Control and Prevention. (2024) About Lassa Fever. [online] <https://www.cdc.gov/lassa-fever/about/> (Accessed May 22, 2024)
25. Happi, A. N., Happi, C. T., and Schoepp, R. J. (2019) Lassa fever diagnostics: past, present, and future Curr Opin Virol **37**, 132-138 10.1016/j.coviro.2019.08.002
26. Salami, K., Gouglas, D., Schmaljohn, C., Saville, M., and Tornieporth, N. (2019) A review of Lassa fever vaccine candidates Curr Opin Virol **37**, 105-111 10.1016/j.coviro.2019.07.006
27. Warner, B. M., Siragam, V., and Stein, D. R. (2019) Assessment of antiviral therapeutics in animal models of Lassa fever Curr Opin Virol **37**, 84-90 10.1016/j.coviro.2019.06.010
28. Loureiro, M. E., D'Antuono, A., and Lopez, N. (2019) Virus(-)Host Interactions Involved in Lassa Virus Entry and Genome Replication Pathogens **8**, 10.3390/pathogens8010017
29. Sanger, L., Williams, H. M., Yu, D., Vogel, D., Kosinski, J., Rosenthal, M. *et al.* (2023) RNA to Rule Them All: Critical Steps in Lassa Virus Ribonucleoparticle Assembly and Recruitment J Am Chem Soc **145**, 27958-27974 10.1021/jacs.3c07325
30. Te Velthuis, A. J., and Fodor, E. (2016) Influenza virus RNA polymerase: insights into the mechanisms of viral RNA synthesis Nat Rev Microbiol **14**, 479-493 10.1038/nrmicro.2016.87

31. Koonin, E. V., Dolja, V. V., Krupovic, M., Varsani, A., Wolf, Y. I., Yutin, N. *et al.* (2020) Global Organization and Proposed Megataxonomy of the Virus World *Microbiol Mol Biol Rev* **84**, 10.1128/MMBR.00061-19
32. Peersen, O. B. (2019) A Comprehensive Superposition of Viral Polymerase Structures *Viruses* **11**, 10.3390/v11080745
33. Venkataraman, S., Prasad, B., and Selvarajan, R. (2018) RNA Dependent RNA Polymerases: Insights from Structure, Function and Evolution *Viruses* **10**, 10.3390/v10020076
34. Agostini, M. L., Andres, E. L., Sims, A. C., Graham, R. L., Sheahan, T. P., Lu, X. *et al.* (2018) Coronavirus Susceptibility to the Antiviral Remdesivir (GS-5734) Is Mediated by the Viral Polymerase and the Proofreading Exoribonuclease *mBio* **9**, 10.1128/mBio.00221-18
35. Voet, D., Voet, J. G., and Pratt, C. W. *Fundamentals of biochemistry: life at the molecular level*, Fifth edition. Ed.,
36. Yoshida, Y., Honma, M., Kimura, Y., and Abe, H. (2021) Structure, Synthesis and Inhibition Mechanism of Nucleoside Analogues as HIV-1 Reverse Transcriptase Inhibitors (NRTIs) *ChemMedChem* **16**, 743-766 10.1002/cmdc.202000695
37. Aidsmap. (2024) Types of antiretroviral medications. [online] <https://www.aidsmap.com/about-hiv/types-antiretroviral-medications> (Accessed June 5, 2024)
38. National Institutes of Health. (2023) FDA-Approved HIV Medicines. [online] <https://hivinfo.nih.gov/understanding-hiv/fact-sheets/fda-approved-hiv-medicines> (Accessed June 5, 2024)
39. Pham, H. T., Xiao, M. A., Principe, M. A., Wong, A., and Mesplede, T. (2020) Pharmaceutical, clinical, and resistance information on doravirine, a novel non-nucleoside reverse transcriptase inhibitor for the treatment of HIV-1 infection *Drugs Context* **9**, 10.7573/dic.2019-11-4
40. Gordon, C. J., Tchesnokov, E. P., Woolner, E., Perry, J. K., Feng, J. Y., Porter, D. P. *et al.* (2020) Remdesivir is a direct-acting antiviral that inhibits RNA-dependent RNA

polymerase from severe acute respiratory syndrome coronavirus 2 with high potency J Biol Chem **295**, 6785-6797 10.1074/jbc.RA120.013679

41. Berger, I., Fitzgerald, D. J., and Richmond, T. J. (2004) Baculovirus expression system for heterologous multiprotein complexes Nat Biotechnol **22**, 1583-1587 10.1038/nbt1036
42. Tchesnokov, E. P., Raesisimakiani, P., Ngure, M., Marchant, D., and Gotte, M. (2018) Recombinant RNA-Dependent RNA Polymerase Complex of Ebola Virus Sci Rep **8**, 3970 10.1038/s41598-018-22328-3
43. Tchesnokov, E. P., Bailey-Elkin, B. A., Mark, B. L., and Gotte, M. (2020) Independent inhibition of the polymerase and deubiquitinase activities of the Crimean-Congo Hemorrhagic Fever Virus full-length L-protein PLoS Negl Trop Dis **14**, e0008283 10.1371/journal.pntd.0008283
44. Tchesnokov, E. P., Feng, J. Y., Porter, D. P., and Gotte, M. (2019) Mechanism of Inhibition of Ebola Virus RNA-Dependent RNA Polymerase by Remdesivir Viruses **11**, 10.3390/v11040326
45. Eydoux, C., Fattorini, V., Shannon, A., Le, T. T., Didier, B., Canard, B. *et al.* (2021) A fluorescence-based high throughput-screening assay for the SARS-CoV RNA synthesis complex J Virol Methods **288**, 114013 10.1016/j.jviromet.2020.114013
46. Todd, B., Tchesnokov, E. P., and Gotte, M. (2021) The active form of the influenza cap-snatching endonuclease inhibitor baloxavir marboxil is a tight binding inhibitor J Biol Chem **296**, 100486 10.1016/j.jbc.2021.100486
47. Monji, F., Al-Mahmood Siddiquee, A., and Hashemian, F. (2020) Can pentoxifylline and similar xanthine derivatives find a niche in COVID-19 therapeutic strategies? A ray of hope in the midst of the pandemic Eur J Pharmacol **887**, 173561 10.1016/j.ejphar.2020.173561
48. Feng, J. Y., Xu, Y., Barauskas, O., Perry, J. K., Ahmadyar, S., Stepan, G., Yu, H., Babusis, D., Park, Y., McCutcheon, K., Perron, M., Schultz, B. E., Sakowicz, R., and Ray, A. S. (2016) Role of Mitochondrial RNA Polymerase in the Toxicity of Nucleotide Inhibitors of Hepatitis C Virus. *Antimicrob Agents Chemother* **60**, 806-817

49. Arnold, J. J., Smidansky, E. D., Moustafa, I. M., and Cameron, C. E. (2012) Human mitochondrial RNA polymerase: structure-function, mechanism and inhibition *Biochim Biophys Acta* **1819**, 948-960 10.1016/j.bbagrm.2012.04.002
50. Shaker, B., Ahmad, S., Lee, J., Jung, C., and Na, D. (2021) In silico methods and tools for drug discovery *Comput Biol Med* **137**, 104851 10.1016/j.combiomed.2021.104851
51. Campagnola, G., Gong, P., and Peersen, O. B. (2011) High-throughput screening identification of poliovirus RNA-dependent RNA polymerase inhibitors *Antiviral Res* **91**, 241-251 10.1016/j.antiviral.2011.06.006
52. Lipinski, C. A., Lombardo, F., Dominy, B. W., and Feeney, P. J. (2001) Experimental and computational approaches to estimate solubility and permeability in drug discovery and development settings *Adv Drug Deliv Rev* **46**, 3-26 10.1016/s0169-409x(00)00129-0
53. Li, Y., Tian, Y., Xi, Y., Qin, Z., and Yan, A. (2020) Quantitative Structure-Activity Relationship Study for HIV-1 LEDGF/p75 Inhibitors *Curr Comput Aided Drug Des* **16**, 654-666 10.2174/1573409915666190919153959
54. Worachartcheewan, A., Prachayasittikul, V., Toropova, A. P., Toropov, A. A., and Nantasenamat, C. (2015) Large-scale structure-activity relationship study of hepatitis C virus NS5B polymerase inhibition using SMILES-based descriptors *Mol Divers* **19**, 955-964 10.1007/s11030-015-9614-2
55. Taoda, Y., Sato, A., Toba, S., Unoh, Y., Kawai, M., Sasaki, M. *et al.* (2023) Structure-activity relationship studies of anti-bunyaviral cap-dependent endonuclease inhibitors *Bioorg Med Chem Lett* **83**, 129175 10.1016/j.bmcl.2023.129175
56. Kaushik, N. K., Kaushik, N., Attri, P., Kumar, N., Kim, C. H., Verma, A. K. *et al.* (2013) Biomedical importance of indoles *Molecules* **18**, 6620-6662 10.3390/molecules18066620
57. Forrestall, K. L., Burley, D. E., Cash, M. K., Pottie, I. R., and Darvesh, S. (2021) 2-Pyridone natural products as inhibitors of SARS-CoV-2 main protease *Chem Biol Interact* **335**, 109348 10.1016/j.cbi.2020.109348
58. Queral-Beltran, A., Marín-García, M., Lacorte, S., and Tauler, R. (2023) UV-Vis absorption spectrophotometry and LC-DAD-MS-ESI(+)-ESI(-) coupled to chemometrics analysis of

the monitoring of sulfamethoxazole degradation by chlorination, photodegradation, and chlorination/photodegradation *Analytica Chimica Acta* **1276**, 341563

<https://doi.org/10.1016/j.aca.2023.341563>

59. Evers, C. E., Vonderach, M., Ferries, S., Jeacock, K., and Evers, P. A. (2018) Understanding protein–drug interactions using ion mobility–mass spectrometry *Current Opinion in Chemical Biology* **42**, 167-176 <https://doi.org/10.1016/j.cbpa.2017.12.013>
60. Jerabek-Willemsen, M., André, T., Wanner, R., Roth, H. M., Duhr, S., Baaske, P., and Breitsprecher, D. (2014) MicroScale Thermophoresis: Interaction analysis and beyond. *Journal of Molecular Structure* **1077**, 101-113
61. Xu, X., Peng, R., Peng, Q., Wang, M., Xu, Y., Liu, S., Tian, X., Deng, H., Tong, Y., Hu, X., Zhong, J., Wang, P., Qi, J., Gao, G. F., and Shi, Y. (2021) Cryo-EM structures of Lassa and Machupo virus polymerases complexed with cognate regulatory Z proteins identify targets for antivirals. *Nat Microbiol* **6**, 921-931
62. Kouba, T., Vogel, D., Thorkelsson, S. R., Quemin, E. R. J., Williams, H. M., Milewski, M., Busch, C., Gunther, S., Grunewald, K., Rosenthal, M., and Cusack, S. (2021) Conformational changes in Lassa virus L protein associated with promoter binding and RNA synthesis activity. *Nat Commun* **12**, 7018

Appendix

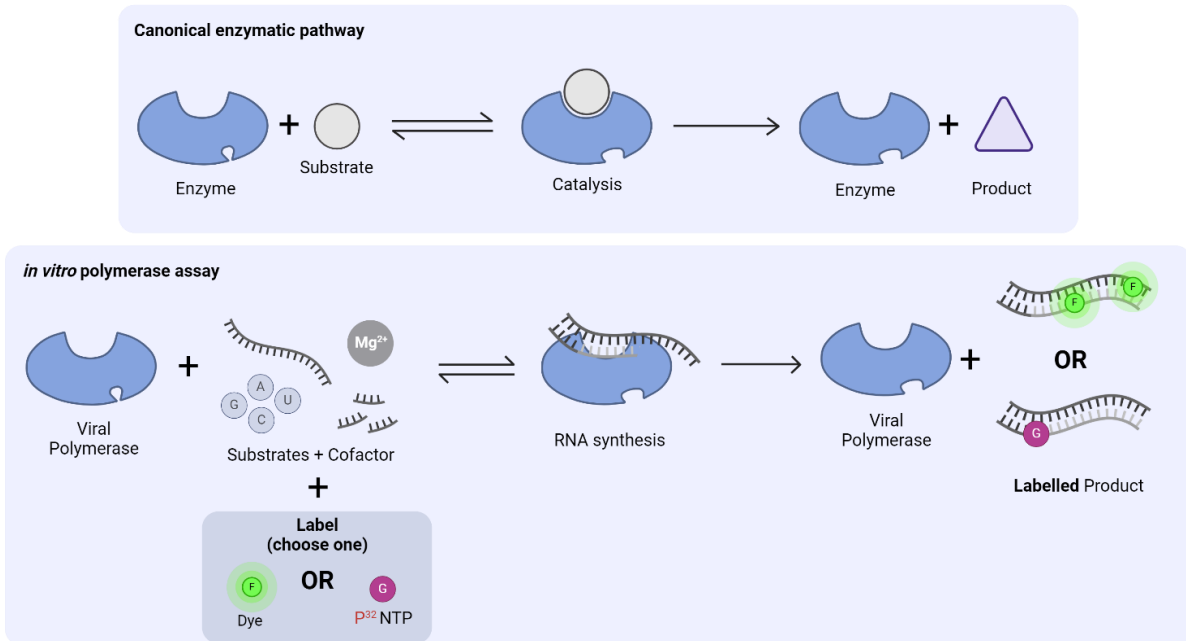


Figure 2.1 *In vitro* polymerase activity assays. Top panel: simplified enzyme catalytic pathway. Bottom panel: *in vitro* polymerase reaction set-up. Purified recombinant polymerase is incubated with substrates (primer, template, nucleotides, and Mg^{2+} co-factor) and a label. In the high-throughput assay (Methods section 2.2), PicoGreen dye fluoresces upon intercalation into double-stranded product RNA. Fluorescence can be monitored over time in a plate reader to quantify product formation. In the gel-based assay (Methods section 2.5), a radiolabelled nucleotide is incorporated into the product RNA. Labelled products can be separated via gel electrophoresis and visualized with a phospho-imager. Created with BioRender.

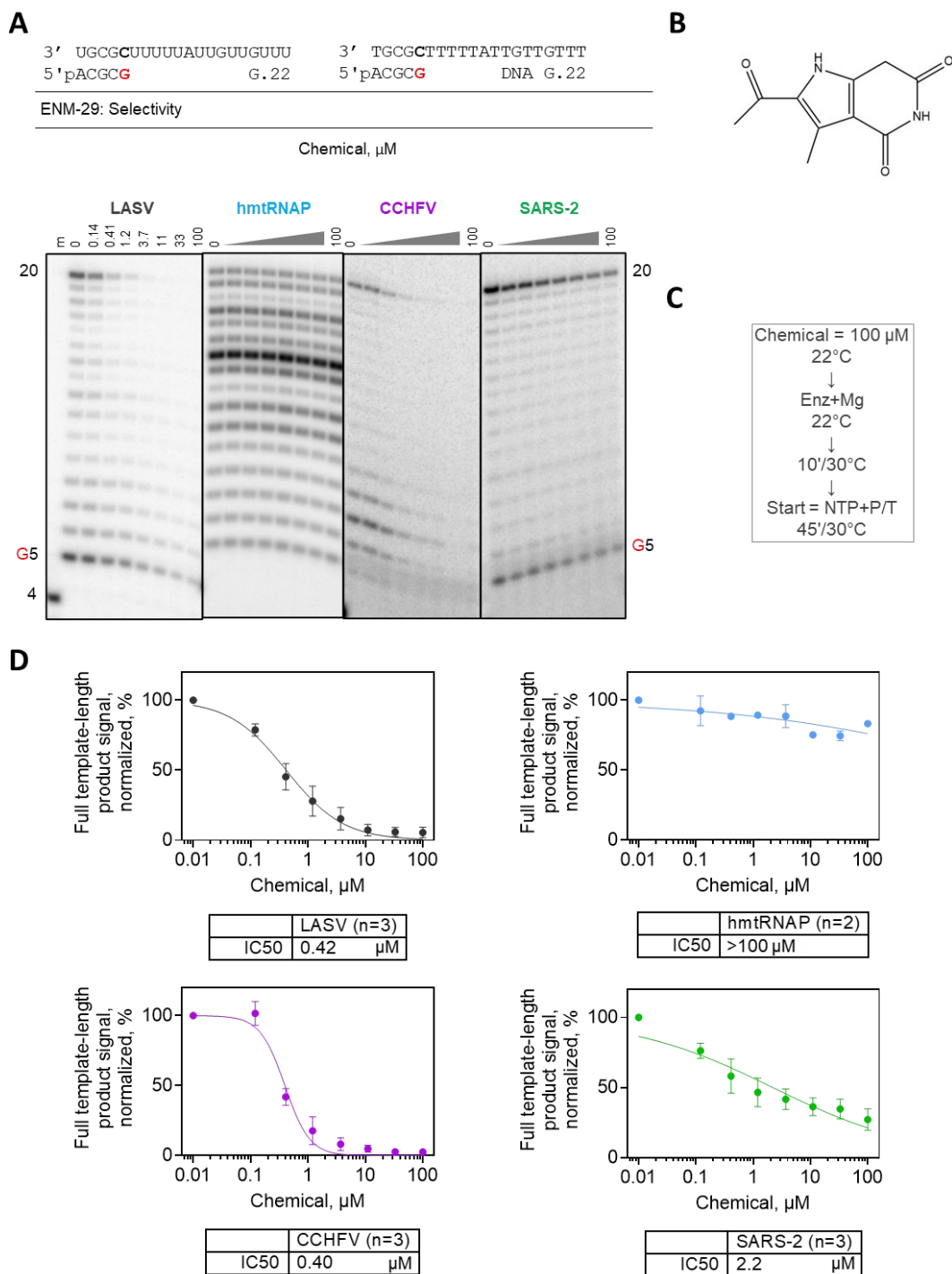


Figure 4.1.1 IC₅₀ of compound ENM-29 against LASV and other polymerases. A) Synthesis of full-template length product by various polymerases at increasing concentrations of chemical. 5'-phosphorylated templates and primers used are shown. A radiolabelled 4 nt RNA serves as a marker. Representative gels are shown for each polymerase. B) Chemical structure. C) Reaction set-up. D) Quantification of full-template length signal in A). IC₅₀ curves and values calculated with Prism software. Note A) and D) are colour-coordinated.

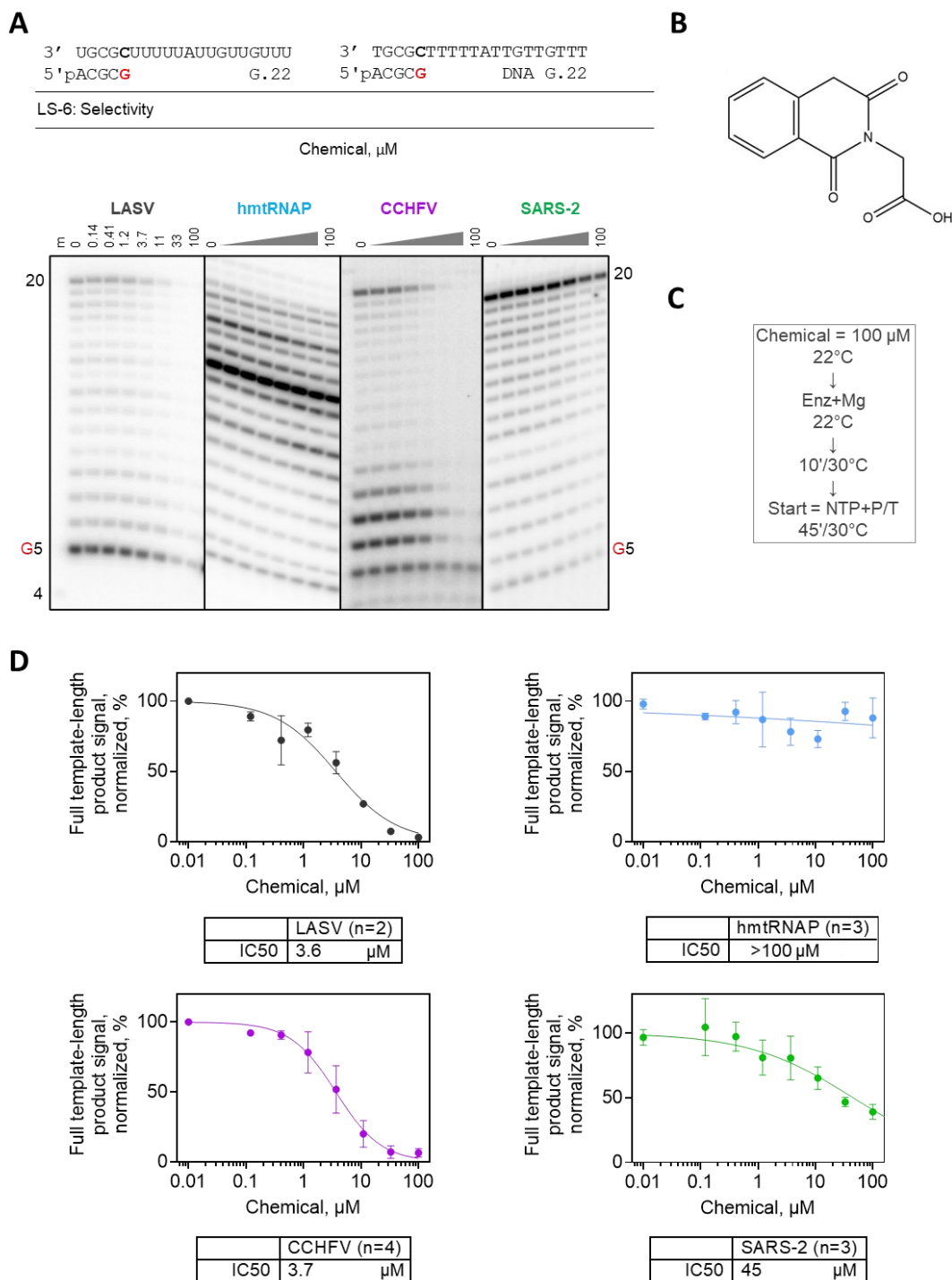


Figure 4.1.2 IC_{50} of compound LS-6 against LASV and other polymerases. A) Synthesis of full-template length product by various polymerases at increasing concentrations of chemical. 5'-phosphorylated templates and primers used are shown. A radiolabelled 4 nt RNA serves as a marker. Representative gels are shown for each polymerase. B) Chemical structure. C) Reaction set-up. D) Quantification of full-template length signal in A). IC_{50} curves and values calculated with Prism software. Note A) and D) are colour-coordinated.

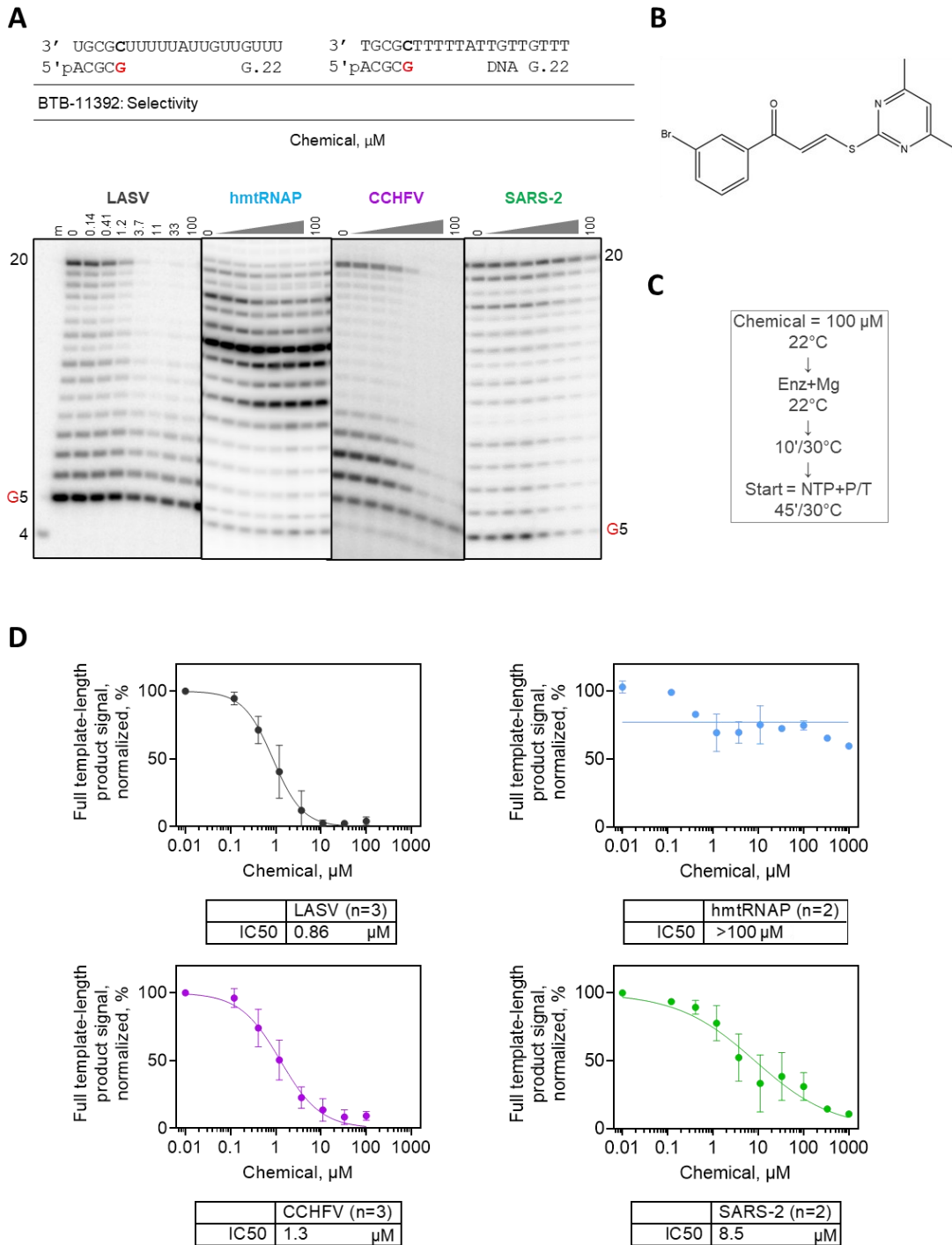


Figure 4.1.3 IC₅₀ of compound BTB-11392 against LASV and other polymerases. A) Synthesis of full-template length product by various polymerases at increasing concentrations of chemical. 5'-phosphorylated templates and primers used are shown. A radiolabelled 4 nt RNA serves as a marker. Representative gels are shown for each polymerase. B) Chemical structure. C) Reaction set-up. D) Quantification of full-template length signal in A). IC₅₀ curves and values calculated with Prism software. Note A) and D) are colour-coordinated.

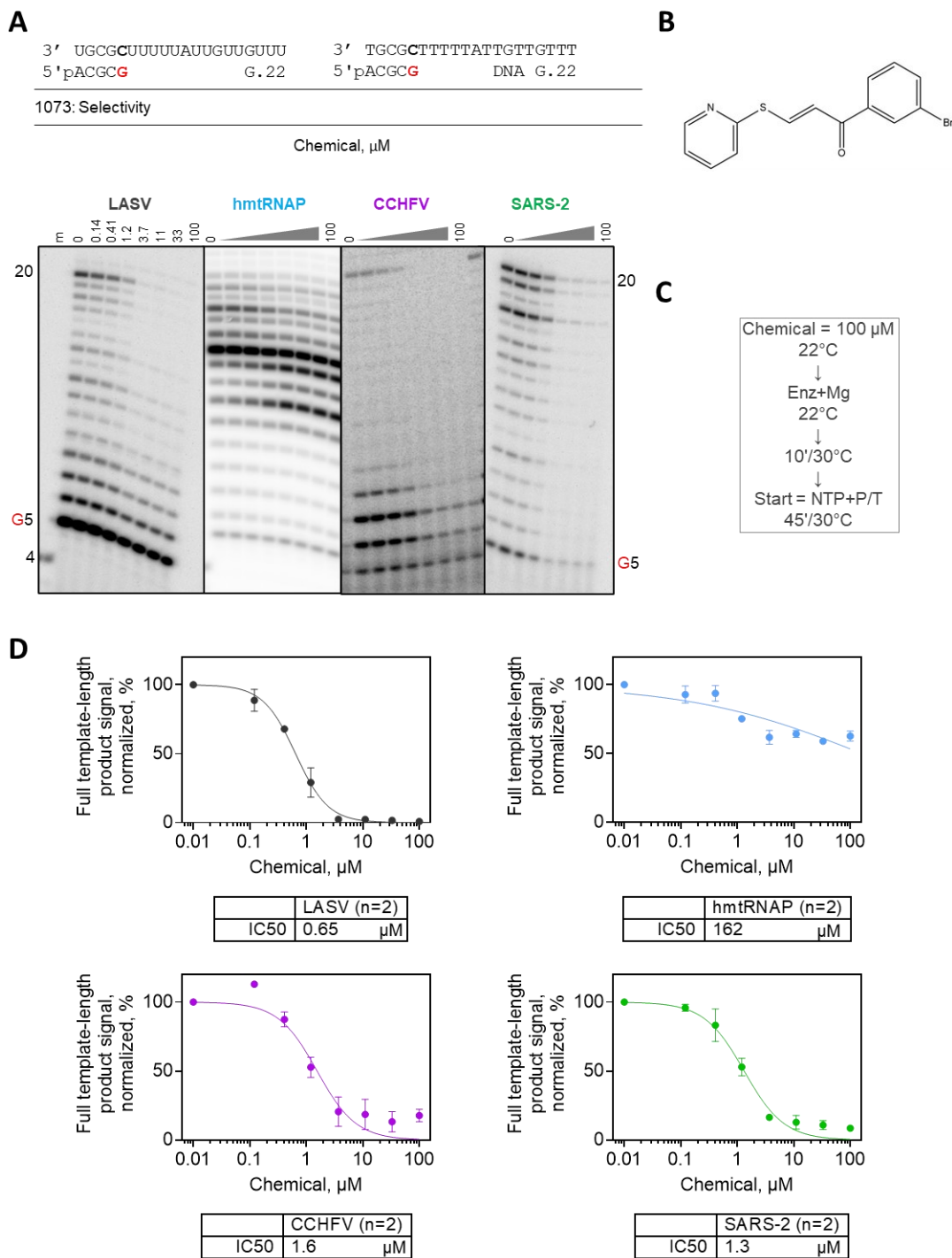


Figure 4.1.4 IC₅₀ of compound 1073 against LASV and other polymerases. A) Synthesis of full-template length product by various polymerases at increasing concentrations of chemical. 5'-phosphorylated templates and primers used are shown. A radiolabelled 4 nt RNA serves as a marker. Representative gels are shown for each polymerase. B) Chemical structure. C) Reaction set-up. D) Quantification of full-template length signal in A). IC₅₀ curves and values calculated with Prism software. Note A) and D) are colour-coordinated.

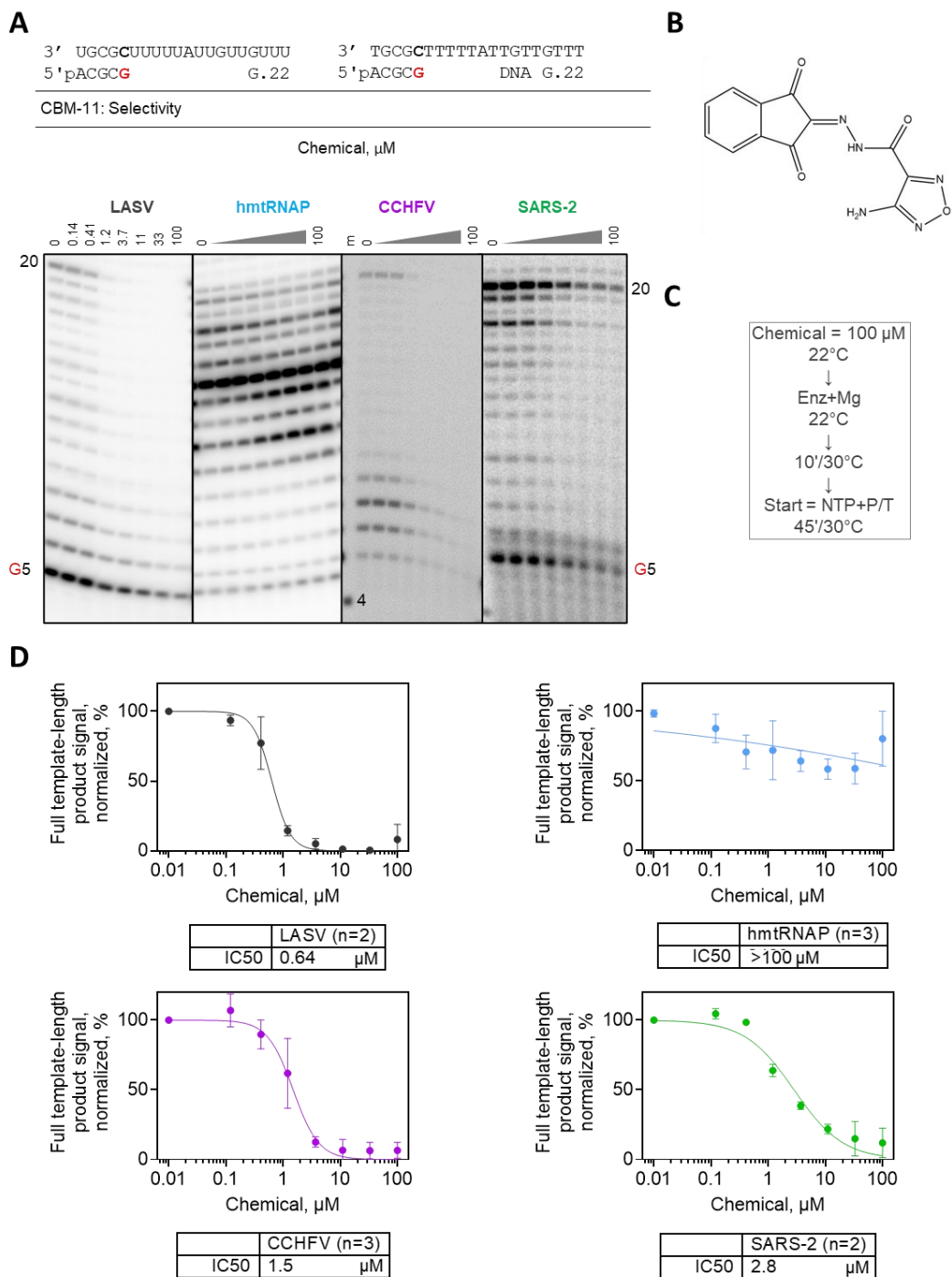


Figure 4.1.5 IC₅₀ of compound CBM-11 against LASV and other polymerases. A) Synthesis of full-template length product by various polymerases at increasing concentrations of chemical. 5'-phosphorylated templates and primers used are shown. A radiolabelled 4 nt RNA serves as a marker. Representative gels are shown for each polymerase. B) Chemical structure. C) Reaction set-up. D) Quantification of full-template length signal in A). IC₅₀ curves and values calculated with Prism software. Note A) and D) are colour-coordinated.

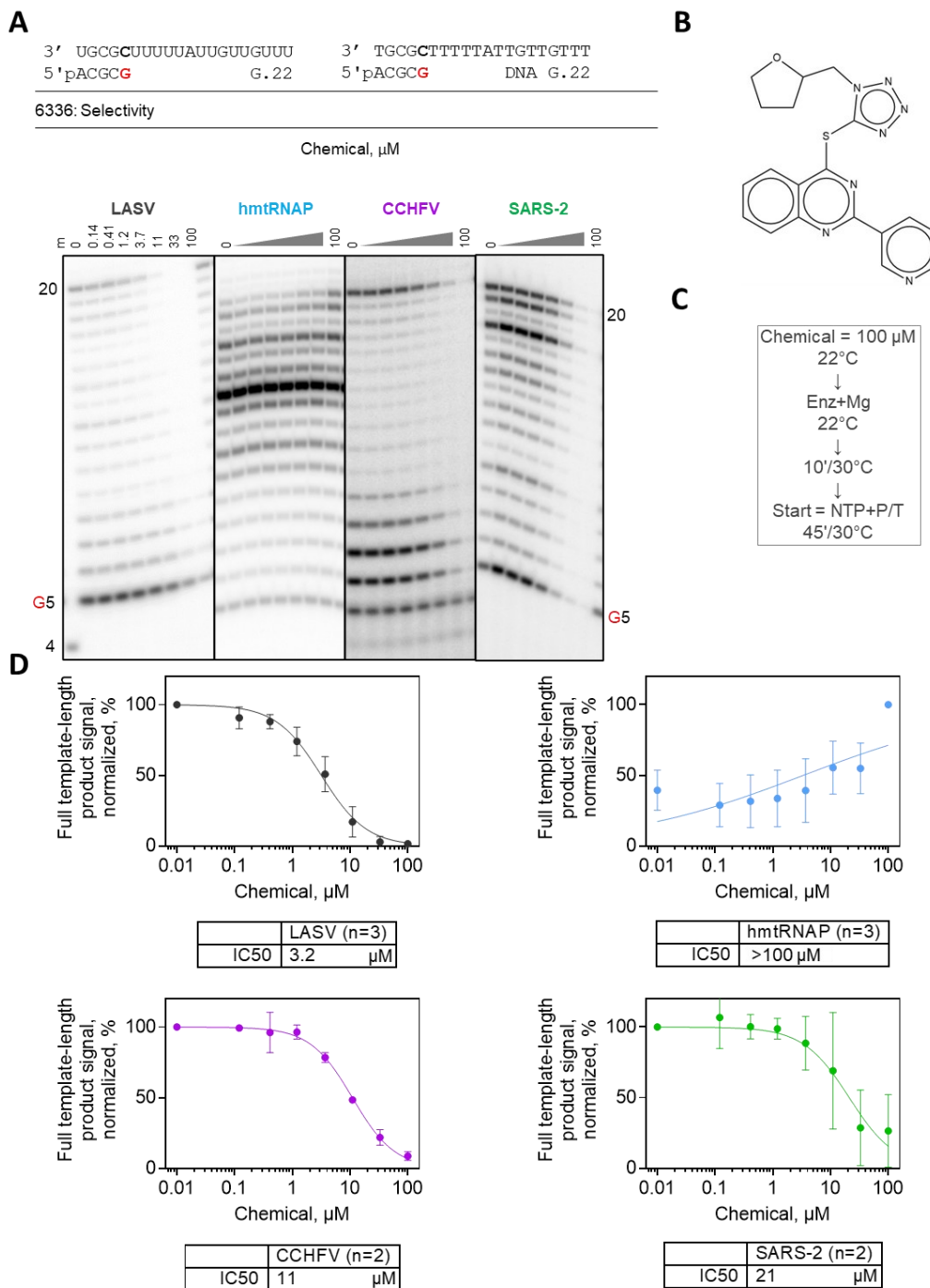


Figure 4.1.6 IC_{50} of compound 6336 against LASV and other polymerases. A) Synthesis of full-template length product by various polymerases at increasing concentrations of chemical. 5'-phosphorylated templates and primers used are shown. A radiolabelled 4 nt RNA serves as a marker. Representative gels are shown for each polymerase. B) Chemical structure. C) Reaction set-up. D) Quantification of full-template length signal in A). IC_{50} curves and values calculated with Prism software. Note A) and D) are colour-coordinated.

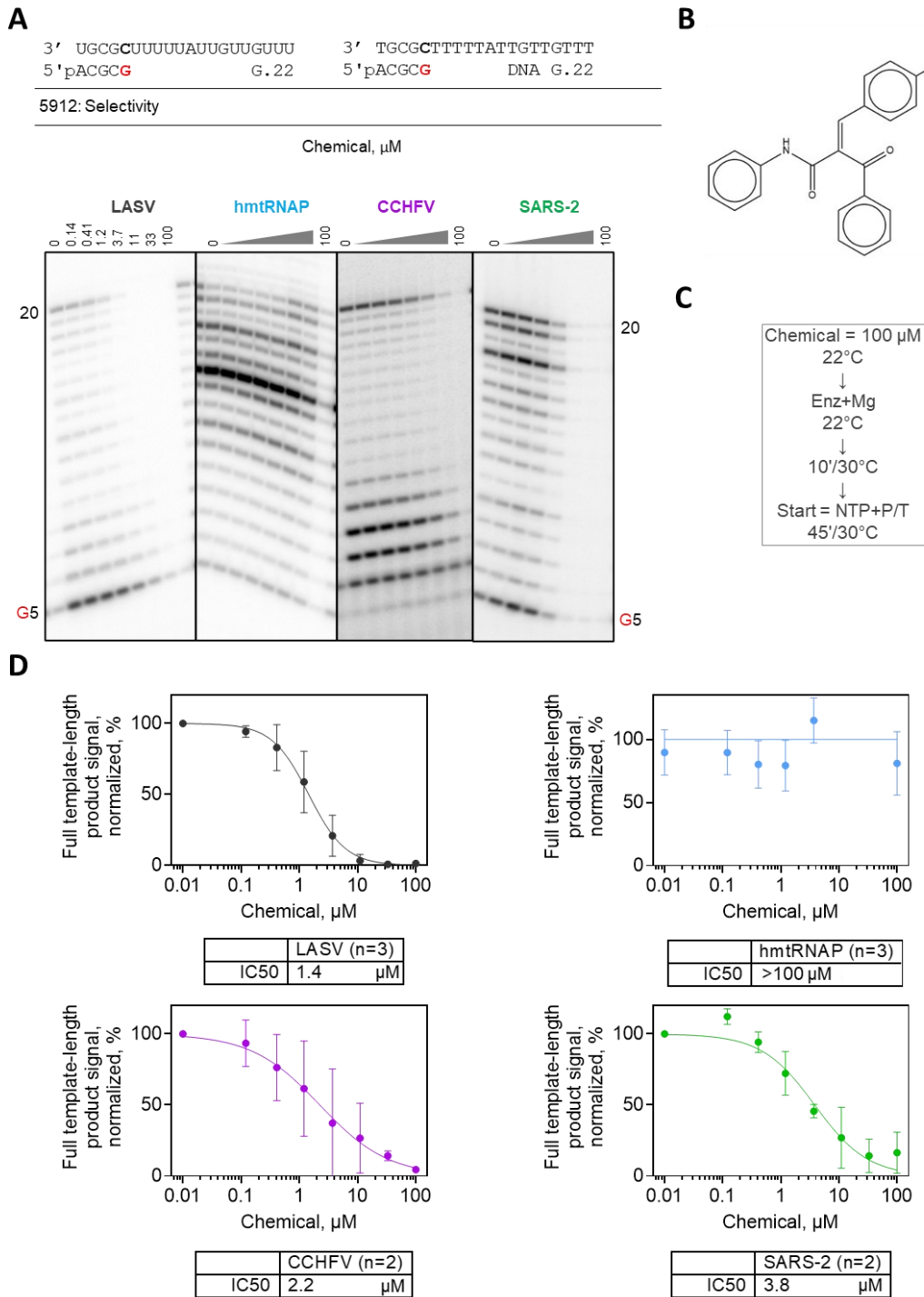


Figure 4.1.7 IC₅₀ of compound 5912 against LASV and other polymerases. A) Synthesis of full-template length product by various polymerases at increasing concentrations of chemical. 5'-phosphorylated templates and primers used are shown. A radiolabelled 4 nt RNA serves as a marker. Representative gels are shown for each polymerase. B) Chemical structure. C) Reaction set-up. D) Quantification of full-template length signal in A). IC₅₀ curves and values calculated with Prism software. Note A) and D) are colour-coordinated.

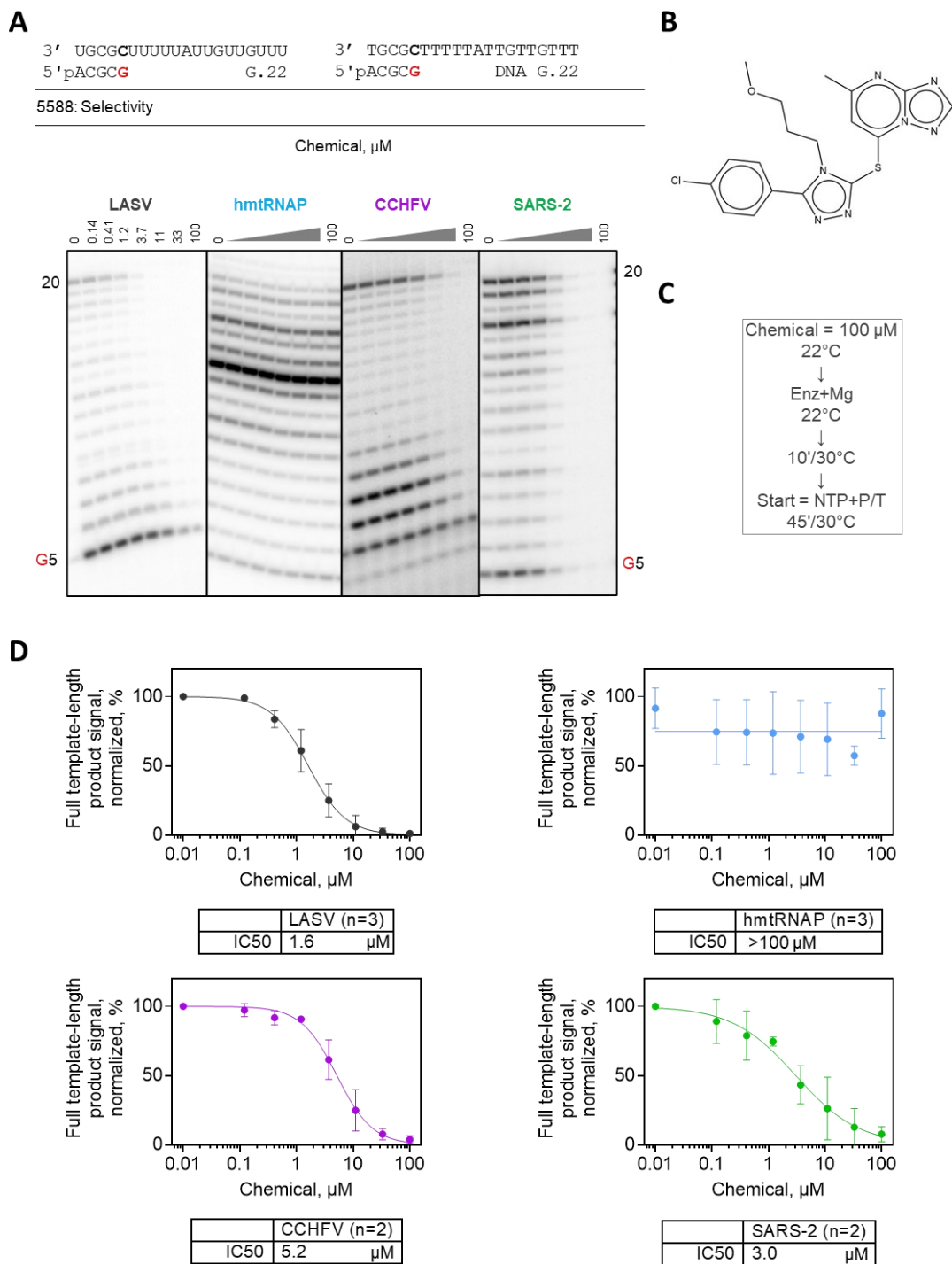


Figure 4.1.8 IC₅₀ of compound 5588 against LASV and other polymerases. A) Synthesis of full-template length product by various polymerases at increasing concentrations of chemical. 5'-phosphorylated templates and primers used are shown. A radiolabelled 4 nt RNA serves as a marker. Representative gels are shown for each polymerase. B) Chemical structure. C) Reaction set-up. D) Quantification of full-template length signal in A). IC₅₀ curves and values calculated with Prism software. Note A) and D) are colour-coordinated.

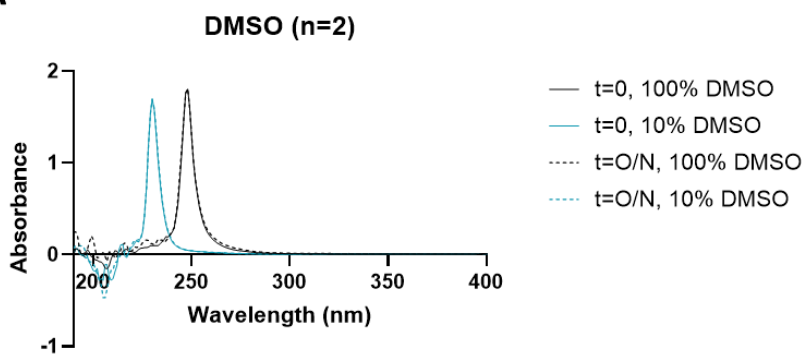
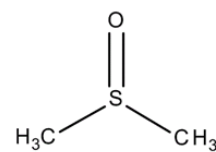
A**B**

Figure 4.2.1 Chemical stability of DMSO in DMSO and reaction buffer (10% DMSO) overnight. A) Absorbance spectrum of compound in DMSO (black) or reaction buffer (teal). Replicate spectra are plotted on the same graph. B) Chemical structure.

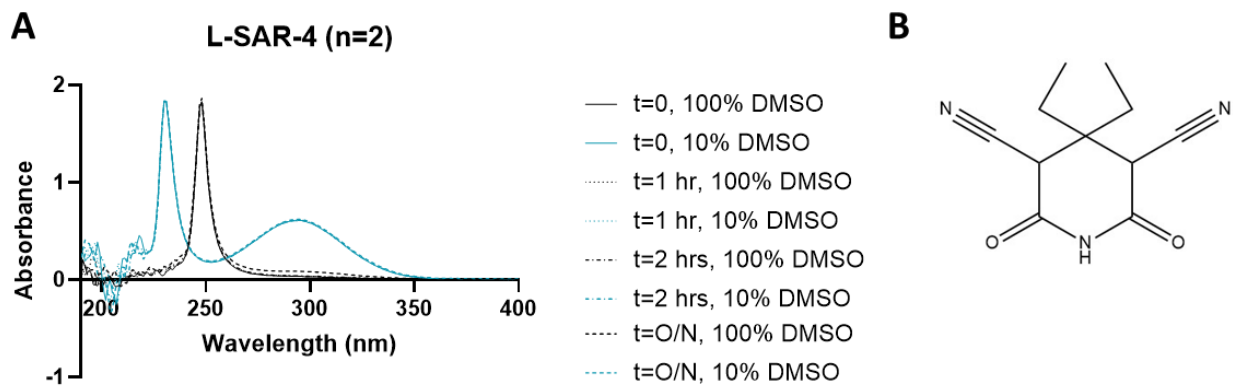


Figure 4.2.2 Chemical stability of L-SAR-4 in DMSO and reaction buffer (10% DMSO) overnight. A) Absorbance spectrum of compound in DMSO (black) or reaction buffer (teal). Replicate spectra are plotted on the same graph. B) Chemical structure.

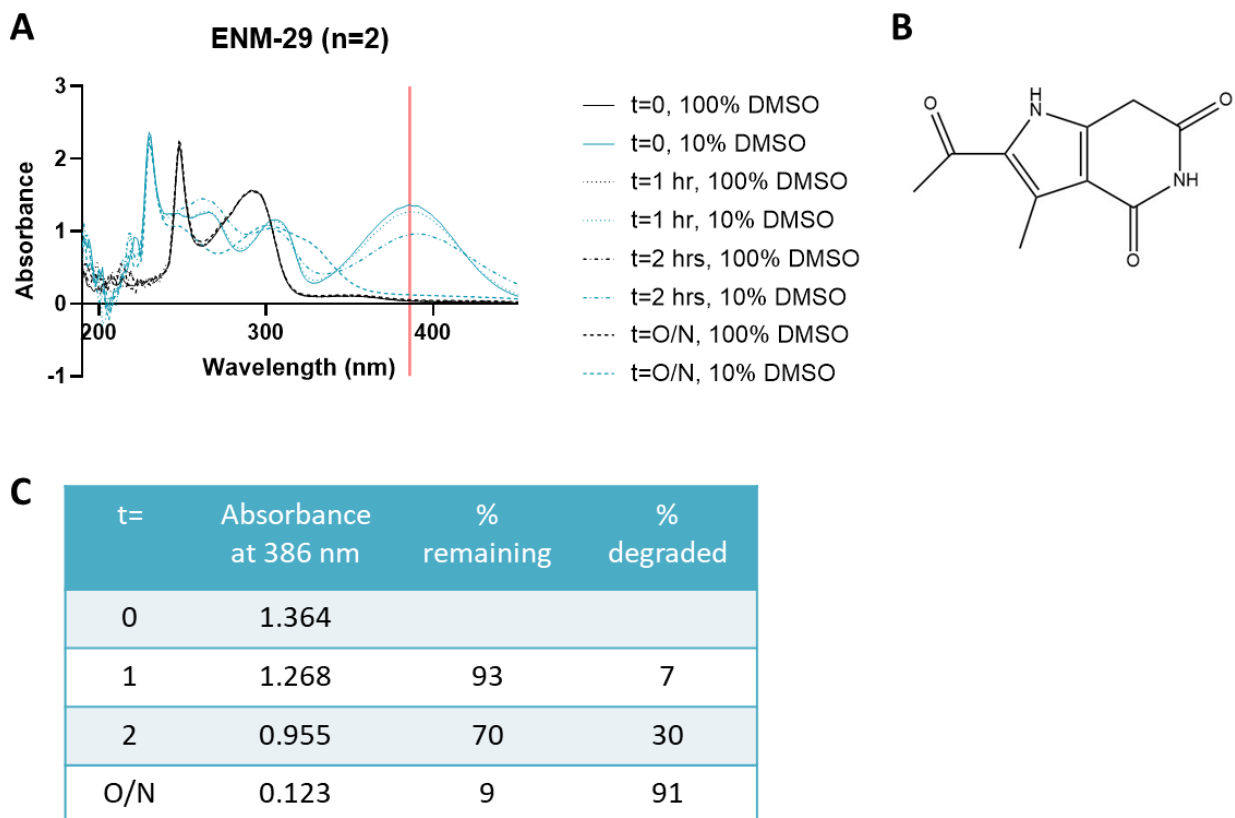


Figure 4.2.3 Chemical stability of ENM-29 in DMSO and reaction buffer (10% DMSO) overnight. A) Absorbance spectrum of compound in DMSO (black) or reaction buffer (10% DMSO) (teal). Replicate spectra are plotted on the same graph. B) Chemical structure. C) Degradation of compound over time, as calculated by disappearance of spectral peak indicated by red line in A).

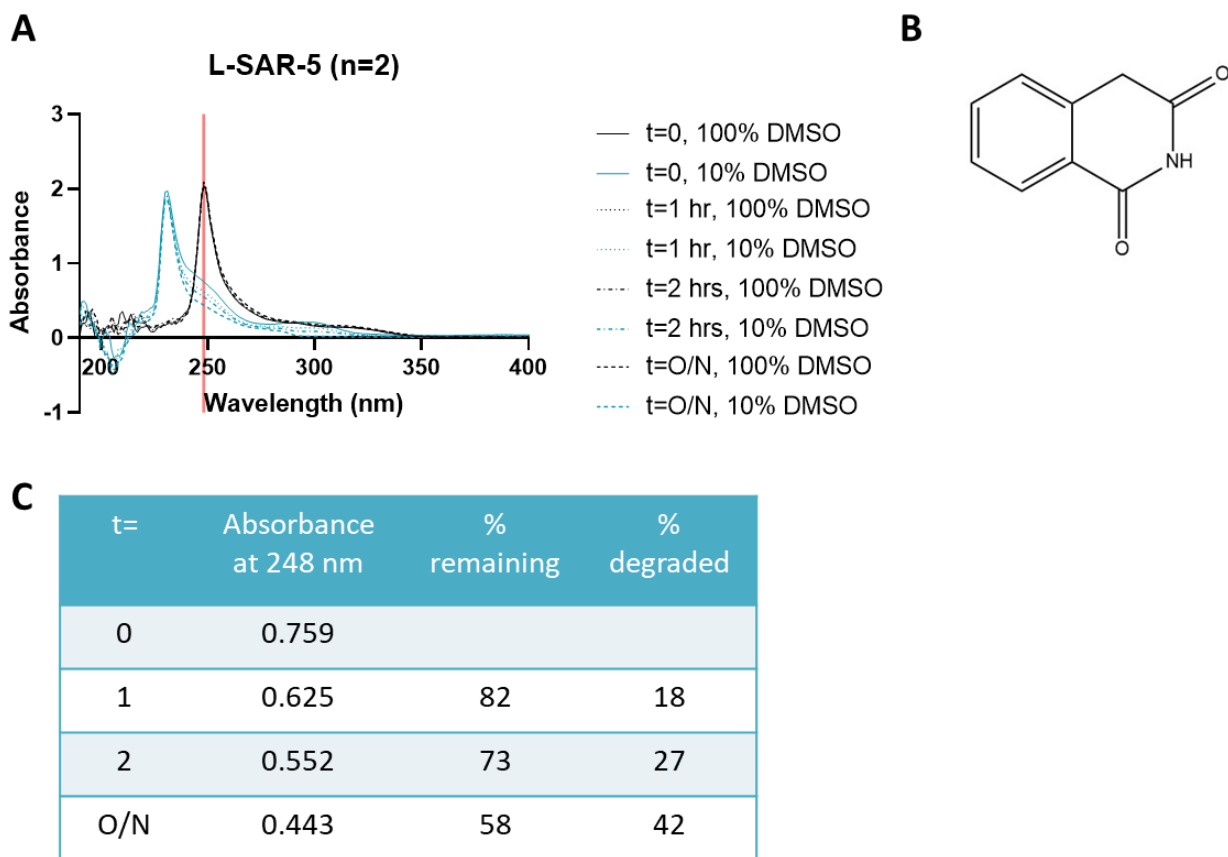


Figure 4.2.4 Chemical stability of L-SAR-5 in DMSO and reaction buffer (10% DMSO) overnight. A) Absorbance spectrum of compound in DMSO (black) or reaction buffer (10% DMSO). Replicate spectra are plotted on the same graph. B) Chemical structure. C) Degradation of compound over time, as calculated by disappearance of spectral peak indicated by red line in A).

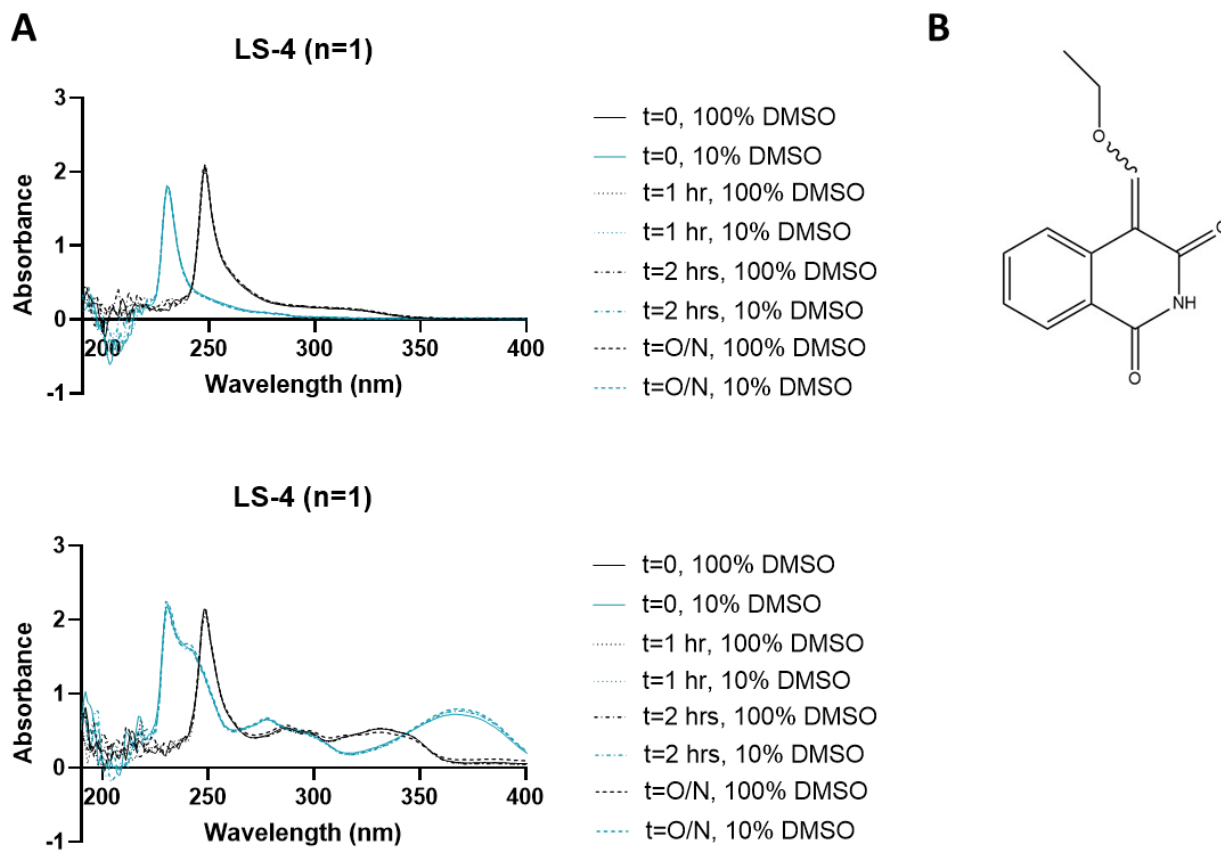


Figure 4.2.5 Chemical stability of LS-4 in DMSO and reaction buffer (10% DMSO) overnight. A) Absorbance spectrum of compound in DMSO (black) or reaction buffer (teal). Individual replicate spectra are shown due to poor reproducibility. B) Chemical structure.

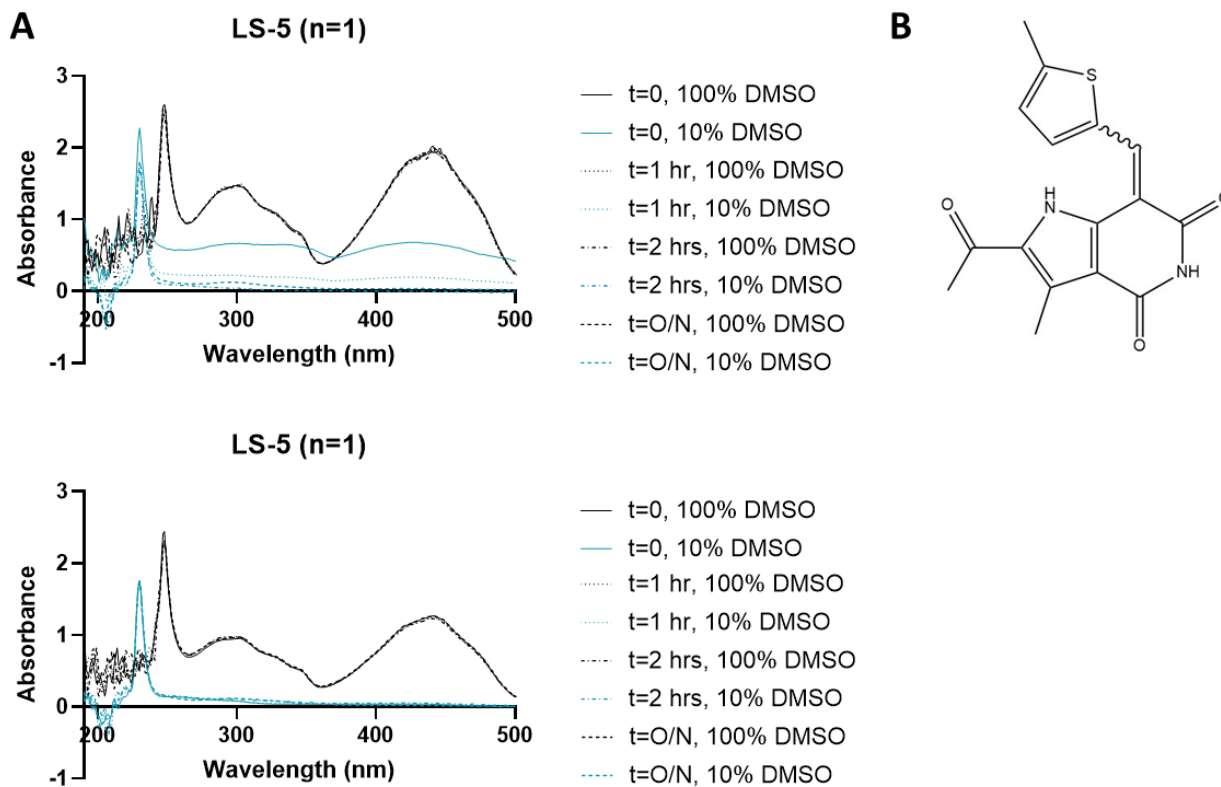


Figure 4.2.6 Chemical stability of LS-5 in DMSO and reaction buffer (10% DMSO) overnight. A) Absorbance spectrum of compound in DMSO (black) or reaction buffer (teal). Individual replicate spectra are shown due to poor reproducibility. B) Chemical structure.

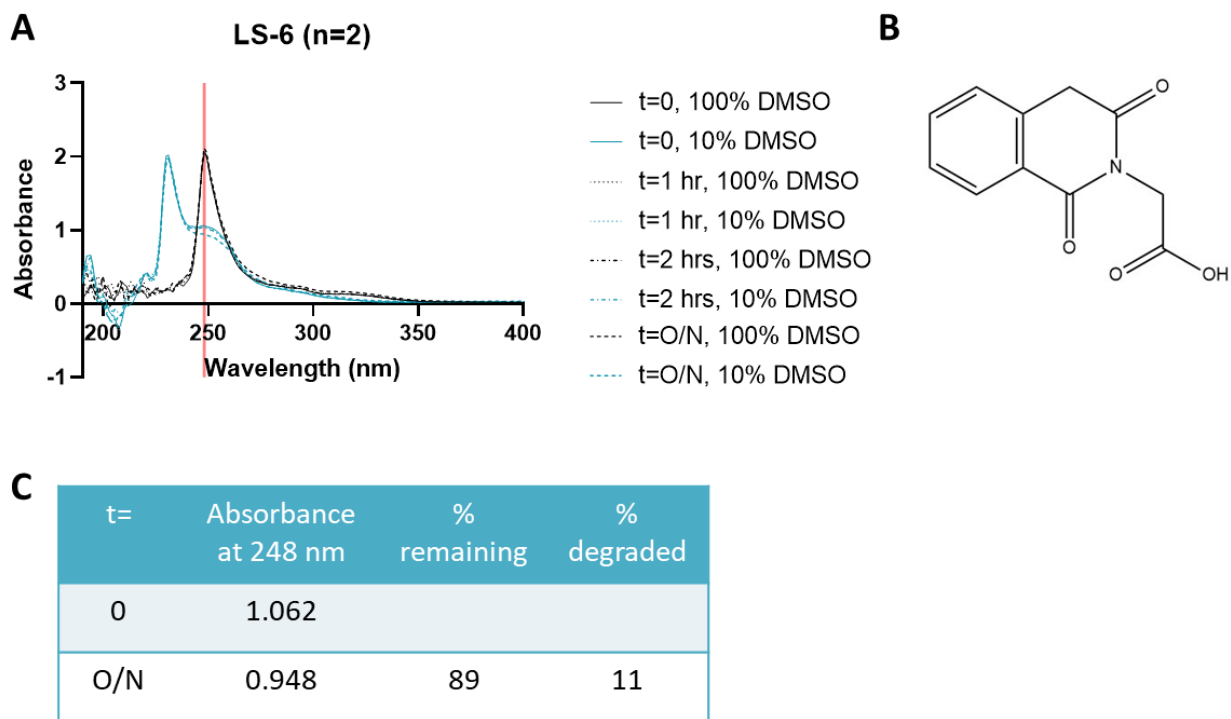


Figure 4.2.7 Chemical stability of LS-6 in DMSO and reaction buffer (10% DMSO) overnight. A) Absorbance spectrum of compound in DMSO (black) or reaction buffer (teal). Replicate spectra are plotted on the same graph. B) Chemical structure. C) Degradation of compound over time, as calculated by disappearance of spectral peak indicated by red line in A).

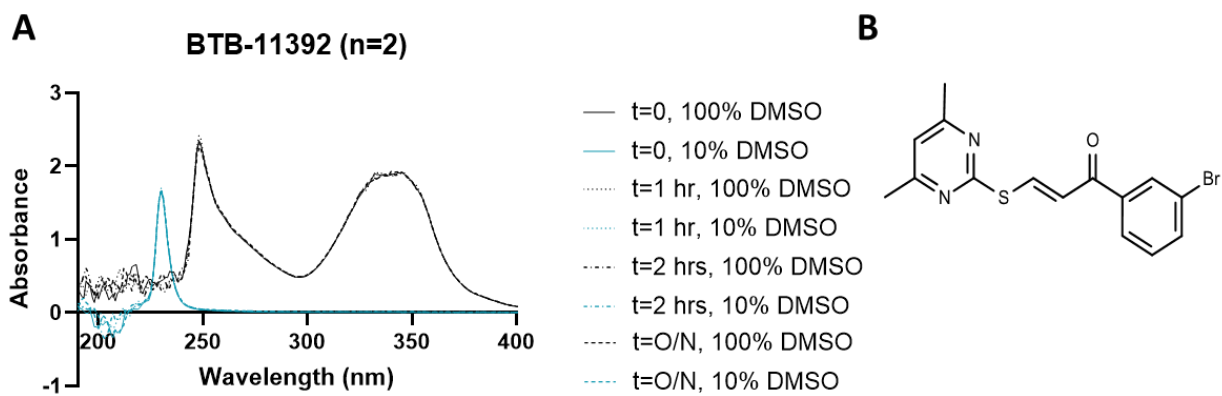


Figure 4.2.8 Chemical stability of BTB-11392 in DMSO and reaction buffer (10% DMSO) overnight. A) Absorbance spectrum of compound in DMSO (black) or reaction buffer (teal). Replicate spectra are plotted on the same graph. B) Chemical structure.

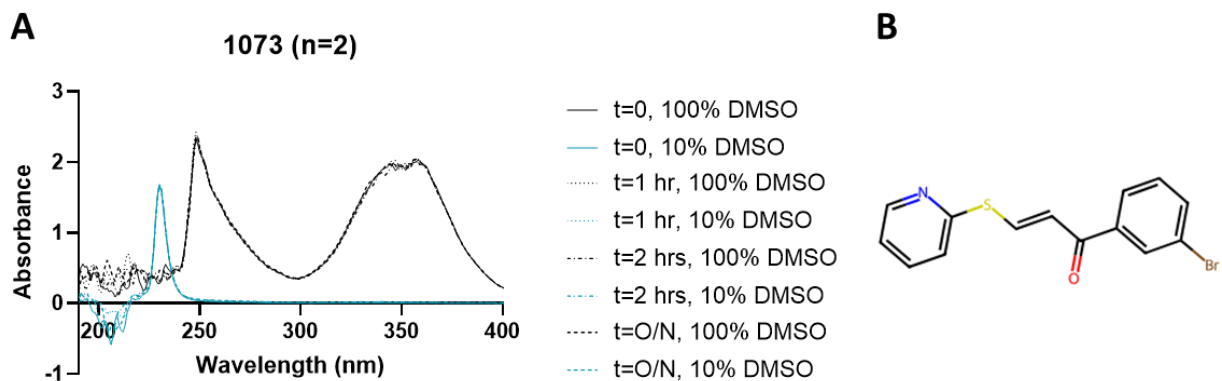


Figure 4.2.9 Chemical stability of 1073 in DMSO and reaction buffer (10% DMSO) overnight. A) Absorbance spectrum of compound in DMSO (black) or reaction buffer (teal). Replicate spectra are plotted on the same graph. B) Chemical structure.

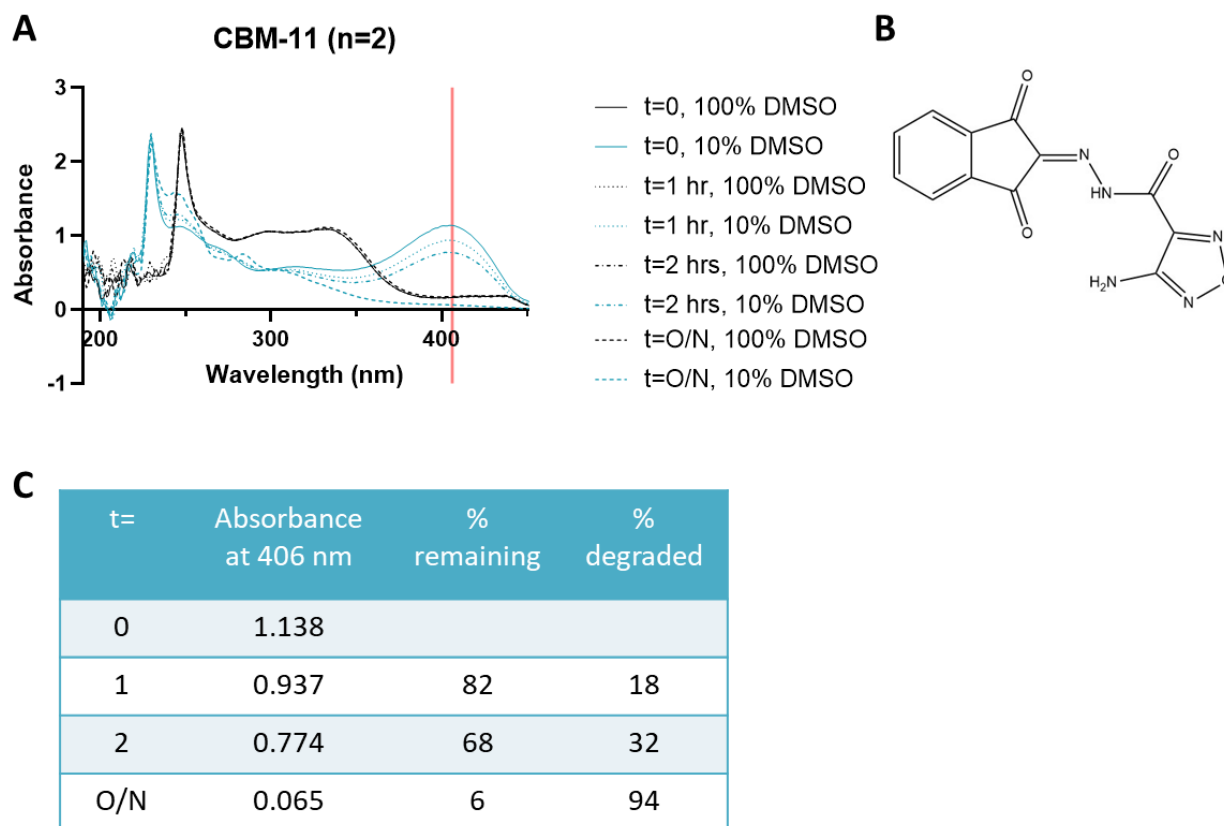


Figure 4.2.10 Chemical stability of CBM-11 in DMSO and reaction buffer (10% DMSO) overnight. A) Absorbance spectrum of compound in DMSO (black) or reaction buffer (teal). Replicate spectra are plotted on the same graph. B) Chemical structure. C) Degradation of compound over time, as calculated by disappearance of spectral peak indicated by red line in A).

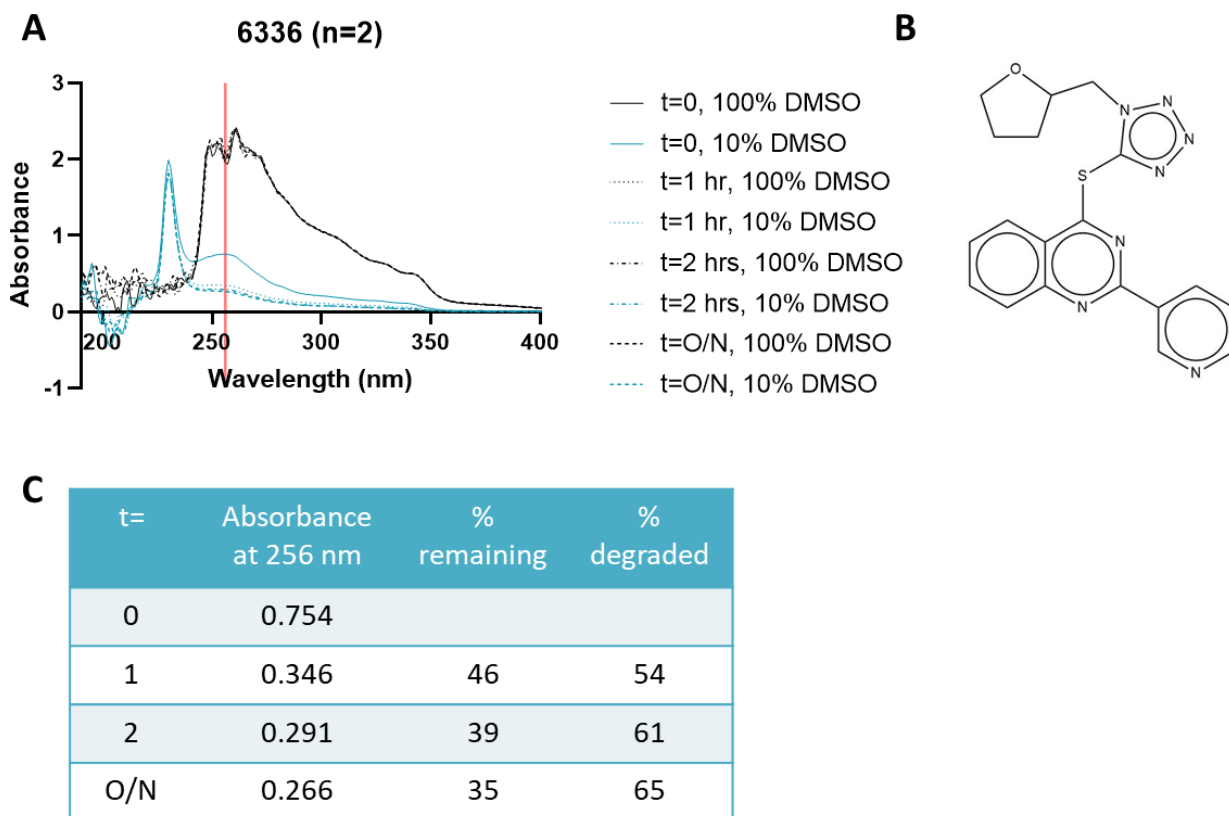


Figure 4.2.11 Chemical stability of 6336 in DMSO and reaction buffer (10% DMSO) overnight. A) Absorbance spectrum of compound in DMSO (black) or reaction buffer (teal). Replicate spectra are plotted on the same graph. B) Chemical structure. C) Degradation of compound over time, as calculated by disappearance of spectral peak indicated by red line in A).

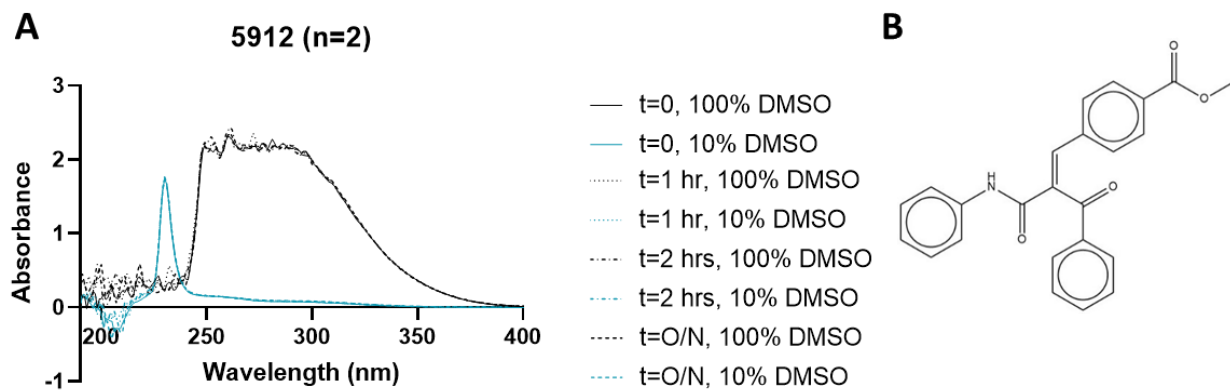


Figure 4.2.12 Chemical stability of 5912 in DMSO and reaction buffer (10% DMSO) overnight. A) Absorbance spectrum of compound in DMSO (black) or reaction buffer (teal). Replicate spectra are plotted on the same graph. B) Chemical structure.

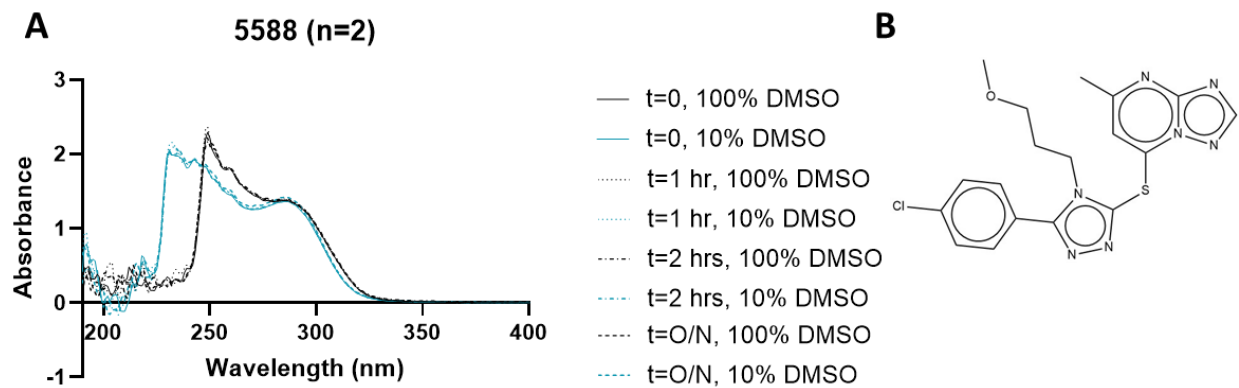


Figure 4.2.13 Chemical stability of 5588 in DMSO and reaction buffer (10% DMSO) overnight. A) Absorbance spectrum of compound in DMSO (black) or reaction buffer (teal). Replicate spectra are plotted on the same graph. B) Chemical structure.

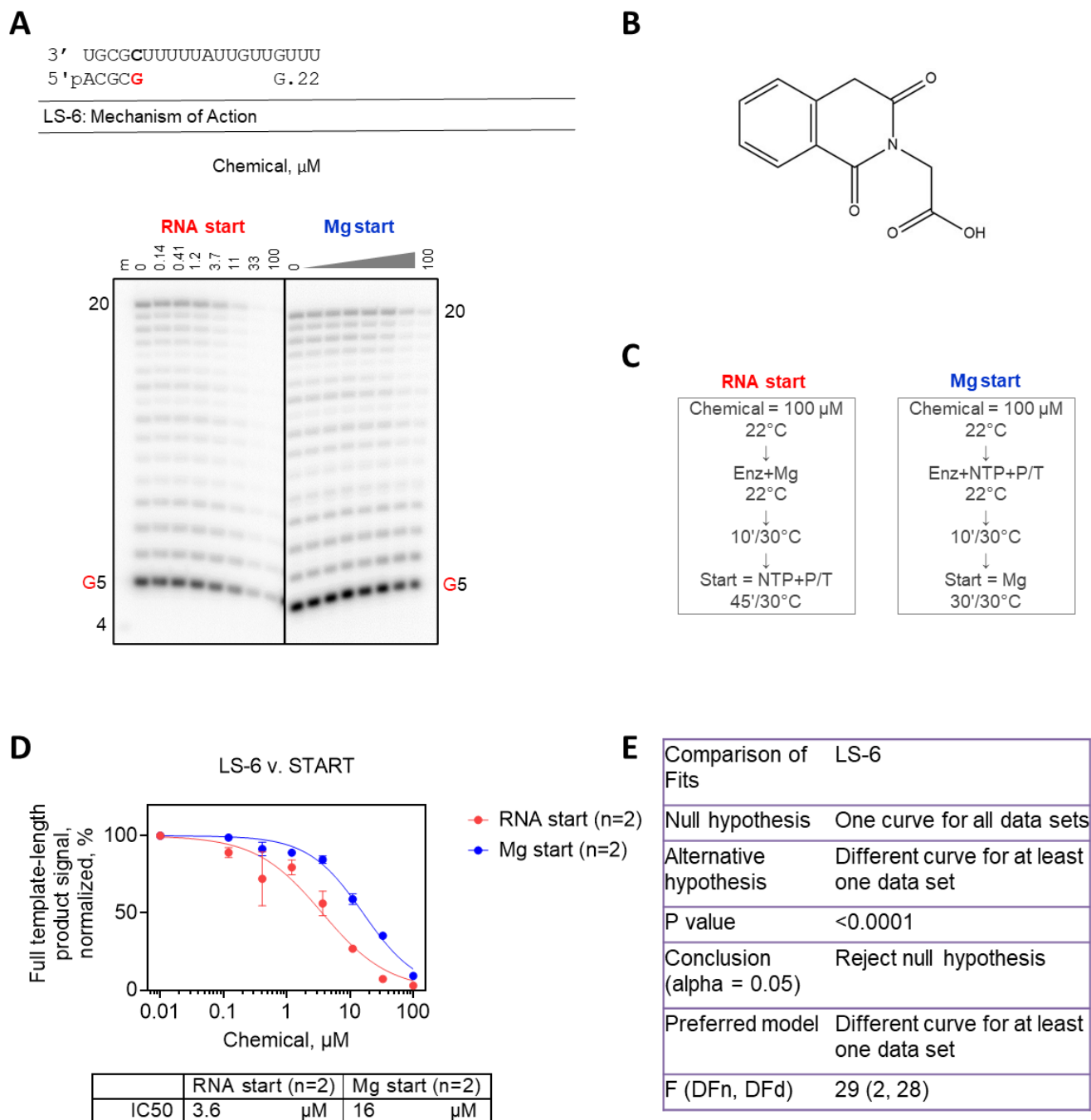
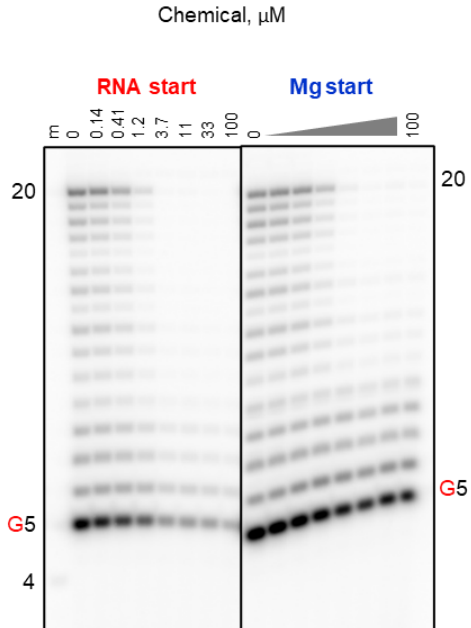
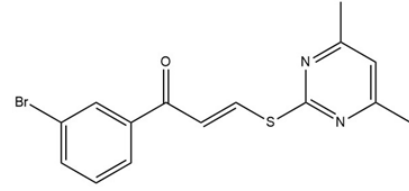
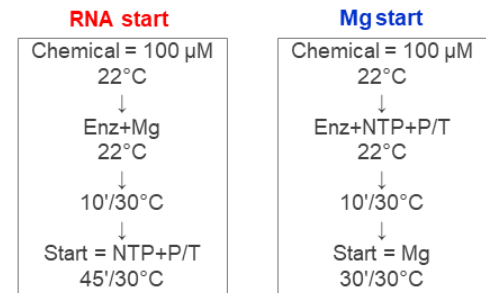
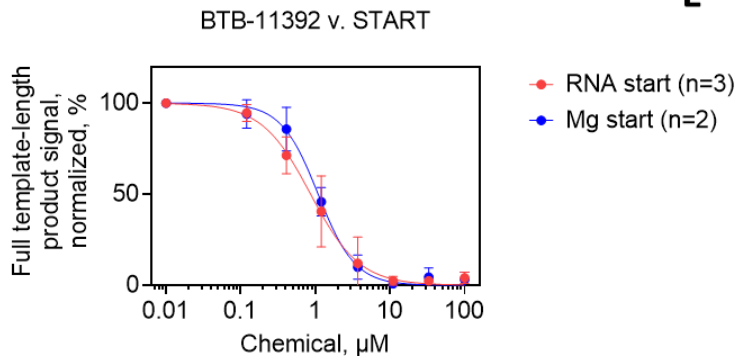


Figure 4.4.2 IC₅₀ of compound LS-6 against LASV under different reaction conditions. A) Synthesis of full-template length product at increasing concentrations of chemical. 5'-phosphorylated templates and primers used are shown. A radiolabelled 4 nt RNA serves as a marker. Representative gels are shown for both conditions. B) Chemical structure. C) Reaction schemes. D) Quantification of full-template length signal in A). IC₅₀ curves and values calculated with Prism software. E) Extra sum of squares F-test. Note A) and D) are colour-coordinated.

A

3' UGCGCUUUUUUUAUUGUUGUUU
 5' pACGCG G.22

BTB-11392: Mechanism of Action

**B****C****D**

	RNA start (n=3)	Mg start (n=2)
IC50	0.86 μM	1.1 μM

E

Comparison of BTB-11392 Fits	
Null hypothesis	One curve for all data sets
Alternative hypothesis	Different curve for at least one data set
P value	0.1173
Conclusion (alpha = 0.05)	Do not reject null hypothesis
Preferred model	One curve for all data sets
F (DFn, DFd)	2.3 (2, 36)

Figure 4.4.3 IC₅₀ of compound BTB-11392 against LASV under different reaction conditions. A) Synthesis of full-template length product at increasing concentrations of chemical. 5'-phosphorylated templates and primers used are shown. A radiolabelled 4 nt RNA serves as a marker. Representative gels are shown for both conditions. B) Chemical structure. C) Reaction schemes. D) Quantification of full-template length signal in A). IC₅₀ curves and values calculated with Prism software. E) Extra sum of squares F-test. Note A) and D) are colour-coordinated.

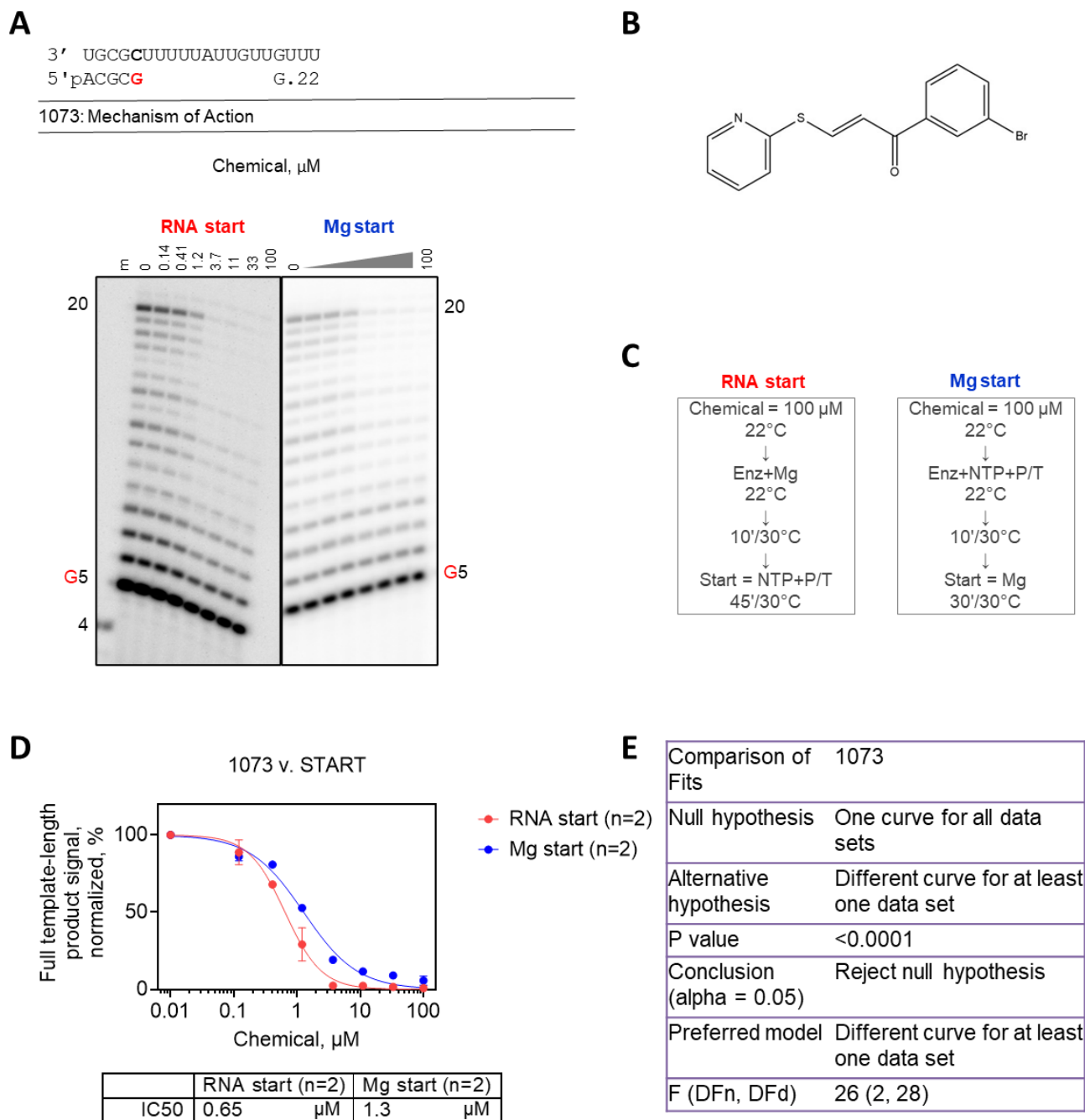


Figure 4.4.4 IC₅₀ of compound 1073 against LASV under different reaction conditions. A) Synthesis of full-template length product at increasing concentrations of chemical. 5'-phosphorylated templates and primers used are shown. A radiolabelled 4 nt RNA serves as a marker. Representative gels are shown for both conditions. B) Chemical structure. C) Reaction schemes. D) Quantification of full-template length signal in A). IC₅₀ curves and values calculated with Prism software. E) Extra sum of squares F-test. Note A) and D) are colour-coordinated.

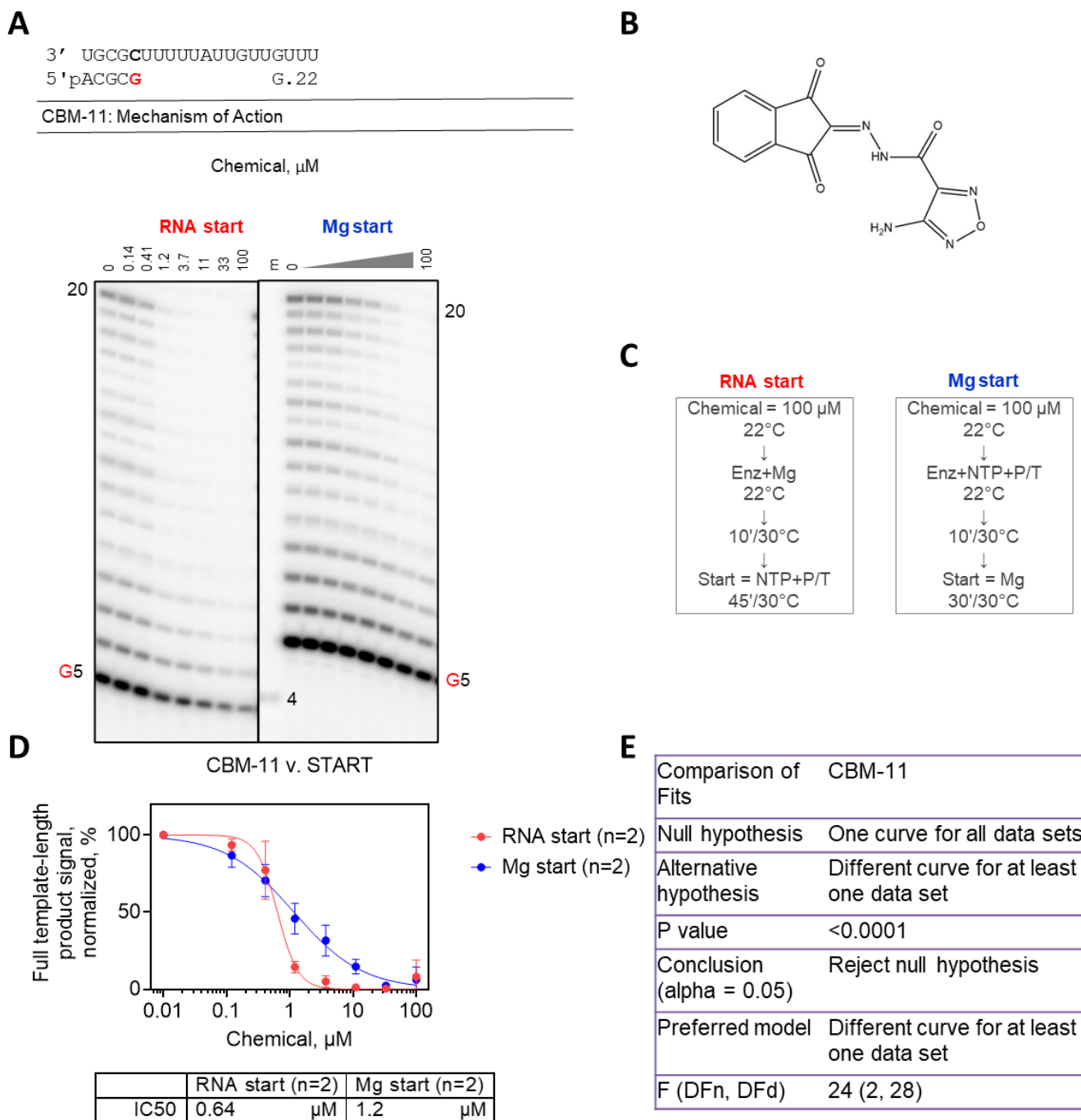


Figure 4.4.5 IC₅₀ of compound CBM-11 against LASV under different reaction conditions. A) Synthesis of full-template length product at increasing concentrations of chemical. 5'-phosphorylated templates and primers used are shown. A radiolabelled 4 nt RNA serves as a marker. Representative gels are shown for both conditions. B) Chemical structure. C) Reaction schemes. D) Quantification of full-template length signal in A). IC₅₀ curves and values calculated with Prism software. E) Extra sum of squares F-test. Note A) and D) are colour-coordinated.

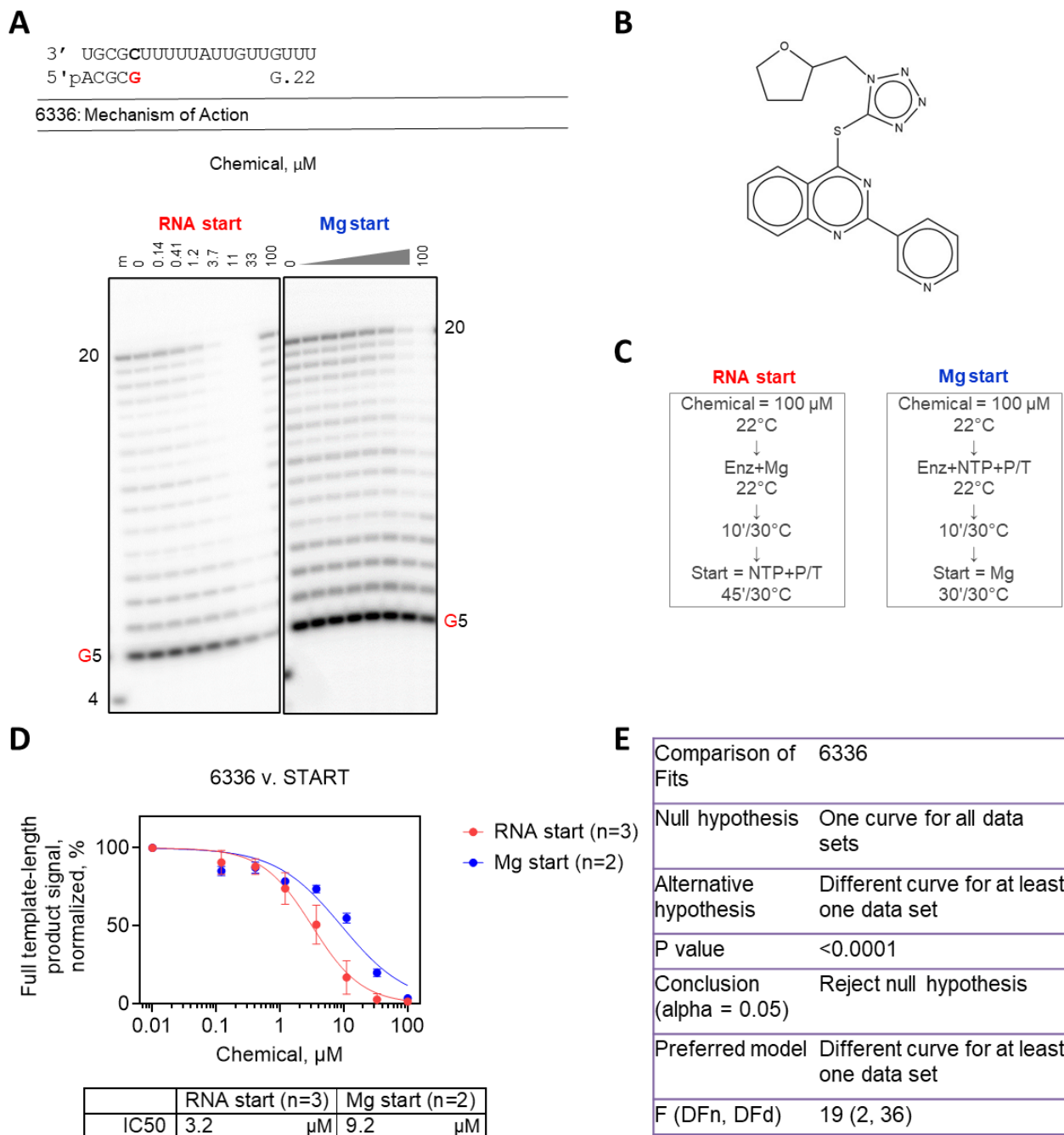


Figure 4.4.6 IC₅₀ of compound 6336 against LASV under different reaction conditions. A) Synthesis of full-template length product at increasing concentrations of chemical. 5'-phosphorylated templates and primers used are shown. A radiolabelled 4 nt RNA serves as a marker. Representative gels are shown for both conditions. B) Chemical structure. C) Reaction schemes. D) Quantification of full-template length signal in A). IC₅₀ curves and values calculated with Prism software. E) Extra sum of squares F-test. Note A) and D) are colour-coordinated.

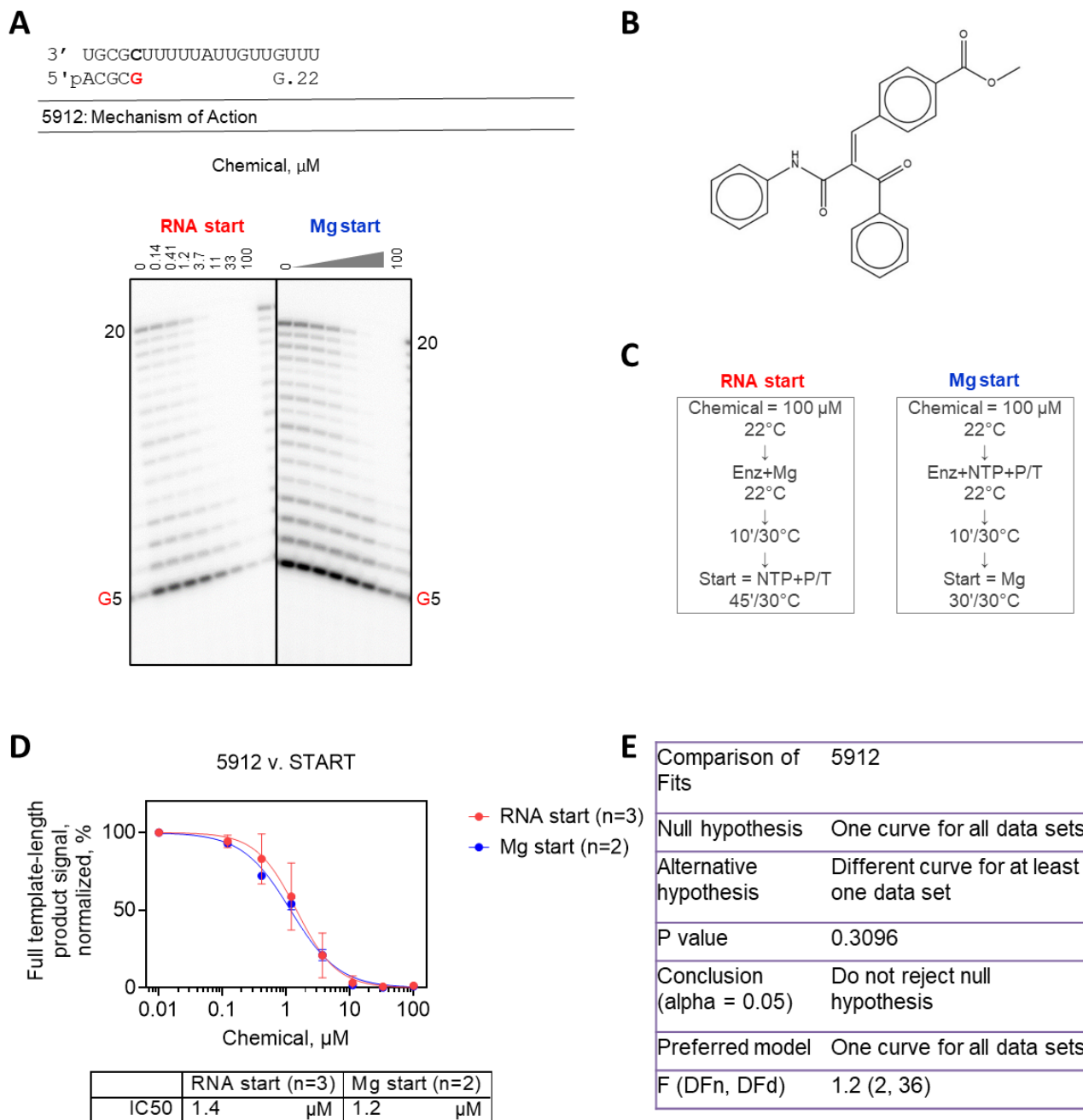


Figure 4.4.7 IC₅₀ of compound 5912 against LASV under different reaction conditions. A) Synthesis of full-template length product at increasing concentrations of chemical. 5'-phosphorylated templates and primers used are shown. A radiolabelled 4 nt RNA serves as a marker. Representative gels are shown for both conditions. B) Chemical structure. C) Reaction schemes. D) Quantification of full-template length signal in A). IC₅₀ curves and values calculated with Prism software. E) Extra sum of squares F-test. Note A) and D) are colour-coordinated.

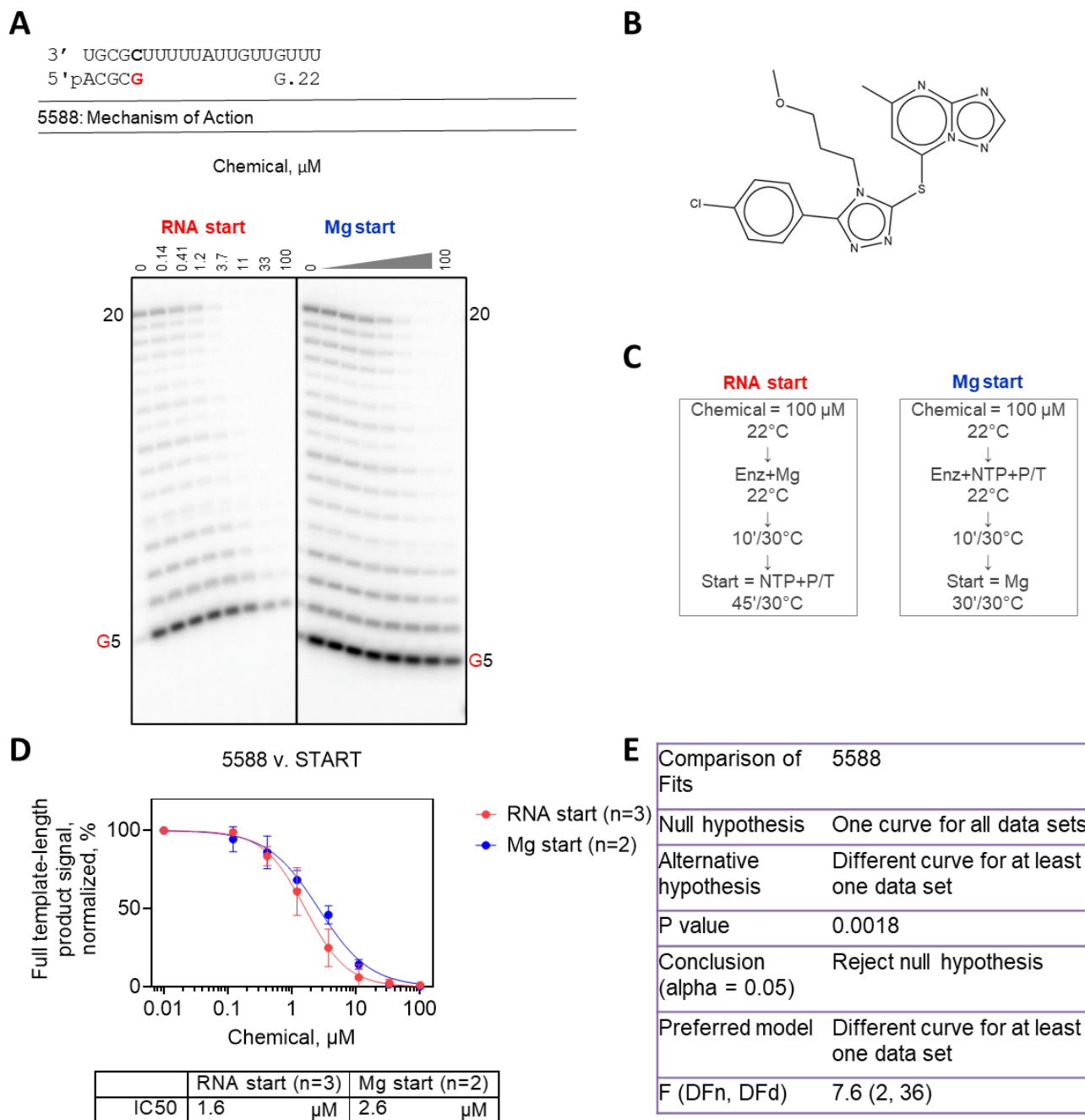


Figure 4.4.8 IC₅₀ of compound 5588 against LASV under different reaction conditions. A) Synthesis of full-template length product at increasing concentrations of chemical. 5'-phosphorylated templates and primers used are shown. A radiolabelled 4 nt RNA serves as a marker. Representative gels are shown for both conditions. B) Chemical structure. C) Reaction schemes. D) Quantification of full-template length signal in A). IC₅₀ curves and values calculated with Prism software. E) Extra sum of squares F-test. Note A) and D) are colour-coordinated.

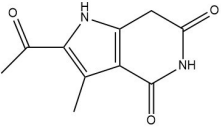
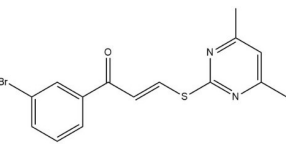
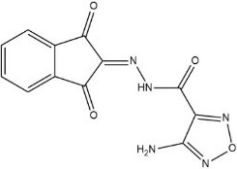
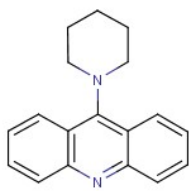
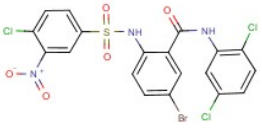
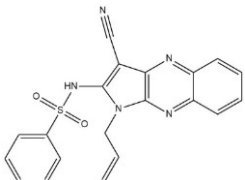
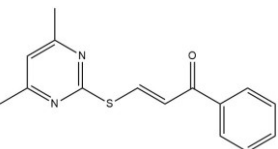
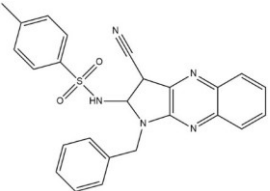
Table 2.1 Polymerase purification buffers

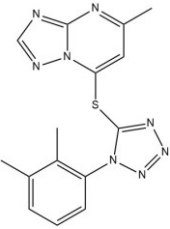
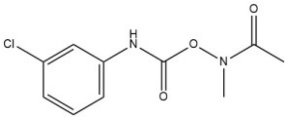
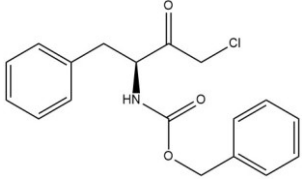
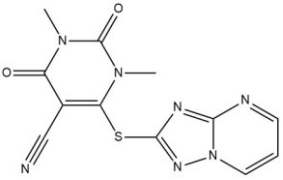
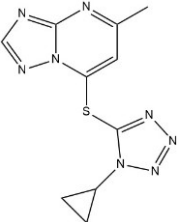
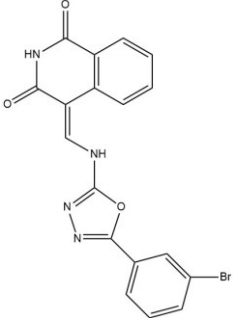
Buffer	Tris HCl, pH 8 (mM)	NaCl (mM)	KCl (mM)	TCEP (mM)	Tween20 (%)	Glycerol (%)	Imidazole (mM)	Sucrose (mM)	PI tablet
Lysis (Cytosolic)	100		100	5	0.1		25	250	yes
Lysis (Whole cell)	100	1000		7.5	1	10	25		yes
Equilibration/Wash	100	1000		5	0.01	10	25		no
Elution 50	100	150		5	0.01	10	50		no
Elution 100	100	150		5	0.01	10	100		no
Elution 200	100	150		5	0.01	10	200		no

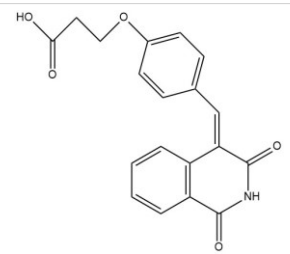
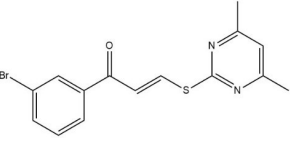
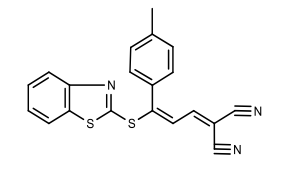
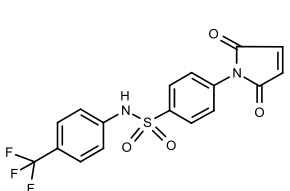
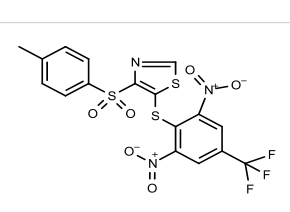
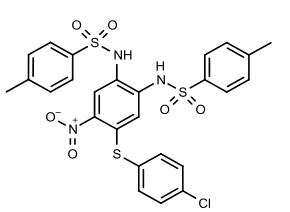
Table 2.2 *in vitro* polymerase activity assay conditions

Enzyme	ACU (μ M)	MgCl ₂ (mM)	0.01% TritonX-100	NaCl (mM)
LASV	0.1	5	yes	50
hmtRNAP	1	10	yes	50
CCHFV	10	5	no	N/A
SARS-2	0.1	1.6	yes	50

Table 3.1 Compounds with $\geq 80\%$ inhibition of LASV polymerase at 100 μM . Blank cells indicate n.d. (not determined). NI = no inhibition.

Structure	ID	% inhibition at 100 μM		% inhibition at 10 μM		IC50 (μM)	
		LASV	hmtRNAP	LASV	hmtRNAP	LASV	hmtRNAP
	ENM-29	95	16			0.42	NI
	BTB-11392					0.86	NI
	CBM-11	99				0.64	NI
	CBM-13	99				0.94	22
	CBM-14	99				5.6	11
	ENM-28	99	57			13	57
	SA-6	99	65				
	ENM-27	99	90				

Structure	ID	% inhibition at 100 μ M		% inhibition at 10 μ M		IC50 (μ M)	
		LASV	hmtRNAP	LASV	LASV	hmtRNAP	
	ENM-43	98			1.2	5.4	
	CBM-12	98			4.4	105	
	SA-2	98	98				
	ENM-44	97			2.5	3.1	
	ENM-70	96			2.5	58	
	ENM-32	96	31		12	>100	

Structure	ID	% inhibition at 100 μ M		% inhibition at 10 μ M		IC50 (μ M)	
		LASV	hmtRNAP	LASV		LASV	hmtRNAP
	ENM-72	81				5.6	8.8
	BTB 11392	99		97		0.86	NI
	BTB 11276	99		92			
	GK 01394	98		99		0.43	0.88*
	DFP 00110	98		96			
	BTB 08547	98		81			

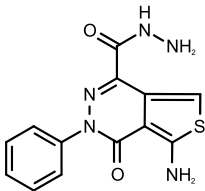
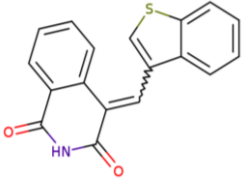
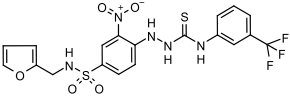
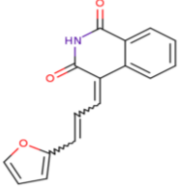
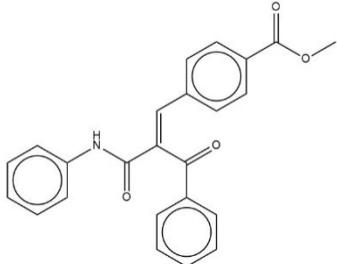
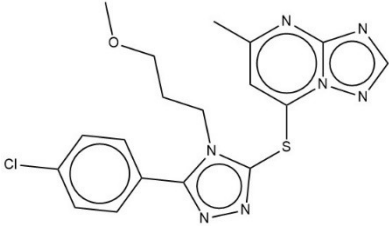
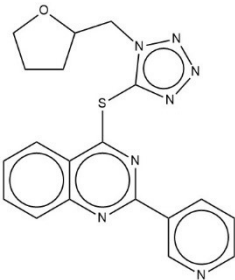
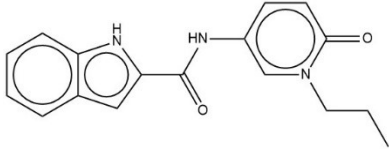
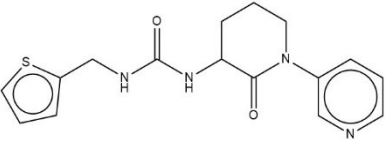
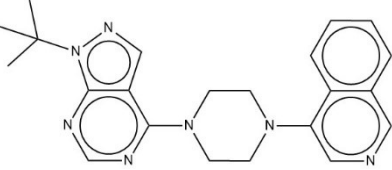
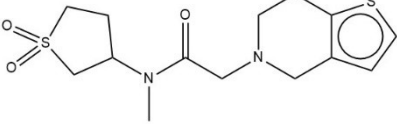
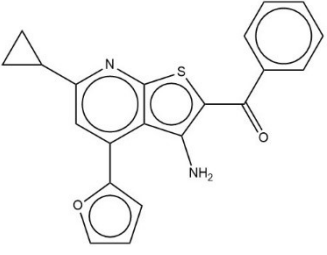
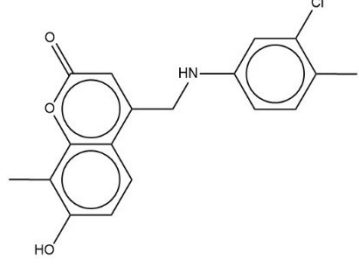
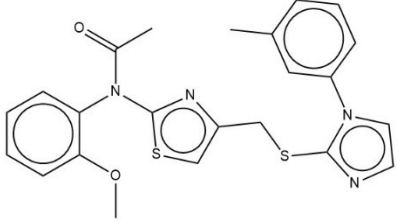
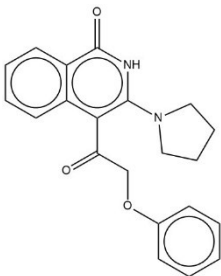
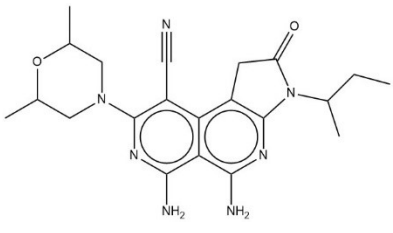
Structure	ID	% inhibition at 100 μ M		% inhibition at 10 μ M		IC50 (μ M)	
		LASV	hmtRNAP	LASV		LASV	hmtRNAP
	HTS 01525	98		58			
	Z217147340	98		43			
	BLT 00211	97		7			
	Z907712176	87		69	11	47*	

Table 3.2 Representative compounds from 16 distinct structural groups. Blank cells indicate n.d. (not determined). NI = no inhibition.

Structure	ID	% inhibition at 100 μ M		IC50 vs LASV (μ M)
		LASV	hmtRNAP	
	5912	99		1.4
	5588	98		1.6
	6336	97		3.2
	ENM-58	0		ND
	702	0		NI
	ENM-71	0		ND

Structure	ID	% inhibition at 100 μ M		IC50 vs LASV (μ M)
		LASV	hmtRNAP	
	2210	0		NI
	8902	32		266
	7891	47		108
	8094	0		NI
	ENM-80			ND, never recv'd
	5949	0		NI

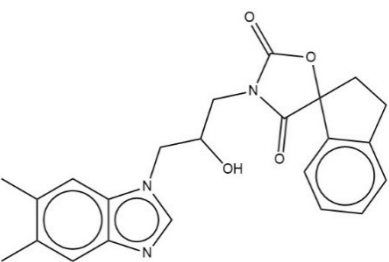
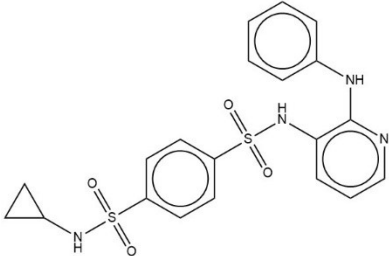
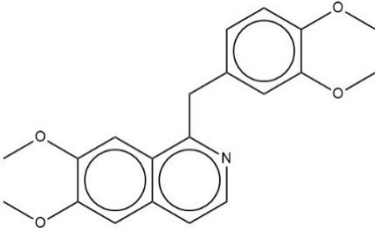
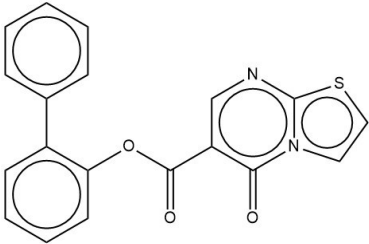
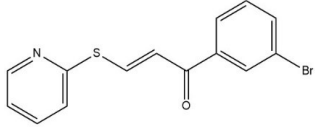
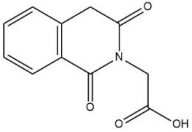
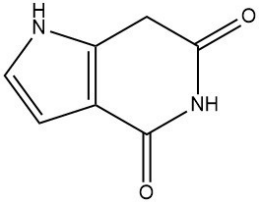
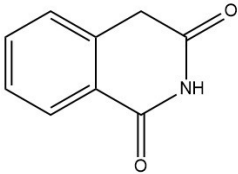
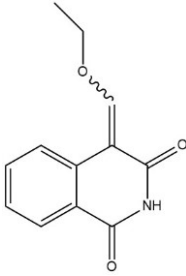
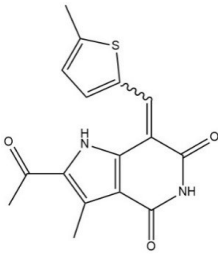
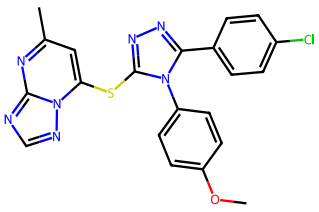
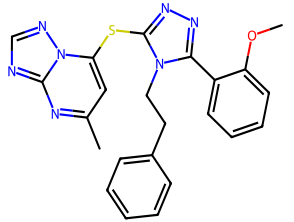
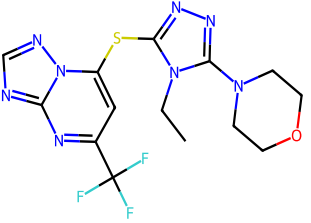
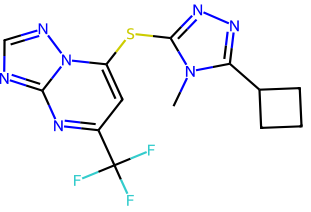
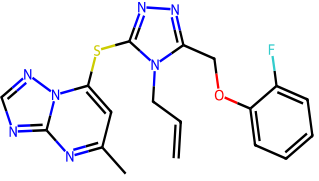
Structure	ID	% inhibition at 100 μ M		IC50 vs LASV (μ M)
		LASV	hmtRNAP	
	8417	0		NI
	5749	0		NI
	PPV	0		NI
	7072	0		NI

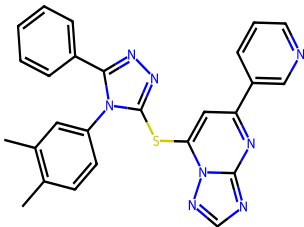
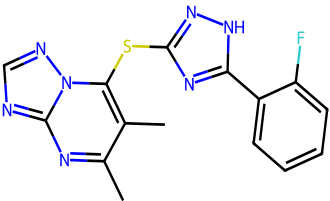
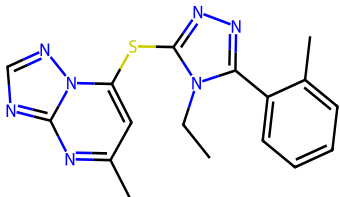
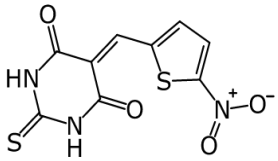
Table 3.3 Summary of derivatives tested for each parent compound

Parent compound	# of derivatives tested	Follow-up "hits"
ENM-29	94	LS-6
BTB-11392	12	1073
CBM-11	0	
6336	3	
5912	3	
5588	12	
TOTAL	124	2

Table 3.4 Derivatives with $\geq 80\%$ inhibition of LASV polymerase at 100 μM . Blank cells indicate n.d. (not determined). NI = no inhibition.

Structure	ID	Parent compound	% inhibition at 100 μM		IC50 (μM)	
			LASV	hmtRNAP	LASV	hmtRNAP
	1073	BTB-11392	98	0	0.65	162
	LS-6	ENM-29			3.6	>100
	L-SAR-2	ENM-29	97	96	3.46	2.63
	L-SAR-5	ENM-29	96	70	1.2	54
	LS-4	ENM-29			2.2	>100
	LS-5	ENM-29			2.5	>100

Structure	ID	Parent compound	% inhibition at 100 μ M		IC50 (μ M)	
			LASV	hmtRNAP	LASV	hmtRNAP
	1118	5588	99	37		
	1117	5588	99	0		
	1120	5588	99	0		
	1129	5588	97	0		
	1121	5588	96	47		

Structure	ID	Parent compound	% inhibition at 100 μ M		IC50 (μ M)	
			LASV	hmtRNAP	LASV	hmtRNAP
	1116	5588	92	62		
	1128	5588	90	0		
	1119	5588	84	0		
	1134	5588	81	0		
	BTB 02101	ENM-29	98		5.3	18*

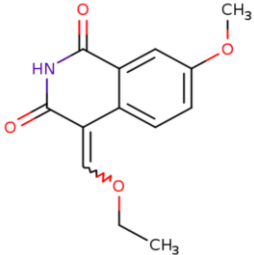
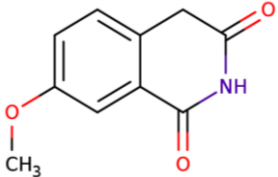
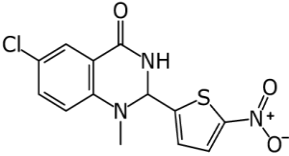
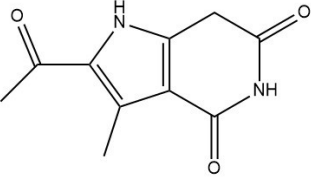
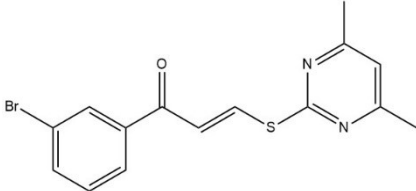
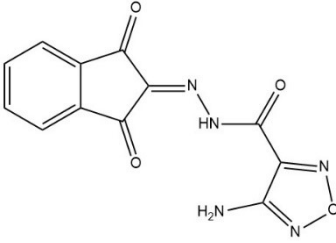
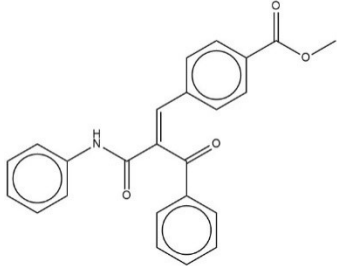
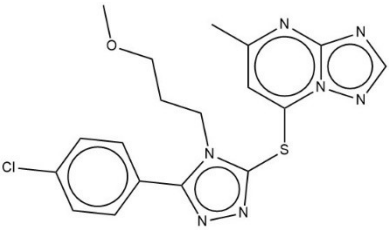
Structure	ID	Parent compound	% inhibition at 100 μ M		IC50 (μ M)	
			LASV	hmtRNAP	LASV	hmtRNAP
	Z56786861	ENM-29	97, 62% at 10 μ M			
	Z56759531	ENM-29	85, 74% at 10 μ M		5.9	>500*
	BTB 02126	ENM-29	83, 44% at 10 μ M			

Table 4.1 IC₅₀ determination of select compounds against LASV and other polymerases.

Structure	ID	IC ₅₀ (μM)			
		LASV	hmtRNAP	CCHFV	SARS-2
	ENM-29	0.42	NI	0.40	2.2
	BTB-11392	0.86	NI	1.3	8.5
	CBM-11	0.64	NI	1.5	2.8
	5912	1.4	NI	2.2	3.8
	5588	1.6	NI	5.2	3.0

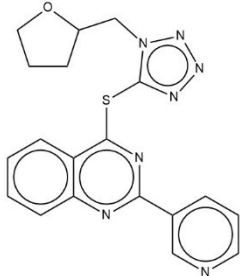
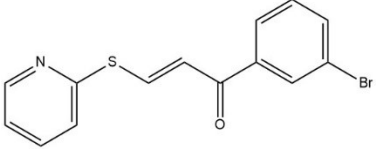
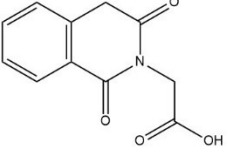
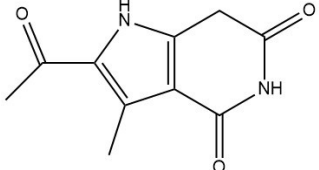
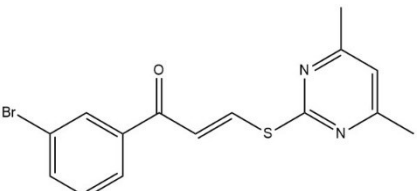
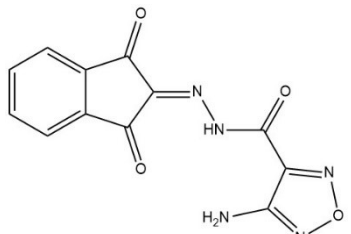
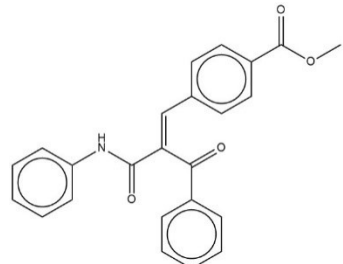
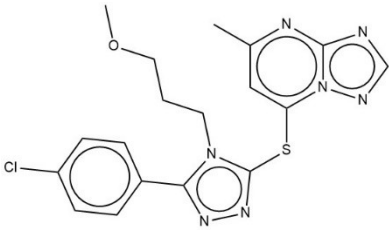
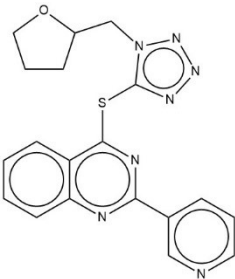
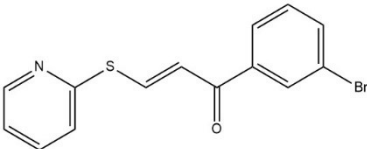
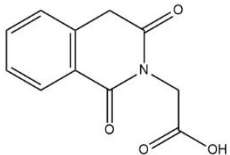
Structure	ID	IC50 (μM)			
		LASV	hmtRNAP	CCHFV	SARS-2
	6336	3.2	NI	11	21
	1073	0.65	162	1.6	1.3
	LS-6	3.6	NI	3.7	45

Table 4.2 IC₅₀ determination of select compounds against LASV under different conditions.

Structure	ID	IC ₅₀ (μM)		F-test	p value
		RNA start	Mg start		
	ENM-29	0.42	61	different curves	<0.0001
	BTB-11392	0.86	1.1	one curve	0.1173
	CBM-11	0.64	1.2	different curves	<0.0001
	5912	1.4	1.2	one curve	0.3096

Structure	ID	IC50 (μM)		F-test	p value
		RNA start	Mg start		
	5588	1.6	2.6	different curves	0.0018
	6336	3.2	9.2	different curves	<0.0001
	1073	0.65	1.3	different curves	<0.0001
	LS-6	3.6	16	different curves	<0.0001